

# **Experimental evolution of parasite life history in bacteriophage $\Phi$ 2**

Thesis submitted in accordance with the requirements of the  
University of Liverpool for the degree of Doctor of Philosophy

by Julie Truman

September 2014



# Abstract

Parasite life history theory predicts that lifetime reproductive success evolves through differential allocation of energy to life history traits constrained by trade-offs. These life history traits govern the characteristics of parasites such as their virulence, transmission and infection phenotypes, so understanding their evolution is a key concern for infectious disease prediction and management. This thesis uses the powerful tool of experimental evolution to gain a fuller understanding of the factors and constraints involved in parasite life history evolution, using bacteriophage  $\Phi 2$  as a model. I found that the evolution of life history in this phage is sensitive to spatial structure, UV-C exposure and co-parasitism with plasmids, and evolution can be mediated by co-evolution with the host.

The high levels of variance I observed here suggest that evolution of parasite life history is more complex than a single trajectory towards a predicted optimum, and likely involves some degree of epistasis or pleiotropy with genes elsewhere on the genome. There was some degree of independent evolution of individual life-history traits, indicating that simple direct trade-offs were not in operation.

I demonstrated that co-evolution with the host provided additional mutational input, resulting in a greater degree of evolution in co-evolved populations than those evolved to a static host. Furthermore, I note that co-parasitism with phage and plasmid may provide the necessary conditions for plasmid persistence

under fluctuating selection for plasmid-encoded traits, and that the efficacy and suitability of phage as therapeutic agents against plasmid-encoded antibiotic resistance is complicated. No direct link between mutation and phenotype could be elucidated in this study, suggesting that evolution in life history is either governed by genes not examined in this thesis, or involves epistasis and pleiotropy with genes elsewhere on the genome.

I concluded that it is important to consider the specific ecology of the focal parasite, its host and any co-occurring symbionts in order to make informed predictions of life history evolution, and general predictions may not be achievable.

## Acknowledgements

I would like to thank: my supervisors; Prof. Steve Paterson for his valuable support, guidance and patience as well as help with statistical analyses and writing style, and Prof. Mike Brockhurst for his enthusiasm and guidance into the world of bacteria-phage co-evolution. Also, Dr. Ellie Harrison for collaboration, enthusiasm, valuable tips and tricks in microbiology and help with statistics in R. I am grateful to the national environment research council (NERC) for funding the project.

Kieran, Carl, Susan and Angela for help with sequencing techniques and technology, Susan, Kieran, Steve, Angela, Leni, Ellie, Beth and Amanda for general support and answering silly questions, and my proof-readers Tom, Steve and Angela for helping with introduction style, clarity and typo removal.

Massive thanks to all my friends and colleagues in Liverpool and beyond for their unending support, after-work fun and thesis cheerleading.

Last but not least, my eternal gratitude to my family and Matt, not only for their support and pride throughout, but also for taking it in turns to keep me fed, housed, out of bankruptcy and sane(ish) in the final months.

Cheers everyone!

## **Declaration of originality**

I declare that all the work presented in this thesis is my own original research with the following acknowledgements:

Chapter 4: The selection experiment was conducted in collaboration with Dr. Ellie Harrison. We jointly performed the experiment and resistance assays, and Dr. Harrison conducted the time-shift analysis.

Chapter 5: The selection experiment was conducted in collaboration with Dr. Ellie Harrison. We designed the experiment together, and Dr. Harrison provided help and guidance with the analysis.

# Contents

Abstract.....	2
Acknowledgements.....	4
Declaration of originality.....	5
1. General introduction.....	9
Life history theory.....	10
Parasite life history.....	11
Spatial structure.....	16
Environmental stress.....	19
Co-parasitism.....	22
Experimental evolution.....	25
The host-parasite system <i>Pseudomonas fluorescens</i> and bacteriophage SWBP25Φ2.....	26
Aims.....	28
Chapter outlines.....	30
Chapter 2.....	30
Chapter 3.....	30
Chapter 4.....	31
Chapter 5.....	31
Chapter 2 – Spatial structure.....	32
Introduction.....	32
Methods.....	35
Media.....	35
Selection experiment.....	36
Population densities.....	36
Phage life history.....	36
Phage amplification.....	37
Growth curves.....	37
Lysis time.....	38
Burst size.....	38
Adsorption rate.....	38
Principal components analysis.....	39
Sequence analysis.....	39
Statistical analysis.....	41
Results.....	41
Phage densities.....	41
Phage life history.....	43
Correlation analysis.....	45
Phage evolution.....	48
Discussion.....	52
Conclusions.....	56
3. UV environmental stress.....	58
Introduction.....	58

Methods.....	62
Pilot.....	62
Selection experiment.....	63
Population densities.....	64
Phage life history.....	65
Life history strategies.....	65
Sequence analysis.....	65
Statistical analysis.....	66
Results.....	66
Phage & bacterial densities.....	66
Phage life history.....	70
Phage evolution.....	75
Discussion.....	81
Conclusions.....	86
4. The effects of phage on bacteria-plasmid dynamics.....	88
Statement of collaboration.....	88
Introduction.....	88
Methods.....	91
Selection experiment.....	91
Population densities.....	92
Plasmid prevalence.....	92
Time-shift resistance assay.....	93
Statistical analysis.....	93
Results.....	94
Plasmid prevalence.....	94
Bacterial & phage densities.....	94
Bacterial resistance.....	97
Discussion.....	99
Conclusions.....	102
5. Effects of plasmid carriage on phage life history and phage-host dynamics.....	103
Statement of collaboration.....	103
Introduction.....	103
Methods.....	107
Selection experiment.....	107
Population densities and bacterial morphology.....	107
Plasmid prevalence.....	108
Resistance assay.....	108
Phage life history.....	109
Life history strategies.....	109
Sequence analysis.....	109
Statistical analysis.....	110
Results.....	111
Plasmid prevalence.....	111
Phage & bacterial densities.....	112
Bacterial resistance and morphology.....	114
Phage life history.....	114

Phage evolution.....	119
Discussion.....	127
Conclusions.....	131
6. General Discussion.....	132
Implications.....	135
Conclusions.....	137
References.....	138
Appendix I – Ancestral phage life history characterization.....	149
Introduction.....	149
Methods.....	149
Host growth curve.....	149
Preparation of high-titre ancestral $\Phi$ 2 stock.....	150
Standard plaque assay.....	150
Purification.....	150
Amplification.....	150
Determination of optimal MOI.....	151
Method.....	151
Growth curve.....	152
Lysis time.....	152
Burst size.....	152
Adsorption rate.....	153
Results.....	153
Host growth curve.....	153
High-titre ancestral $\Phi$ 2 stock.....	154
Optimal MOI.....	154
Ancestral life history.....	155
References.....	156
Appendix II – Sequencing methods.....	158
PCR.....	158
ExoSAP digest.....	158
Cycle sequencing reaction.....	159
Precipitation and sequencing.....	159
Analysis.....	159

# 1. General introduction

Parasitism is a highly successful mode of life. There are parasitic species found in all taxa, from viruses through to complex multicellular plants and animals (Combes 2001; Poulin 2011). No known species are completely resistant to parasitism, and most hosts support multiple species of parasites, making parasites considerably more numerous than free-living organisms (Windsor 1998). As such a dominant presence, parasites play an important role in shaping the evolutionary ecology of their hosts (Barber et al. 2000; Combes 2001). By nature, parasitic exploitation causes some degree of harm to their individual hosts (Combes 2001). The degree of harm ranges from the energetic costs of replicating additional genetic material in plasmids (Bergstrom et al. 2000) or transposable elements (Charlesworth & Langley 1989), through causing deleterious disease symptoms such as fever and vomiting due to *Plasmodium falciparum* (e.g. Gouagna et al. 2004), to castration as in *Sacculina* infections of crabs (e.g. Phillips & Cannon 1978), and certain death as caused by parasitoids and lytic phage such as SBWP25Φ2 (Buckling & Rainey 2002).

On a population level, parasites can regulate host population density (Anderson & May 1978; Redpath et al. 2006; Combes 2001) through their effects on host death rates and fecundity. The first example of this effect was discovered in wild red grouse (*Lagopus lagopus scoticus*) infection with the parasitic nematode *Trichostrongylus tenius* (Hudson et al. 1998). Red grouse populations exhibit cyclical fluctuations with occasional crashes in density. Treatment of grouse

with the anthelmintic Levamisole hydrochloride reduced fluctuations in the population proportionally to the percentage of animals treated, with 20% treatment almost completely removing fluctuations (Hudson et al. 1998). This dampening of fluctuations was associated with reduced worm load and increased fecundity in female birds, demonstrating that individual effects of parasite infection are sufficient to cause population-level effects. These population-level effects combine to act upon communities, by maintaining diversity, stabilising communities and influencing speciation (Combes 2001). Aside from their inherent ecological interest, a better understanding of the adaptation and evolution of parasites is crucial for disease prediction and prevention measures (Galvani 2003).

## **Life history theory**

A valuable framework for understanding the evolution of parasites is life history theory. Life history theory posits that an individual's fitness is determined by the values of a suite of traits acting together to bestow lifetime reproductive success (Stearns 1992). These traits are those directly involved in survival and reproduction such as size and age at maturity, number and size of offspring, and age-specific parental investment (Stearns 1992). The basic tenet of life history theory is that individuals cannot maximise all life history traits at once. A theoretical organism operating without constraint would be sexually mature at birth, produce infinite offspring and live forever, but in reality phylogenetic, physiological and ecological constraints prevent such a “Darwinian demon” from

arising (Law 1979). Instead, individuals possess a finite amount of resources and face trade-offs between traits, which are shaped by the environment and their mode of life (Law 1979; Partridge & Harvey 1988; Stearns 1989; Gadgil & Bossert 1970; Clutton-Brock et al. 1982). The particular balance of allocation of resources/effort to each of these traits exhibited by an individual is termed its life history strategy, and the optimal strategy is that which maximises lifetime reproductive success in a given environment (Partridge & Harvey 1988; Stearns 1992; Stearns 1989; Gadgil & Bossert 1970).

## **Parasite life history**

Although general life-history theory was developed with free-living species in mind, there are many parallels among parasitic organisms, and life history theory has been adapted to address the selection pressures faced by parasites (Poulin 1996). For parasites, reproductive success is not governed solely by the acquisition and conversion of resources into progeny, but also by successful transmission of progeny from one host to the next.

As with free living organisms, parasites experience trade-offs between growth and reproduction, reproduction and survival, number of offspring and offspring quality, and current reproduction and future reproduction (Stearns 1992; Stearns 1989). Additionally, due to their dependence on host organisms, parasites face unique trade-offs between: within-host growth and reproduction (virulence) and transmission, virulence and within-host survival, virulence and

extra-host survival and host range and infectivity (Poulin 1996; Combes 2001; Goldhill & Turner 2014).

One of the most important trade-offs for parasite success is believed to be that between virulence and transmission. Virulence is generally defined as the negative effects of parasite growth and reproduction on host physiology (Anderson & May 1982), although the specific definition varies from study to study for logistical reasons. For parasites that cause chronic or non-lethal infections, virulence can be defined as the degree of debilitation of the host or reduction of host reproductive potential, which can be difficult to quantify (Read 1994). For obligate killing parasites such as lytic bacteriophage, virulence is often more simply defined as the rate of host death (Kerr et al. 2006), percentage clearance of the host population (Nidelet et al. 2009) or the time to host lysis (Abedon et al. 2003a; Bull 2006). Similarly, although transmission is most correctly defined using the term  $R_0$ , or the number of secondary infections resulting from one primary infection (Alizon et al. 2009), in reality the difficulty in correctly measuring this number requires that simpler approximations of transmission are used. Transmission is often therefore defined as the reproductive output of the parasite, or simply the number of progeny produced in a given reproductive cycle (e.g. Messenger et al. 1999).

The virulence-transmission trade-off theory assumes that virulence is a side-effect of within-host reproduction, and transmission to new hosts. The theory, first described in its current form by Anderson & May (1982), postulates that whilst maximising the rate of progeny production may increase an individual

parasite's within-host fitness, the associated increase in virulence can debilitate and even prematurely kill the host. This exhaustion of the host can reduce the transmission likelihood of progeny to new hosts and destroy the resources needed for further progeny production (Levin & Pimentel 1981; Frank 1996). As the fitness of a parasite depends on both the production of offspring and transmission of offspring to new hosts, parasites must evolve a life history strategy that allows the optimal balance between virulence and transmission. This optimal balance is predicted to vary with transmission mode, for instance parasites transmitted by a vector can "afford" to be more virulent than those transmitted by direct host-to-host contact (Day 2001; Ewald 1983). This trade-off has been documented in bacteriophage f1 selected under two different regimes of horizontal and vertical transmission (Messenger et al. 1999). This phage establishes non-fatal infection and can be transmitted vertically. Vertical transmission selects for reduced virulence, as healthy hosts are more able to replicate and hence transmit the phage. Horizontal transmission, on the other hand, selects for higher virulence due to the selection for increased numbers of progeny for transmission to multiple new hosts. Long interval ratio of vertical to horizontal transmission in this system produced phage with low rates of virion production and hence reduced virulence, while short interval ratios produced virulent phage with a higher reproductive rate. Jensen et al. (2006) also found support for the virulence-transmission trade-off in the castrating bacterium *Pasteuria ramosa*, which produces spores that are only released after host death, allowing for a direct estimate of lifetime

transmission success based on the abundance of spores. When infecting a clonal population of *Daphnia magna*, this parasite displayed wide variation in virulence (measured as time to host death) and spore production. Maximal spore production was reached at intermediate virulence, suggesting that a trade-off is in operation, and an optimal virulence value is achievable in this system.

The virulence-transmission trade off is an attractive hypothesis due to its simplicity and generality, and is at the heart of most of the popular recent theories of parasite virulence evolution, but it is far from universally accepted (for a review of the debate, see Alizon et al. 2009). The fact that, under this hypothesis, the optimal virulence varies with host genotype, immunology and physiology, spatial structure, relatedness of co-infecting parasites, transmission mode and host density makes trade-offs difficult to detect empirically often leads to criticism of the hypothesis (e.g. Weiss 2002). Ebert & Bull (2003) also noted that increased virulence is not always detrimental to parasite fitness, and that virulence is rarely controlled solely by the parasite, but is also influenced by host-associated characteristics such as tolerance and immunology. Alizon et al. (2009) counter, however, that these details do not undermine the basic tenet of the virulence-transmission trade-off hypothesis, but highlight the need for modification of the basic model under certain conditions. For instance, when hosts are infected by multiple strains of a parasite, the basic model must be modified to allow for within-host competition and kin-selection. When two unrelated strains are competing for host resources, selection will favour the

more productive strain, leading to an overall increase in virulence when co-infections are common (Levin & Bull 1994). Conversely, when co-infecting strains are related, co-operative prudence can drive lower virulence than expected (Hamilton 1972). Therefore, the probability and degree of co-infections and the relatedness of co-infecting strains should be incorporated into the virulence-transmission model in order to make accurate predictions. If we accept that the basic model is a starting point which requires additional information in order to accurately predict parasite life history evolution, it remains a useful theoretical framework which continues to be widely utilised. Many species of bacteriophage may only transmit by lysis of the bacterial cell (lytic phage), which kills the host and causes the destruction of the replicative machinery needed to produce further virions (Abedon et al. 2003). In many phage, therefore, the virulence-transmission trade-off is likely to be a crucial determinant of reproductive success.

In lytic phage, virion production is predicted to show a linear relationship with time spent within a host cell, so a trade-off between lysis time and burst size (the number of virions produced per infected cell) is predicted.

This thesis will use a bacteriophage model to focus on three common abiotic and biotic factors predicted to influence the trade-off between virulence and transmission: Spatial structure, environmental stress and co-parasitism.

Virulence is here defined as host death, and is measured by the time taken for a given population of phage to lyse 50% of infected cells (lysis time). Transmission is not directly measured, but rather inferred from the adsorption rate of phage

to host cells and the number of progeny produced in a given reproductive cycle (burst size).

## Spatial structure

Spatial structure is the phenomenon of reduced connectivity within an environment caused by the physical attributes of that environment, which leads to a reduced encounter rate between organisms, and localised interactions. The majority of habitats have a spatially heterogeneous element to them which can cause patchy aggregation within populations with reduced gene flow between patches compared to within patches (Slatkin 1987); a metapopulation (as defined by Hastings & Harrison, 1994). The degree of isolation of these population patches depends both on the physical attributes of the landscape and the dispersal ability of the organisms. Spatial structure is an important evolutionary driver in natural populations which can promote or erode genetic diversity within populations, provide the necessary heterogeneity for coexistence and promote specificity to local hosts (Hastings & Harrison 1994). Theoretically, spatial structure is the degree of localisation of a given population, or the effective distance between individuals (Watts & Strogatz 1998). Effective distance is influenced by actual physical distance, factors that affect movement such as physical barriers on land or viscosity in liquids, and the dispersal ability of organisms, which combine to confer a theoretical probability of encounter between individuals. The larger the effective distance between individuals, the lower the encounter probability and the more localised interactions will be,

promoting the development of ephemeral or permanent patchiness of the population (Boots & Sasaki 1999).

For parasites, an individual host plant or animal may constitute a patch, with patches connected through social interactions or pollinating insect movement, for example. Many microbial communities also exist naturally in structured environments such as in biofilms, on plant or animal tissue or in soil or sediments (Abedon & Yin 2009), so understanding the consequences of spatial structure on parasite adaptive trajectory is essential to our understanding of parasite ecology in general.

In host-parasite interactions, spatial structure limits the dispersal of both hosts and parasites, effectively reducing the local pool of susceptible hosts through reduced host immigration and limiting transmission opportunities for parasite progeny (Boots & Sasaki 1999). When susceptible hosts are abundant in spatially unstructured environments, encounter rate is high so transmission between hosts is fast and easy. Parasites are limited by their rate of development and the number of progeny produced rather than their transmission ability. Short reproductive cycles and large numbers of offspring, resulting in high virulence are favoured (Abedon & Culler 2007a; Abedon et al. 2003a). In spatially structured environments, parasites face increased competition for hosts with related genotypes (kin-shading; Lion & Baalen 2008) and identical genotypes (self-shading; Boots & Sasaki 2000), and risk exhaustion of their local pool of susceptible hosts leading to local extinctions (the tragedy of the commons; Kerr et al. 2006; Boots & Sasaki 2002). In highly structured

environments therefore, parasites with lower infectivity and virulence, that produce progeny with greater transmission ability are favoured, even if fewer progeny are produced over all (Boots & Meador 2007).

Studies modelling the effects of increased connectivity warn that there may be a critical connectivity threshold above which diseases will rapidly evolve higher virulence, which could have serious consequences for human and agricultural disease as human populations become ever-more connected (Boots & Sasaki 1999). Understanding the effect of spatial structure and local adaptation on parasite evolution and dynamics is therefore crucial from an anthropogenic point of view, both for predicting the spread of human and agriculturally important diseases and informing intervention design.

In a comparative study between 33 strains of the obligate fungal pathogen *Podosphaera plantaginis* infecting *Plantago lanceolata*, life history traits such as sporulation speed and abundance were positively correlated on their locally-adapted hosts within a metapopulation structure (Susi & Laine 2013). These correlations became negative when the same strains infected allopatric (geographically isolated) host populations, which was associated with reduced prevalence of disease, highlighting the importance of local adaptation on the effects of spatial structure on life history traits. Evolution experiments with spatial structure in phage are also beginning to show general support for theoretical predictions. The *Escherichia coli* phage ID11 challenged with a spatially structured environment evolved a single substitution in the major capsid protein. This resulted in a reduced infection rate, but greater numbers of

progeny produced when grown on the spatially structured surface of an agar plate (Roychoudhury et al. 2014).  $\lambda$  phage which had been engineered to have a fast adsorption rate suffered reduced productivity when grown in semi-solid agar (Gallet, Shao, et al. 2009). Spontaneous evolution of mutants with a slower adsorption rate occurred in these populations, suggesting that selection for slow adsorption rate is strong in structured environments. In contrast, no deleterious effects of high productivity were found in phage  $\Phi 6$  when compared with the less-productive  $\Phi 6_M$ .  $\Phi 6$  was superior to  $\Phi 6_M$  in all environments regardless of host density or spatial structure, although the relative fitness of  $\Phi 6_M$  in structured environments increased with host density (Dennehy 2009). The success of  $\Phi 6$  across all environments was attributed to its high burst size, which may compensate for a reduced dispersal ability.

Kerr et al. (2006) manipulated migration between host sub-populations in phage T4 in 96-well microtitre plates. Movement restricted to local patches promoted more prudent (less virulent) strategies, whilst unrestricted migration promoted high virulence (Eshelman et al. 2010). Neither life history traits nor genetic mutations were measured in this study however, so it is not clear how the differences in productivity between the migration regimes arose in this system.

## Environmental stress

There are many abiotic factors which may act as environmental stressors to parasites, such as temperature, acidity, dessication, UV or X-ray irradiation,

salinity and deoxygenation. In macroparasites, particularly ectoparasites, temperature sensitivity is an important factor affecting life-history (Poulin 1996). For terrestrial microparasites, UV-irradiation plays an important role (Rodriguez et al. 2014; Murray & Jackson 1993; Weinbauer & Wilhelm 1997), and for aquatic organisms salinity and acidity are key factors (Miracle & Serra 1989; Dupont & Thorndyke 2009). Whilst endoparasites may be able to escape direct abiotic environmental influence whilst inhabiting a host, all parasites with free-living or transmission stages must face the extra-host environment at some stage in their life-cycle (Poulin 1996).

A general prediction for parasites in harsh environments is that adaptation to withstand environmental stress results in a trade-off with reproductive rate, mirroring the classic life history trade-off between survival and reproduction in free-living species (Goldhill & Turner 2014). In a comparative study of 16 phage families that infect *E. coli*, De Paepe & Taddei (2006) examined the multiplication and decay rates of these phage at different temperatures. They discovered a robust negative correlation between reproduction and survival across phage families, which was related to the density of their packaged DNA and capsid thickness.

Evolution experiments with phage have highlighted the diversity in the degree to which this trade-off operates and the mechanisms by which it is generated (Goldhill & Turner 2014). The RNA phage  $\Phi 6$  evolved in an environment characterised by regular brief heat shocks causing high rates of mortality and thus evolved greater thermal stability at the expense of reduced reproduction

(Dessau et al. 2012). Conversely, in the RNA phage Q $\beta$ , no such costs of thermostability were found in evolution to heat shocks, and thermostable phage were found to also be more resistant to acidity, suggesting a general robustness to mutagenesis (Domingo-Calap et al. 2010).

Parasites whose transmission modes are through free-living stages and host contact with contaminated surfaces generally show the opposite effect – persistence in the environment selects for high virulence (Bonhoeffer et al. 1996). This is termed the “sit and wait”, or “curse of the pharaoh” hypothesis. This hypothesis suggests that extreme longevity in the environment reduces the costs associated with high virulence, as associated decreases in transmission from the host are offset by the increased transmission ability afforded by extreme environmental persistence (Walther & Ewald 2004). This effect has been demonstrated in a comparative study of respiratory tract pathogens of humans, conducted by reviewing the epidemiological and medical literature of such diseases. Walther & Ewald (2004) found a correlation between persistence and virulence using both across-species and phylogenetically controlled studies. These contrasts in the outcomes of environmental stress suggest that evolutionary responses are both variable and specific to the ecology of the species, suggesting that general predictions may be unsuitable in the case of environmental stress *per se*.

## Co-parasitism

Host individuals often carry more than one strain, species or taxon of parasite at once (Windsor 1998), and co-occurring parasites will impact upon each other's fitness either directly or indirectly. Interactions between co-occurring species within a host determine the epidemiology of each species through their impact on host fitness, severity of disease symptoms and the release of infective stages into the environment (Pedersen & Fenton 2007). A general prediction is that when co-infecting strains are closely related, their interests are aligned and a prudent exploitation of the host may be favoured, but when co-infections occur between distantly related strains or different species, competition for resources is fierce, selecting for increased growth rate and high virulence (Hamilton 1972).

In temperate lambdoid phage of *E. coli* induced to lyse, lysis timing was always controlled by the faster-lysing phage type in double infections (Refardt 2011). This fast lysis was associated with a competitive advantage over types with much later lysis, with competitive ability following a hierarchical pattern between 11 phage varying in lysis timing.

Experimental evolution with phage  $\Phi 2$  found that at high multiplicity of infection (MOI) where co-infection is common, phage evolved a plastic lysis time (Leggett et al. 2012). Phage evolved at high MOI were able to detect co-infections and lysed the cell earlier in mixed than single infections. In contrast, phage adapted to low MOI conditions did not lyse faster in mixed infections, indicating that plastic lysis is an adaptation to mixed infection conditions rather

than an artefact of increased phage numbers within a cell. The method by which phage were able to detect infection status was not discovered. This early lysis in phage evolved to mixed infections was associated with a reduced population density, indicating a trade-off between within-host competitive ability and transmission to new hosts. Conversely, in the RNA phage  $\Phi 6$ , the effects of multi-parasitism followed a classical prisoner's dilemma strategy of game theory due to shared intracellular products produced by these phage. When co-infecting strains were closely related, intracellular products were produced cooperatively. Cheats, which sequester the intracellular products made by cooperators, evolved when two co-infecting strains were unrelated. This reduced the overall productivity of phage and consequently reduced rather than increased virulence in mixed infections (Turner & Chao 1999).

Understanding how lysis timing is controlled by phage has been a major research focus in recent years. It has long been known that the phage-encoded endolysins and holins were jointly responsible for cell membrane degradation (Wang et al. 1996; Young 1992) and that timing was mainly controlled by alleles in the gene encoding for holins (Young et al. 2000; Wang et al. 2000), but only recently have we gained a fuller picture of lysis regulation (Young 2014; Young 2013). In brief, holins accumulate in the cytoplasmic membrane of the host cell, and endolysins accumulate in the cytoplasm harmlessly throughout virion production (Young 2014). Lysis begins when the holin triggers at a time genetically pre-programmed by alleles that alter the primary structure of the holin protein. At this time, the holins cause permeabilisation of the cytoplasmic

membrane, and the endolysins escape and begin breaking down the peptidoglycans in the cell wall. Therefore, lysis can be genetically controlled by mutations that alter the structure of the holin proteins, which in turn alter the critical concentration of holins required to activate permeabilisation (Young 2013). In mixed infections, therefore, phage could be responding to the accumulation of non-self holins and endolysins in the host cell, and responding plastically through regulation of gene expression. However, this is simple conjecture and the method of detecting co-infections is still unknown.

Co-parasitism by vertically transmitted and horizontally transmitted parasites causes conflict due to the differences in optimal virulence (Rigaud & Haine 2005). Vertically transmitted parasites require healthy reproducing hosts for transmission so optimal virulence is low whilst horizontally transmitted parasites generally have higher virulence due to the need for a high transmission rate. Jones et al. (2010) modeled this interaction and found that co-parasitism with vertically transmitted parasites selected for increased virulence in horizontally transmitted parasites due to the competition for resources, particularly when the vertically transmitted parasite was feminising. Horizontally transmitted parasites select for intermediate virulence in vertically transmitted parasites, and shorter host life span drives higher virulence in both parasites when co-infecting. In the amphipod *Gammarus roeseli*, vertically transmitted *Dictyocoela* parasites interfered with the host-manipulation of the horizontally transmitted *Polymorphus minutus* (Haine et al. 2005). *G. roeseli* is the intermediate host of *P. minutus*, which manipulate the host's geotaxis in

order to increase predation rate by its definitive host, freshwater birds. When co-infecting with *Dictyocoela*, however, this geotaxis was markedly reduced, suggesting sabotage by the vertically transmitted *Dictyocoela*, although the mechanism of this interference was not discovered.

## Experimental evolution

Historically, the majority of studies on life history evolution were theoretical, comparative or based only on a few generations, leading to a lack of empirical data on the causes and evolution of trade-offs and associated traits (Roff & Fairbairn 2007). There was good reason for this dearth of information – examination of life history and trade-offs was concerned with long-lived free-living organisms, and evolution studies would have been both onerous and excessively lengthy.

The development of experimental evolution with microbes has opened up the field of life history evolution to empirical testing of theoretical predictions, allowing researchers valuable insights into the nature of life history. Microbial experimental evolution is a powerful tool for investigating the evolution and co-evolution of parasites and their hosts (Brockhurst & Morgan 2007; Ebert 1998; Brockhurst & Koskella 2013), and a wealth of information is rapidly emerging from such studies, providing many of the examples discussed here.

The fast generation times and large population sizes of microbial populations allow for experimental studies of evolution that track hundreds or even thousands of generations through evolutionary time in manageable timescales

within a laboratory (Lenski & Levin 1985). These populations can be frozen and stored for long periods at any time point, allowing the direct comparison of ancestral and evolved genotypes (Lenski et al. 1991). The small size of microbial cultures allows for large-scale propagation and replicate populations, permitting the investigation of population-level questions. Populations can be initiated isogenically and carefully controlled to ensure that confounding variables are kept to a minimum, and observed changes can be directly ascribed to mutation and selection (Brockhurst & Morgan 2007). Furthermore, small genomes and high population densities permit the exploration of genetic mutation alongside phenotypic change.

## **The host-parasite system *Pseudomonas fluorescens* and bacteriophage SBWP25Φ2**

*Pseudomonas fluorescens* is a common gram-negative rod-shaped bacterium which inhabits soil, plant surfaces and water (Rainey & Bailey 1996). Isolate SBW25 was isolated in 1989 from a sugar beet plant in Oxfordshire, and has become a model organism for studies of bacterial adaptation due to its ease of culture and manipulation. Bacteriophage SBWP25Φ2, hereafter referred to as Φ2, is a naturally associated obligate lytic phage of *P. fluorescens* (Buckling & Rainey 2002). This host-parasite system is well-characterised, since the genomes of both host and parasite have been sequenced and the system is well-suited to experimental evolution (Brockhurst & Morgan 2007).

Lytic bacteriophage such as  $\Phi 2$  disperse freely through the environment and attach to bacterial hosts using tail fibres, which contract to irreversibly bind the phage to the bacterial cell wall (adsorption). The phage genome is then injected into the bacterial cytoplasm, where it hijacks the cellular apparatus used for reproduction to replicate, and replicate genomes are packaged into new virions. When a certain number of virions have been fully assembled (the burst size), the phage activate cell lysis and the bacterial cell wall is broken down, releasing the new virions into the environment to find and infect new hosts.

The lytic phage life cycle can be broken down into 3 key measurable life history traits, which are regulated by the phage genome: the adsorption rate, the lysis time, and the burst size, which are expected to be subject to trade-offs (Fig 1.1).

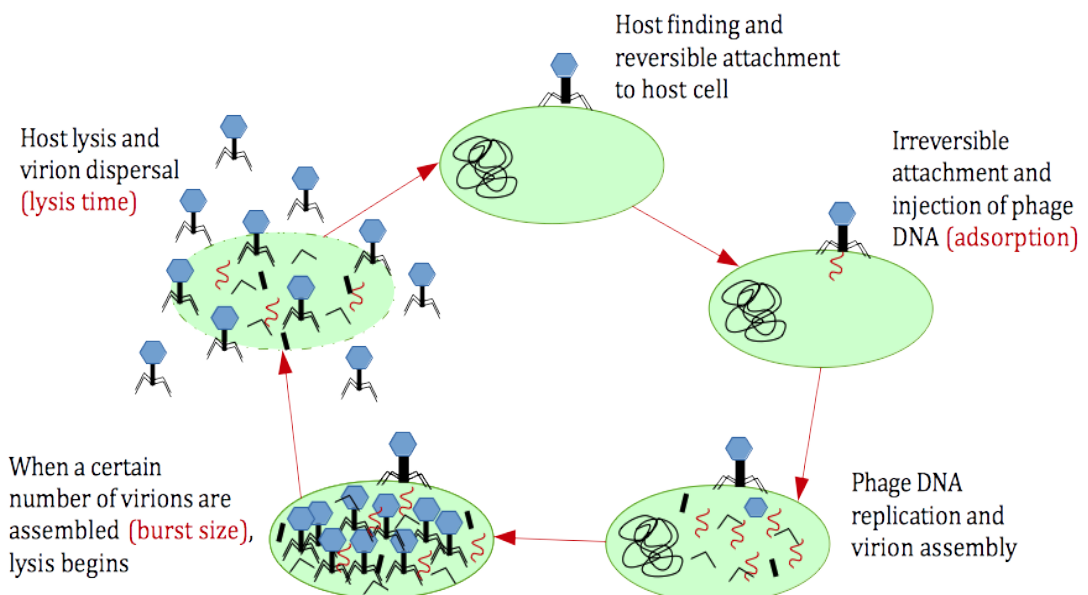


**Figure 1.1.** Lytic phage life cycle

The genetic basis of life history evolution in bacteriophage is not well understood, despite a wealth of knowledge of phage genetics and physiology (Bull 2006). For this reason, predictions of phage life history evolution are often based solely on basic optimality models without regard for the genetic details, as first developed by Maynard Smith (1978). This approach has been heavily criticised as an over-simplified view of evolution (Lewontin 1989), but it continues to be a common approach. For lysis timing, the assumptions of optimality models have been found to be generally compatible with what is known about the genetic control of lysis in bacteriophage, but inclusion of genetic details substantially improves optimality models by revealing constraints, pleiotropy and plasticity (Bull et al. 2004). Host-parasite co-evolution experiments have demonstrated an accelerated mutation rate in  $\Phi 2$  genes predicted to be involved in infection and lysis during co-evolution (Paterson et al. 2010), but it is not yet clear how these mutations affect life history phenotypes.

## Aims

In order to gain a fuller understanding of the evolution of parasite life history, this thesis will consider the effects of both biotic and abiotic environmental variables on life history traits and their trade-offs.

The aim of this thesis is to investigate the selection pressures on parasites produced by a shift in common environmental variables and the direction, strength and repeatability of the phenotypic response and the underlying

genetic evolution. An increase in our understanding of the selection pressures faced by parasites and their responses will help inform disease prevention and control measures, as well as helping to describe the natural distribution and variation of parasites.

The following questions are addressed: Does a reduction in encounter rate through increased spatial structure drive the evolution of a more prudent life history? Does the common environmental stressor UV irradiation cause a reduced capacity for phenotypic evolution, or provide additional mutational input for a higher rate of phenotypic evolution? Does indirect competition between two symbionts affect host capacity to resist either symbiont? Does this competition result in decreased prevalence of either symbiont? Does selection for mutualism in one of the symbionts alter the outcomes of this competition? Do all populations under the same selective conditions follow the same evolutionary trajectory or are there multiple adaptive strategies in play?

This thesis explores these questions with the bacteria-phage system *Pseudomonas fluorescens* and bacteriophage SBWP25Φ2. Using an experimental evolution approach, the effects of spatial structure, exposure to UV-C irradiation and both sides of the interaction with the competing symbiont plasmid pQBR103 are investigated. Phenotypic evolution in the key phage life history traits adsorption rate, lysis timing and burst size are measured, with a view to examining the evolution in trade-offs between these traits. In addition, the genetic basis of life history evolution is investigated through Sanger sequencing

of key host-associated genes in order to elucidate the link between genotypic and phenotypic evolution in life history trade-offs.

## **Chapter outlines**

### **Chapter 2**

Spatial structure is a common feature of many habitats and is predicted to be an important driver of ecological processes. Parasites are predicted to evolve high virulence in non-structured environments, but prudence in highly structured environments to avoid over-exploitation of the host and local extinction. Using viscous growth medium, I will experimentally evolve populations to assess the effects of spatial structure on life history evolution in a bacteriophage model. A combination of life history assays and genetic analysis should afford me a deeper understanding of the mechanisms and trade-offs in life history evolution.

### **Chapter 3**

UV irradiation is an environmental stress known to cause high mortality in phage, but its effect on phage life history is unknown. Experimental evolution of phage exposed to different doses of UV-C irradiation will allow me to determine the evolutionary trajectory of phage under UV stress. I will conduct both evolutionary and co-evolutionary experiments, to look for the effects of increased mutational input with co-evolution.

## Chapter 4

Co-parasitism is ubiquitous in nature and each parasite can have profound effects on the fitness of the other. Plasmids that confer a benefit to the host in certain environments range from parasitic to mutualistic, and the effects of positive selection for plasmids on the outcome of co-parasitism is not known. Using the naturally-associated plasmid pQBR103 which confers mercury resistance on *P. fluorescens*, I will assess the effects of different degrees of positive selection for plasmids on the effects of phage predation.

## Chapter 5

Following on from chapter 4, in this chapter I will assess the effects of positively-selected plasmids on phage life history evolution and phage-host dynamics under co-evolution. As plasmid carriage is predicted to limit the host resources available to phage for reproduction, a more virulent life history strategy may be favoured. Alternatively, the predicted reduction of bacterial density in plasmid-carrying populations may select for a more prudent life history strategy.

## Chapter 2 – Spatial structure

### Introduction

Microbial communities often inhabit spatially structured environments such as soils, sediments, in or on animal or plant tissue and the bacterial biofilms that are readily formed by many species (Abedon & Culler 2007a). Spatial structure is predicted to be an important driver of evolutionary processes (Hastings & Harrison 1994), so studying the effects of structured environments on phage life history evolution is an important step towards our understanding of life history and trade-offs (Galvani 2003). When hosts are abundant and there is no spatial structure, parasites are limited by their rate of reproduction, so the classic virulence-transmission trade-off is skewed towards high virulence and fast transmission (Boots & Meador 2007). When host populations are highly structured, however, host-parasite interactions become localised, and highly virulent parasites risk driving their local pool of susceptible hosts (and therefore themselves) to extinction (Messinger & Ostling 2009). The transmission-virulence trade-off therefore becomes skewed towards slow rates of reproduction and increased dispersal ability of offspring (Wild et al. 2009; Kamo & Boots 2006). At low spatial structure, life history theory predicts that phage will evolve fast adsorption, early lysis and large burst size, unless constrained, in order to maximise reproductive rate and competitive ability (Abedon & Culler 2007b; Abedon et al. 2003a). At high spatial structure, theory

predicts parasites to become more prudent in order to avoid kin and self shading (Wild et al. 2009; Lion & Boots 2010), so phage should evolve slow adsorption for increased dispersal, late lysis and small burst size.

Empirical studies of parasite life history evolution under spatial structure in phage are beginning to show general support for theoretical predictions. A study by Gallet et al. (2009) found that fast adsorption rate was highly disadvantageous in terms of plaque size, productivity and emigration in structured environments in  $\lambda$  phage growing in semi-solid agar. Mutants with a slower adsorption rate spontaneously evolved in strains engineered to have fast adsorption rates, suggesting that selection for slow adsorption rate is strong in structured environments. Additionally, phage ID11 grown with *E. coli*, serially passaged for ~550 generations on agar plates evolved a slow adsorption mutant, governed by a single substitution in the major capsid protein (Roychoudhury et al. 2014). This mutant had a lower adsorption rate than the ancestor, but no changes in lysis time or burst size were observed. The slower adsorption rate was associated with both a larger plaque size and greater density of phage within a plaque when plated, suggesting an adaptive advantage of low adsorption rate mutants in spatially structured environments.

Conversely, (Dennehy et al. 2007) found no deleterious effects in spatially structured environments on the more productive (higher burst size) phage  $\Phi 6$  when compared with the less-productive  $\Phi 6_M$ .  $\Phi 6$  was superior to  $\Phi 6_M$  in all environments regardless of host density or spatial structure, although the

relative fitness of  $\Phi 6_M$  in structured environments increased with host density. The success of  $\Phi 6$  across all environments was attributed to its high burst size. A study manipulating migration between host populations in phage T4 in 96-well microtitre plates showed that movement restricted to local patches promoted prudent strategies when compared to global movement across the plate (Kerr et al. 2006). Wells were inoculated with phage and/or bacteria or left empty initially based on simulations, and mixed either with local wells or with any well on the plate (global mixing) according to simulated patterns, at each transfer. Global migration regimes exposed phage to competition between genotypes, and greater availability of hosts, promoting a rapacious life history and the subsequent rapid extinction of both hosts and phage. Local mixing, however, reduced the contact rates with hosts and competing genotypes, and more prudent host exploitation strategies evolved as predicted by theory (Boots & Meador 2007; Boots & Sasaki 1999). Neither life history traits nor genetic mutations were measured in this study however, so it is not clear how the differences in productivity between the migration regimes arose in this system. This chapter aims to test the prediction that increased spatial structure selects for a more prudent life history. Investigating the phenotypic response of experimental populations allows us to elucidate the capacity of parasites to respond to selection imposed by increase structure, and may help to inform future disease management and prevention efforts.

Experimental evolution of phage against a static ancestral host allows phage to adapt to structured environments both phenotypically and genetically, without any confounding effects of co-evolutionary adaptation. Sequencing of key genes involved in host-parasite interactions will help to identify the genetic basis of life history evolution. I predict the evolution of slower adsorption rates, later lysis times and smaller burst sizes in populations from structured than non-structured environments. I expect to see mutations on genes associated with host-parasite interactions in all treatments, but different identities of mutations in structured than non-structured treatments.

## Methods

### Media

Media used were standard King's B (KB) growth medium supplemented with the gelling agent Pluronic F-127. Pluronic F-127 (henceforth: Pluronic) is a non-toxic block copolymer of polypropylene oxide and ethylene oxide which is soluble at low temperatures but forms a stable gel at temperatures above 10°C (Gardener & Jones 1984). 16% Pluronic solutions are roughly equivalent to 0.6% semi-solid agar, a commonly used concentration in microbiology, which is known to allow movement of microbes through the medium, but at a reduced rate compared to liquid media. The advantage of using Pluronic rather than agar is that it forms a stable gel at 28°C, but liquefies quickly when placed on ice, allowing the recovery and transfer of live heat-sensitive virions from one structured solution to the next.

## Selection experiment

Six replicate populations were initiated in each of five levels of structure: 0 (liquid), 2, 4, 8 and 16% Pluronic (total 30 microcosms). Each of these were inoculated with 60  $\mu\text{l}$  saturated overnight culture of *P. fluorescens* SBW25 ( $\sim 10^7$  cells  $\text{ml}^{-1}$ ) and 6  $\mu\text{l}$  ancestral phage stock ( $10^{11}$  virions  $\text{ml}^{-1}$ ). After incubation standing statically at 28°C for 48 hours, structure was destroyed by placing cultures on ice, and a 1 ml sample filter sterilised to remove host cells. 60  $\mu\text{l}$  phage filtrate was transferred to a fresh microcosm with the same concentration of Pluronic and 60  $\mu\text{l}$  fresh saturated *P. fluorescens* culture. This regime was continued for 20 48 hour serial transfers (c. 130 bacterial generations).

## Population densities

At every 2<sup>nd</sup> transfer, cultures were sampled and filter sterilised. Filtrates were spot-plated for phage titration and aliquots frozen at -80°C. Bacteria were discarded.

## Phage life history

Filter-sterilised samples of phage populations from the 0% and 16% Pluronic treatments were taken at the end of the selection experiment and assayed for life history traits. Due to the low densities of phage in evolved populations and initial assay issues, some samples at transfer 20 were exhausted before reliable life history estimates could be made. Therefore, all final assays were conducted on samples from transfer 18.

### *Phage amplification*

Each population (transfer 18) first underwent a round of phage amplification. Phage suspensions were serially diluted; 100  $\mu$ l mixed with 100  $\mu$ l saturated *P. fluorescens* culture ( $\sim 10^7$  cells  $\text{ml}^{-1}$ ) in 6 ml 0.6% KB agar and poured onto a standard 1.2% KB agar plate as a semi-solid overlay. After overnight growth inverted at 28°C, the plates exhibiting semi-confluent lysis were flooded with 6 ml KB liquid medium and phage allowed to adsorb for  $\sim 1$  hour. The supernatant was then collected into a sterile 30 ml glass universal, and the semi-solid agar layer scraped into the same universal. 1% (v/v) chloroform was added and the mixture incubated at room temperature for  $\sim 1$  hour. The mixture was then filter-sterilised and the filtrate spot-plated for titration and stored in aliquots of 1 ml at -80°C as high-titre phage suspension.

### *Growth curves*

33 replicate microcosms were initiated with 100  $\mu$ l saturated *P. fluorescens* culture ( $\sim 10^7$  cells  $\text{ml}^{-1}$ ) in 6 ml KB liquid medium in sterile 30 ml glass universals. These microcosms were incubated shaken at 180 rpm at 28°C. At mid-log host growth (3.5 hours after initiation), microcosms were inoculated with phage suspension at a multiplicity of infection (MOI) of 0.001. Immediately after inoculation and every 8 minutes for 80 minutes, 3 replicate microcosms were selected at random, sampled and removed. A 1 ml sample was taken and immediately filter sterilised to prevent further growth. At the end of the assay, all samples were spot-plated for titration. A one-step growth curve was obtained for each evolved phage population and used to calculate life history values.

For each phage growth curve, a generalised additive model (GAM) was fitted to  $\log_{10}$  PFU ml<sup>-1</sup> against smoothed time and used to predict values to fit a smoothed curve to the data.

### *Lysis time*

Lysis time was calculated as the point of inflection during the exponential growth period, which equates to 50% of infected cells lysed.

### *Burst size*

Burst size was calculated as  $\frac{P_{max}}{P_{ads}}$  where  $P_{max}$  is the maximum free phage following burst, and  $P_{ads}$  is the number of adsorbed phage, obtained by calculating  $P_0 - P_{min}$  where  $P_0$  is free phage at time 0, and  $P_{min}$  is free phage following adsorption, immediately before the exponential growth period.

### *Adsorption rate*

24 replicate microcosms were initiated with 100 µl saturated ( $\sim 10^7$  cells ml<sup>-1</sup>) *P. fluorescens* culture in 6 ml KB liquid medium in sterile 30 ml glass universals. These microcosms were incubated shaken at 180 rpm at 28°C. At mid-log host growth (3.5 hours after initiation), microcosms were inoculated with phage suspension at an MOI of 0.001. Immediately after inoculation and at 3, 6, 10, 15, 20, 25 and 30 minutes, 3 replicate microcosms were selected at random, sampled and removed. A 1 ml sample was taken and immediately filter sterilised. At the end of the assay, all samples were spot-plated for titration. Adsorption rate was calculated as (adapted from Shao & Wang 2008):

$$r = \frac{\mu \ln(P_t/P_0)}{-(e^{\mu t} - 1)N_0} \quad \text{where } P_t \text{ is free phage density at 30 minutes, } P_0 \text{ and}$$

$N_0$  are phage and bacterial density at time 0, respectively,  $\mu$  is bacterial growth rate and  $r$  is the rate to be measured.

### *Principal components analysis*

As life history strategies are made up of combinations of life history trait values rather than any individual trait in isolation, a principal components analysis was conducted on lysis time, burst size and adsorption rate to assess covariance and look for groupings by strategy.

### **Sequence analysis**

At the end of the experiment (Transfer 18), filter-sterilised  $\Phi 2$  populations were Sanger sequenced (Applied Biosystems: ABI PRISM 3130xl Genetic Analyzer) for 5 genes believed to be important in interactions with the host and a control (Table 2.1). These genes are those identified in Paterson et al. (2010) as most rapidly evolving divergence in  $\Phi 2$  under co-evolution with *P. fluorescens*. As these genes diverged during antagonistic interactions with the host, they are predicted to be involved in controlling phenotypes associated with the host-associated infection and virulence traits such as adsorption rate, lysis time and burst size. The full sequencing protocol is outlined in appendix II. Genes were assembled and aligned using Geneious R7 (created by Biomatters. Available from <http://www.geneious.com/>). Fixed mutations were identified as single clear peaks that differed from the reference genome in both the forward and

**Table 2.1.** Genes Sanger sequenced in all evolved populations and the ancestor. Genes *SBWP25\_0027* - *0036* are those previously identified by Paterson et al. (2010) as rapidly evolving divergence in co-evolution with the host. Gene *SBWP25\_0040* was included as a control.

Gene	Function
SBWP25_0027*	Predicted virion structural protein
SBWP25_0032*	Tail tubular protein
SBWP25_0034*	Predicted lysozyme
SBWP25_0035*	Internal virion structural protein
SBWP25_0036*	Predicted tail fibre protein
SBWP25_0040	Predicted phage lysozyme

reverse sequences (NCBI accession number NC\_012660). Polymorphisms were identified as overlapping double high peaks that occurred in both the forward and reverse sequences. Euclidean distances were calculated in R statistical package (R Core Team 2013) based on binary data of base differences from the ancestor. At each position where a particular base mutation occurred in at least one population, all populations were given a score of 1 if they carried that particular base, 0 if they carried the ancestral base or 0.5 if there was a polymorphism of ancestral and mutant bases. Where two different base mutations occurred between populations at any particular position, that position was scored twice. A neighbour-joining tree of genetic distances between the populations was constructed and rooted by the ancestor.

## Statistical analysis

All statistical analyses were conducted in R statistical package (R Core Team 2013). Life history traits and mutation events were analysed using standard ANOVAs of trait by treatment, correlations between traits were analysed using Pearson's product moment correlations and variance in life history traits was analysed using Bartlett's tests of homogeneity of variances between treatments.

## Results

### Phage densities

The density of phage in evolving populations at five levels of structure with a static host was recorded at every second 48h transfer by spot plating filter-sterilised samples. In all structure treatments except the highest level of structure (16%), phage density increased rapidly at the beginning of the experiment, and remained constantly high in all populations throughout the selection experiment, with some fluctuation in the 8% Pluronic treatment (Fig. 2.1). At 16% Pluronic, phage density trajectories were more variable, with some populations showing an initial decline in density followed by a recovery. One population declined to extinction within the first few transfers and has been excluded from analysis. All remaining populations (n=5) at 16% had a hump-shaped density trajectory over time, rising to a peak density between transfers 8-12 and declining towards the end of the experiment.

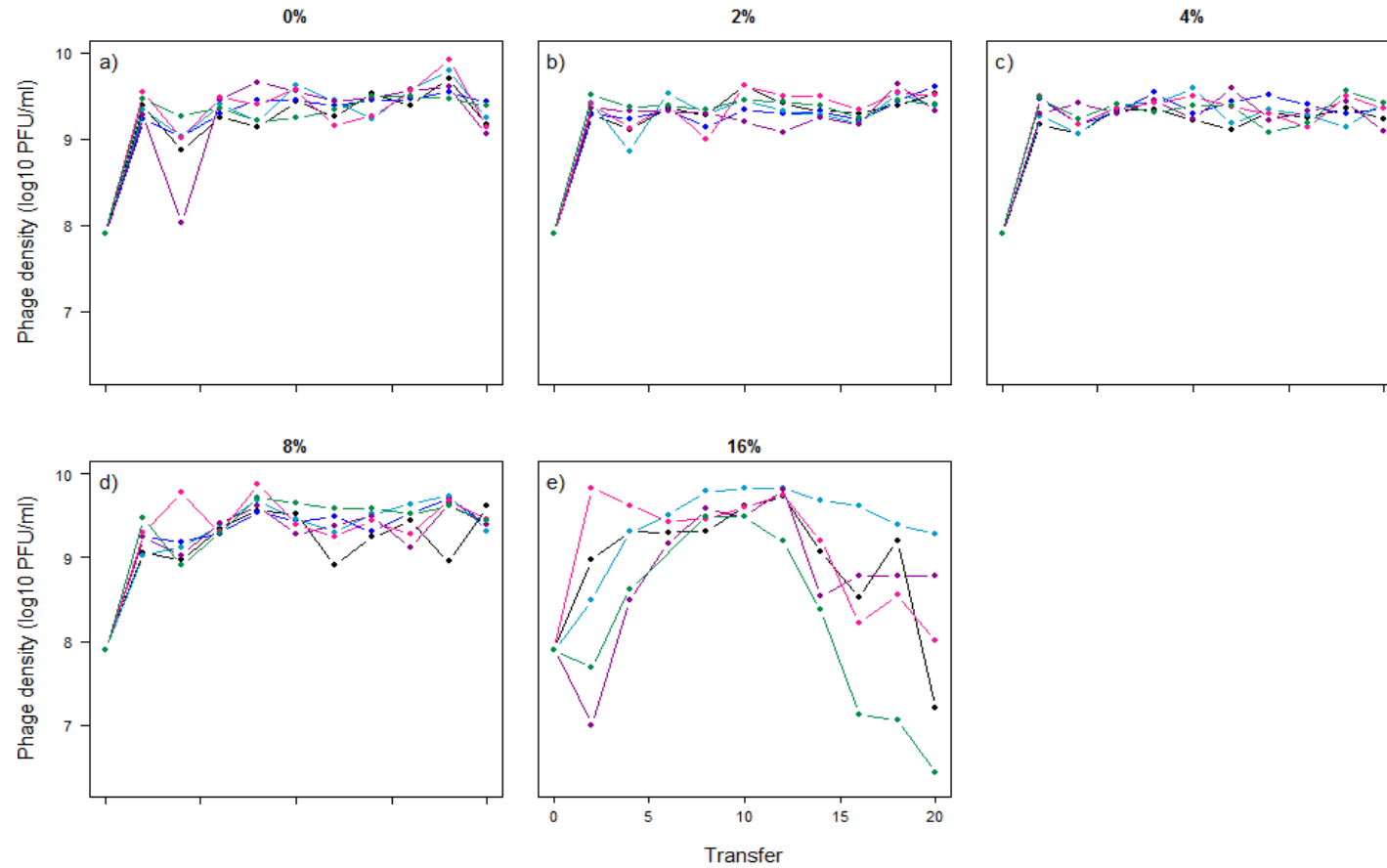


**Figure 2.1.** Phage density measured every second transfer throughout the selection experiment. Colours represent individual populations from 6 replicate populations in each structure treatment: 0 (a), 2 (b), 4 (c), 8 (d) and 16% (e) Pluronic. Phage density was significantly lower in high structure 16% Pluronic treatment at the end of the experiment (transfer 20) than in other treatments (ANOVA;  $F = 10.96$ , d.f. = 4, 24,  $p < 0.001$ )

End densities (transfer 18) were significantly lower at 16% Pluronic (ANOVA;  $F = 10.96$ , d.f. = 4, 24,  $p < 0.001$ ), with no significant difference in variance of end densities between replicate populations (Bartlett test of homogeneity of variances;  $K^2 = 0.7025$ , d.f. = 4,  $p = 0.951$ ).

0% (no structure) and 16% (high structure) treatments were chosen for further analysis as the extremes of the selection conditions, which would be most likely to elucidate the effects of spatial structure on life history evolution. Intermediate structure treatments were excluded in order to reduce the time and expense needed for analysis.

### Phage life history

Samples of filter-sterilised phage populations from the end of the selection experiment (transfer 18) were assayed for life history traits adsorption rate, lysis time and burst size. Adsorption rate was significantly slower in both treatments than the ancestor (Fig. 2.2.a. ANOVA;  $F = 6.6$ , d.f. = 2,8,  $p = 0.02$ . Post-hoc Tukey comparisons; Ancestor-16%: difference =  $7.4 \times 10^{-9}$ ,  $p < 0.001$ , Ancestor-0%: difference =  $7.25 \times 10^{-9}$ ,  $p < 0.001$ ), but not significantly different between high and no structure treatments (ANOVA;  $F = 0.41$ , d.f. = 1,9,  $p = 0.54$ ). There was also no significant difference in variance of adsorption rate between the two treatments (Bartlett test of homogeneity of variances;  $K^2 = 1.255$ , d.f. = 1,  $p = 0.263$ ).

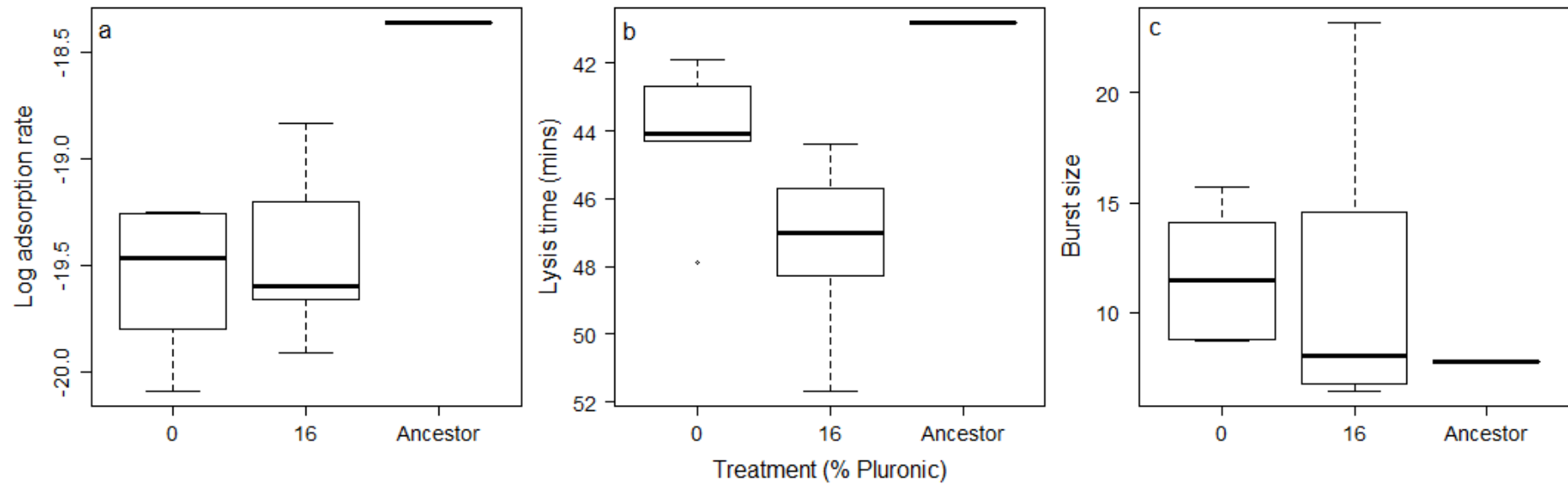


**Figure 2.2.** Life history box and whisker plots of evolved (transfer 18) populations from 0% (n=6) and 16% (n=5) Pluronic treatments, and the ancestor (n=1). Boxes display the median and interquartile range, and whiskers display the maximum and minimum values of the traits. Panel a shows adsorption rate, which was significantly slower in both treatments than the ancestor (ANOVA;  $F = 6.6$ , d.f. = 2,8,  $p = 0.02$ ), but not significantly different between 0% and 16% Pluronic treatments (ANOVA;  $F = 0.41$ , d.f. = 1,9,  $p = 0.54$ ). Panel b shows lysis time, which was significantly later in the 16% Pluronic treatment than 0% (ANOVA;  $F = 4.94$ , d.f. = 1,9,  $p = 0.05$ ) and the ancestor (ANOVA;  $F = 6.1$ , d.f. = 2,8,  $p = 0.042$ ). Panel c shows burst size, which was not different from the ancestor in either treatment (ANOVA;  $F = 1.56$ , d.f. = 2,8,  $p = 0.27$ ), nor significantly different between 0% and 16% Pluronic treatments (ANOVA;  $F = 8 \times 10^{-4}$ , d.f. = 1,9,  $p = 0.07$ )

Lysis time was significantly later than the ancestor in evolved populations from the 16% Pluronic high structure treatment, but not the 0% Pluronic no structure treatment (Fig. 2.2.b. ANOVA;  $F = 6.1$ , d.f. = 2,8,  $p = 0.025$ . Post-hoc Tukey comparisons; Ancestor-16%: difference = -0.55,  $p = 0.042$ , Ancestor-0%: difference = -0.26,  $p = 0.37$ ). Lysis time was also significantly later in evolved populations from the 16% Pluronic high structure treatment compared to the 0% Pluronic no structure treatment (ANOVA;  $F = 4.94$ , d.f. = 1,9,  $p = 0.05$ ). There was no significant difference in variance of lysis time between the two treatments (Bartlett test of homogeneity of variances;  $K^2 = 0.3752$ , d.f. = 1,  $p = 0.54$ ).

There was no significant difference in burst size between evolved populations from either treatment and the ancestor (Fig. 2.2.c. ANOVA;  $F = 1.56$ , d.f. = 2,8,  $p = 0.27$ ), or between evolved populations from each treatment (ANOVA;  $F = 8 \times 10^{-4}$ , d.f. = 1,9,  $p = 0.98$ ). There was no significant difference in variance of burst size between the two treatments (Bartlett test of homogeneity of variances;  $K^2 = 3.2053$ , d.f. = 1,  $p = 0.073$ ).

## Correlation analysis

Correlations between pairs of traits were sought in order to elucidate trade-offs. Lysis time and adsorption rate were significantly correlated with each other in 0% Pluronic no structure populations (Fig. 2.3. Pearson's product-moment correlation;  $t = -3.7$ , d.f. = 4,  $p = 0.02$ ), but not in 16% Pluronic high structure populations (Fig. 2.3. Pearson's product-moment correlation;  $t = -0.37$ , d.f. = 3,  $p$

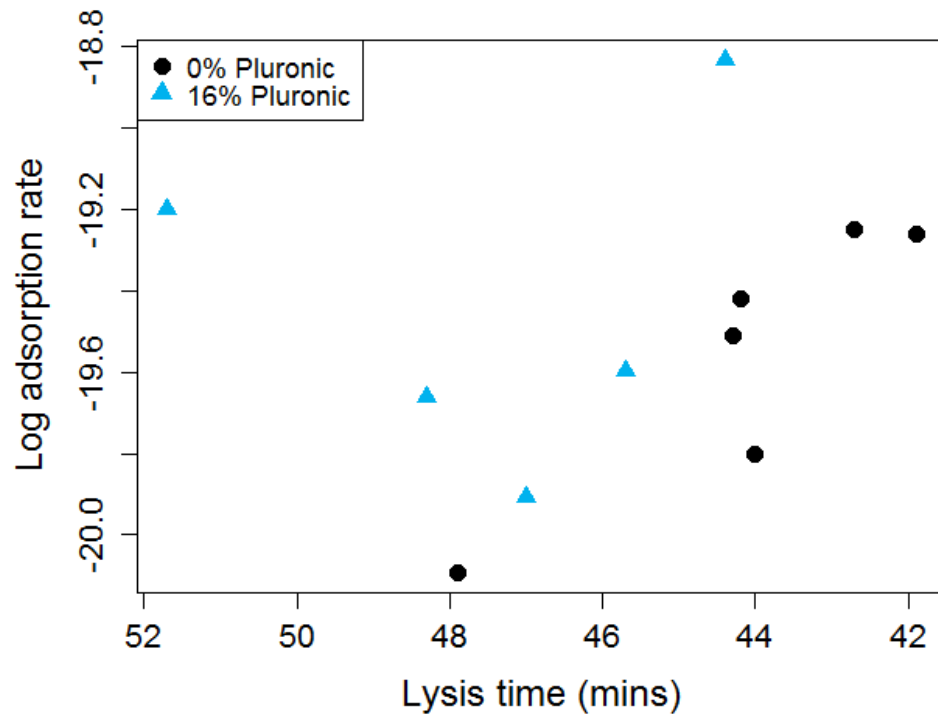


**Figure 2.3.** Correlation between adsorption rate and lysis time in evolved (transfer 18) populations from 0% (n=6, black circles) and 16% (n=5, blue triangles) Pluronic treatments. Lysis time and adsorption rate were significantly correlated at 0% Pluronic (Pearson's product-moment correlation;  $t = -3.7$ , d.f. = 4,  $p = 0.02$ ), but not at 16% Pluronic (Pearson's product-moment correlation;  $t = -0.37$ , d.f. = 3,  $p = 0.74$ ), nor across both treatments combined (Pearson's product-moment correlation;  $t = -0.54$ , d.f. = 9,  $p = 0.6$ ).

= 0.74), nor across both treatments combined (Fig. 2.3. Pearson's product-moment correlation;  $t = -0.54$ , d.f. = 9,  $p = 0.6$ ). There were no other significant correlations between life history traits in either treatment nor overall (data not shown).

In order to investigate holistic life history strategies among these key traits, covariance was analysed using principle components analysis. The principal components analysis explained all of the variation in the data in principal components 1 (79%) and 2 (21%). PC1 was associated with burst size, while

PC2 was associated with lysis time (Fig. 2.4.a). There was some indication of groupings by treatment (Fig. 2.4.b), although these groupings may overlap. These postulated groupings suggest the emergence of divergent life history strategies both between the two treatments, and between populations within the high structure treatment (16% Pluronic).

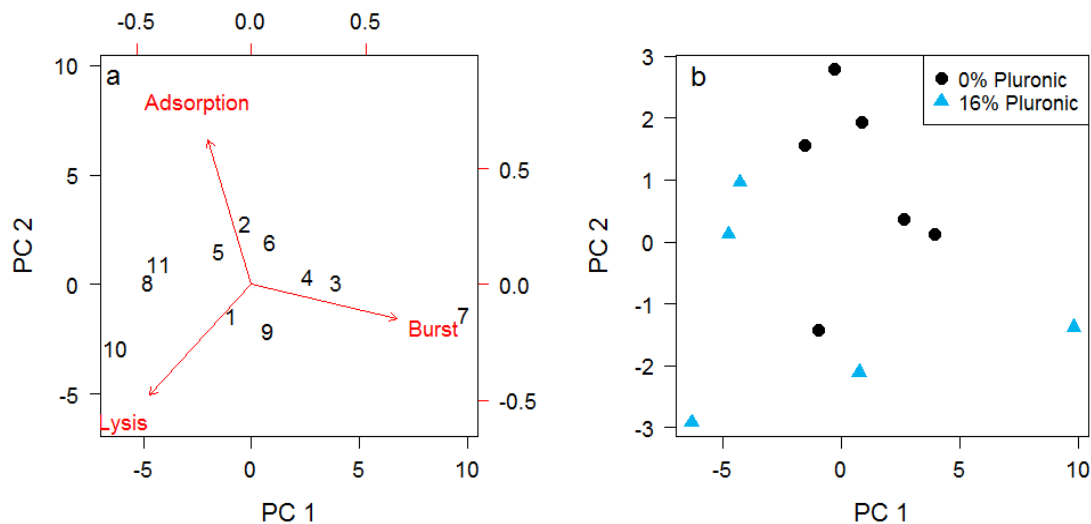


**Figure 2.4.** Principal components analysis. Panel a is the loadings biplot showing the principal component scores of the individual populations (lower x axis = PC1, left y axis = PC2), and the relative loadings of the life history variables (red arrows, upper x and right y axes). Numbers correspond to individual populations. Panel b is the traits biplot, which shows the location of each population from the 0% (n=6, black circles) and 16% (n=5, blue triangles) Pluronic treatments in trait space according to principal components scores on PC1 and PC2.

## Phage evolution

Evolved phage populations were Sanger sequenced at the end of the selection experiment (transfer 18) in 5 genes believed to be important in controlling interactions with the host, and a control (see table 2.1). Sequences analysed from all populations were identical to the ancestor in all but one of the genes investigated. Mutations on gene *SBWP25\_0036*, which encodes for the tail fibre protein, are identified in table 2.2. There was no significant difference in the number of mutational events between 0% Pluronic no structure (range = 2-3, mean = 2.5 mutations) and 16% Pluronic high structure (range = 2-4, mean = 2.6 mutations) treatments (Fig. 2.5. ANOVA;  $F = 0.05$ , d.f. = 1,9,  $p = 0.82$ ), and there was no significant difference in the variance between

**Table 2.2.** The locations and identities of mutations on gene *SBWP25\_0036* in the evolved (transfer 18) populations. Positions (in base pairs from the start of the gene) are indicated at the top of the table, and the mutations found at that position (base differences from the ancestor) are identified at the bottom of the table. Rows correspond to individual populations. + indicates the presence of the identified mutation in the population, and = indicates the presence of the identified polymorphism.

Gene	SBWP25_0036										
Position	281	290	928	992	995	1204	1291	1433	1435	1562	1675
0% Pluronic:											
1	-	-	-	=	=	-	-	-	-	-	+
2	-	-	-	-	+	-	-	-	-	-	+
3	-	-	=	-	-	-	-	-	=	-	-
4	-	-	=	-	=	=	-	-	-	-	-
5	-	-	-	-	+	-	-	-	-	=	=
6	-	-	-	-	+	-	-	-	-	-	=
16% Pluronic:											
1	+	-	-	=	-	-	=	-	-	-	+
2	-	-	-	+	-	-	-	-	-	-	+
3	-	+	-	-	-	-	-	=	-	-	-
5	+	-	-	-	-	-	-	+	-	-	+
6	-	-	-	-	+	-	-	-	-	-	+
Type (+)	A-G	A-G		C-A	T-A			T-G			A-G
Poly (=)			M	M	W	R	R	K	M	M	R

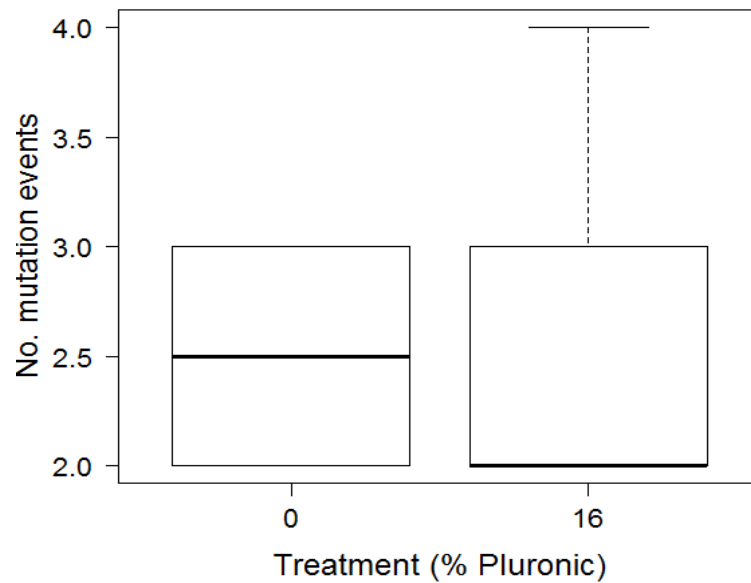


**Figure 2.5.** The number of mutations in gene *SBWP25\_0036* in 0% (n = 6) and 16% (n = 5) populations. Boxes display the median and interquartile range, and whiskers display the maximum and minimum values. There was no significant difference in the number of mutations between 0% and 16% Pluronic treatments (ANOVA;  $F = 0.05$ , d.f. = 1,9,  $p = 0.82$ ).

the two treatments (F-test of variance;  $F = 0.375$ , d.f. = 5,4,  $p = 0.31$ ). However, the frequency of mutations varied between treatments, and some mutations were found exclusively in one of the two treatments (Fig. 2.6). A neighbour-joining tree of Euclidean distances is displayed in figure 2.7. There were no distinct clusters by treatment. The longest branches were found in high structure populations, and the shortest branches were found in no structure populations.

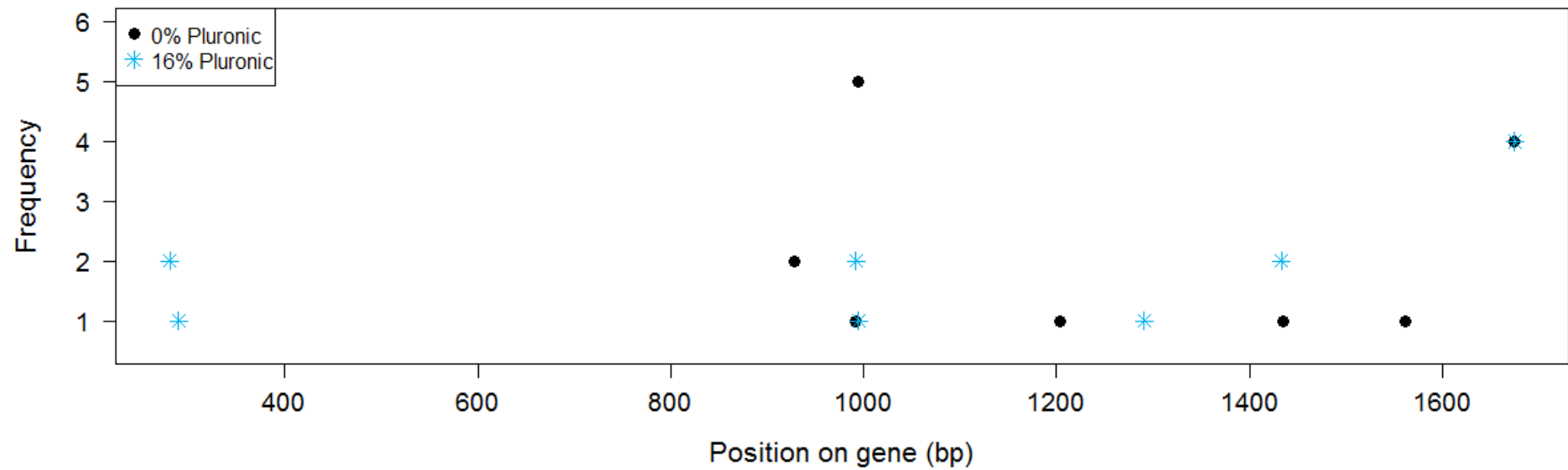


**Figure 2.6.** Frequency of each identified mutation in gene *SBWP25\_0036* in evolved (transfer 18) populations from 0% Pluronic low structure (n= 6, black circles) and 16% Pluronic high structure (n= 5, blue asterisks) populations. The x axis shows the bp position of mutations on the gene.

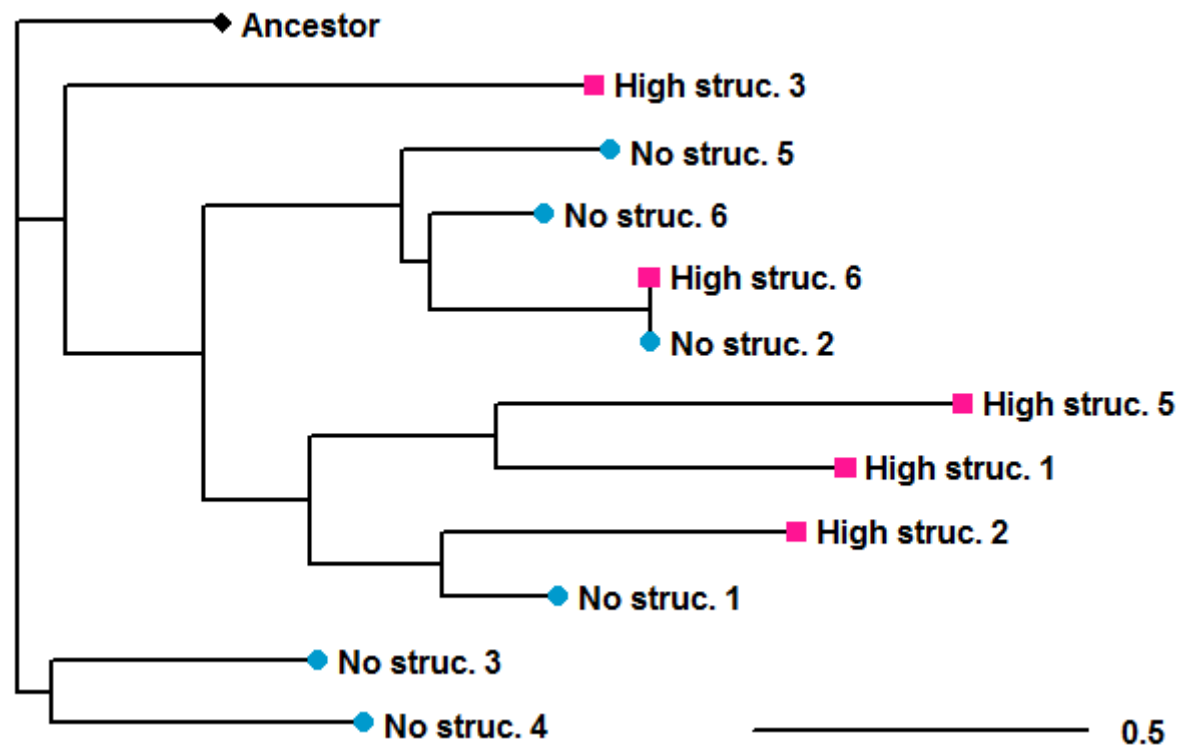


**Figure 2.7.** Neighbour-joining tree of pairwise Euclidean distances between 11 evolved (transfer 18) populations and the ancestor in gene *SBWP25\_0036*. Based on binary data of base substitutions from the ancestor, rooted by the ancestor (black diamond). 0% Pluronic populations are labelled No struc, blue circles. 16% Pluronic populations are labelled High struc, pink squares.

## Discussion

Parasite life history evolution in high and low spatial structure has been examined theoretically with life history theory and mathematical models, but few empirical studies have directly assessed life history evolution in spatially structured environments. My data suggest that increased spatial structure selects for later lysis as predicted by life history theory, but not slower adsorption or smaller burst size than at low structure. Although life history traits do not generally appear to be correlated with one another, there is some limited evidence for divergent life history strategies between populations evolved to high and low spatial structure. There was a lot of variation between populations in all traits in both spatial structure treatments, which indicates that life history evolution in phage  $\Phi 2$  may be more complex than suggested by life history theory and simple models.

Life history theory predicts that in non-structured environments, interactions are global and parasites with as short a reproductive cycle as possible will be favoured, particularly when they also produce large numbers of progeny. Conversely, in highly spatially structured environments, interactions become localised. Parasites should evolve longer reproductive cycles and produce fewer progeny with greater dispersal ability.

The evolution of a much slower adsorption rate in both treatments than the ancestor may indicate a general adaptation to experimental conditions rather than an adaptation to either treatment. It is worth noting that the no structure

treatment employed in this study, although liquid, was incubated statically rather than shaken. Shaking cultures is known to break up any structure caused by bacterial formations such as biofilms within the microcosms and is used in microbiology to ensure a homogeneous environment. Therefore, it may be the case that in each 48 hour growth period, sufficient bacterial structure formed to cause selection for a reduced adsorption rate. Static incubation of *P. fluorescens* encourages the formation of biofilms, which cause sufficient structure to promote adaptive radiation of bacterial morphology (Rainey & Travisano 1998), so reduced adsorption rate in my no-structure treatment may in fact be an adaptation to low structure. Alternatively, the ancestral stock preparation may have by chance selected a genotype with an unusually fast adsorption rate, which was non-optimal in both environments, causing the evolution of reduced adsorption rate in both.

The evolution of later lysis in highly structured environments was consistent with theoretical predictions (Wild et al. 2009; Lion & Boots 2010). Later lysis allows time for the immigration of susceptible hosts into the local patch and diffusion of kin before burst, increasing the likelihood of progeny encountering a susceptible host, and decreasing the risk of kin shading.

Burst size did not differ between structure treatments nor deviate significantly from the ancestor in either treatment. Failure to map the pattern seen in lysis time is inconsistent with the idea that virions are assembled at a given rate and burst size is therefore dependent on lysis time, as is often assumed in the literature (Abedon & Yin 2009; Goldhill & Turner 2014). The large variation

seen in burst size between populations at high structure suggests that there may be more than one life history strategy emerging in high structure populations. The principal components analysis suggests two or more separate strategies may be in operation in the high structure treatment, with points forming two distinct groups, which may be divisible into further groups, although the boundaries of these further divisions are not well defined. With no correlations between traits at high structure it is difficult to define the strategies in play. The interrelationships between traits are complex, and likely to be strongly influenced by the first slight deviations from the ancestral state. Abedon & Culler (2007) highlight the importance of initial trait values on the influence of changes in these trait values on phage movement in semi-solid agar. When adsorption rate is high, a decrease in latent period (earlier lysis) will improve the diffusion of phage, although latent period length becomes less important if burst sizes are large and as adsorption rate decreases. Similarly, increases in burst size will improve phage diffusion ability, but only when burst sizes are initially small. An increase in adsorption rate will improve diffusion when adsorption rate is very slow, but have a negative effect on diffusion when adsorption rate is already fast. Any initial differences in trait values between populations, therefore, may alter the adaptive trajectory. Kin and self-shading avoidance can be achieved by more than one adaptive route – individuals can either delay adsorption, delay lysis time or reduce burst size, or modify a combination of any of these traits to achieve similar fitness benefits. This study demonstrates that multiple strategies are both possible and viable.

Of the genes investigated, mutations were found only on gene *SBWP25\_0036*, which encodes for the tail fibre protein. There is no difference in the number of mutations between treatments, so these mutations are likely to be responsible only for the reduced adsorption rate in both treatments. No single mutation was identified in every population, so none can be directly attributed to reducing the adsorption rate, although the most common mutation in both treatments (at position 1675) is likely to have been an important step for many of the populations. It is conceivable that there are many mutational routes to slower adsorption rate, as this is predicted to be governed mainly by the length of tail fibres in  $\Phi 2$ . The shorter the tail fibres, the further the virions diffuse before encountering a cell within reach, so any mutations that reduce the length of tail fibres will reduce the rate of adsorption. The variation in the mutational pathways that lead to a reduced adsorption rate are likely to be responsible for the large variation in adsorption rate between replicate populations in both treatments. It is perhaps surprising not to find mutations on the genes predicted to be important in lysis timing given the phenotypic adaptation observed. However, the measure of lysis time employed here encompasses both the adsorption time and the time spent reproducing within a cell, so it can be expected to vary with mutations in genes that determine adsorption rate also. Lysis time was indeed correlated with adsorption rate at no structure, but not at high structure, and we do not see the same pattern of reduced adsorption rate in high structure environments as we do with lysis. The relationship between genotype and phenotype is likely more complex than previously thought.

Mutations elsewhere on the genome that this study was not able to detect may have contributed to lysis time evolution through epistatic effects. Scanlan et al. (2011) studied the genetic basis of infectivity evolution in  $\Phi 2$  and also concluded that the relationship between genotype and phenotype is unclear and likely to involve epistasis between genes. Alternatively, lysis timing may be a relatively plastic trait, controlled by differential gene expression rather than mutational evolution.

The lack of genetic evolution and phenotypic differentiation between treatments in this study may be due to a lack of mutational input because phage evolved to a static ancestral host. It has been demonstrated by Paterson et al. (2010) that under co-evolution these genes evolve much faster than under evolution alone due to the Red Queen dynamics of infectivity and resistance evolution. In nature, phage will undoubtedly be co-evolving with their local hosts, so the extra mutational input provided by co-evolution may be a necessary driver of life-history evolution. Alternatively, mutation may have occurred elsewhere on the genome which this study was unable to detect. Further study with whole-genome sequencing is necessary to elucidate whether or not mutations in other genes interact with phage life history in spatially structured environments.

## Conclusions

This study was designed to assess whether the experimental evolution of bacteriophage in a spatially structured environment aligned with theoretical predictions, and identify the underlying genetic evolution behind phenotypic

adaptation. Lysis time evolved in the direction predicted by theory, but adsorption rate and burst size did not show any significant divergence between treatments. There is a suggestion of multiple life history strategies being employed, which indicates that parasite life history adaptation may be more complex than imagined by theory. There was little genetic evolution on the genes studied which indicates a lack of mutational input without co-evolution with the host. Mutations identified on the tail fibre gene do not directly explain the adaptation in lysis time, suggesting a more complex genotype-phenotype relationship with epistatic interactions, or a possible phenotypic plasticity. Further studies would benefit from whole genome sequencing to identify genetic influences, co-evolution with the host to boost evolutionary potential and larger numbers of replicate populations in order to tease out multiple strategies.

### 3. UV environmental stress

#### Introduction

Bacteriophage which naturally inhabit environments exposed to direct sunlight, such as leaf surfaces, soil surface and shallow marine environments, regularly encounter high levels of UV exposure. The effects of UV on the viability and death of phage and repair mechanisms have been extensively studied both in the lab and in the marine environment for over 70 years (Bernstein 1981), but the effects of UV stress on the evolution of phage life history remains to be investigated.

In the marine environment, DNA damage caused by UV-A and B in direct sunlight can cause significant deactivation and death of phage in depths of up to 60 m below the surface in clear waters (Suttle & Chen 1992). UV exposure is predicted to be the primary factor in the decay of phage viability in these marine systems, deactivating and killing more phage than all other phage-clearing mechanisms combined (Suttle & Chen 1992). Despite the extensive damage to phage caused by exposure to direct sunlight, phage numbers in nature remain high, outnumbering bacteria 3 to 10 times in natural water systems (Wommack et al. 1996). Wommack et al. (1996) suggested that as sunlight removes phage viability at a greater rate than it kills them, many of the phage present (as counted by electron microscope) are likely to be non-viable. Conversely,

Wilhelm et al. (1998) showed that most of the phage remained infective, indicating a significant amount of DNA damage repair occurring within host cells. Reactivation of phage infectivity within host cells by multiplicity reactivation (Luria 1947; Luria & Dulbecco 1949, later termed recombination reactivation), photo-reactivation (Dulbecco 1949; Dulbecco 1950) and excision (a.k.a dark repair, Luria 1950; Streisinger 1956) had already been discovered and documented in laboratory systems. However, the extent of these processes in natural communities was not realised until the experiments of Wilhelm et al. (1998), which suggested that up to 50% of damaged phage are reactivated in marine environments, and Kellogg & Paul (2002), where up to 100% reactivation was achieved in laboratory conditions.

The mechanisms of phage DNA repair are well documented for the T and  $\lambda$  phage (reviewed in Bernstein 1981), and comprise of both phage-encoded (primarily in large T4 phage) and host-encoded (particularly for the smaller  $\lambda$  phage) repair mechanisms. Phage  $\Phi$ 2 is a relatively small phage at ~43 Kbp, so it is likely that reactivation in this system is mainly governed by the host-encoded mechanisms of excision and photo-reactivation. Excision repair is a general bacterial response to DNA damage and involves the release of a multi-enzyme complex which works to remove lesions of various types from DNA (Kellogg & Paul 2002). Photo-reactivation is the light-dependent release of the enzyme photolyase, which specifically targets pyrimidine dimers (Kellogg & Paul 2002), the type of lesion commonly caused by UV (Wood et al. 1984).

The current literature on phage and UV is focused on the effects of UV on phage infectivity (Wood et al. 1984; Suttle & Chen 1992; Wommack et al. 1996) and the mechanisms and efficiency of repair (Cavilla & Johns 1964; Wilhelm et al. 1998; Dulbecco 1949; Dulbecco 1950; Ellison et al. 1960) in the short-term, the genetic basis of inactivation and reactivation (Harm 1963; Bernstein 1981), and the effects of UV-inactivation and reactivation on the composition of phage communities (Wilhelm et al. 1998; Wilhelm & Weinbauer 1998) and interference between phage (Bawden & Kleczkowski 1953). To my knowledge there have been no studies conducted to date on the effects of repeated exposure to UV on phage life history and host-parasite interactions on an evolutionary timescale. A general prediction for parasites in harsh environments is that adaptation to withstand environmental stress results in a trade-off with reproductive rate (Goldhill & Turner 2014). For example, across 16 phage families that infect *E. coli*, there is a robust negative correlation between reproduction and survival under heat stress, which is related to the density of their packaged DNA and capsid thickness (De Paepe & Taddei 2006). UV irradiation is another example of such an environmental stressor. Phage within a host cell at the time of exposure may be afforded some protection by the cell membrane, and will have the additional advantage of immediate reactivation by host-mediated responses when compared to their ex-host conspecifics. Additionally, phage with larger burst sizes may increase the chances of some of their offspring surviving UV irradiation whether they happen to be in-host or ex-host at the time of exposure.

The present study aims to measure the effects of regular exposure to lethal doses of UV on life history evolution in the *Pseudomonas fluorescens* phage  $\Phi 2$ , evolved against both a static ancestral host and a co-evolving host. Evolution against a static ancestral host allows us to observe phage adaptation to UV treatments without any confounding effects of co-evolution with the host, whilst co-evolution allows phage to evolve with the higher mutational input driven by co-evolutionary processes (Paterson et al. 2010), and with the benefit of host-mediated reactivation. I predict the evolution of faster adsorption, later lysis and larger burst sizes in populations regularly exposed to UV in both evolution and co-evolution treatments. The elevated mutation rates associated with both co-evolution and UV reactivation is predicted to result in a larger evolutionary potential, allowing phage in co-evolution treatments to evolve closer to an optimum life history strategy than their counterparts in evolution treatments. Alternatively, co-evolution could limit the evolution of UV resistance in phage. In experiments with the same study system (*Pseudomonas fluorescens* and phage  $\Phi 2$ ), Zhang & Buckling (2011) discovered that co-evolution with the host reduced the capacity of the phage to resist increasing temperatures. They concluded that the reduction in population size and accumulation of costly infectivity mutations caused by co-evolution contributed to the extinction of phage populations in their experiments.

## Methods

### Pilot

A pilot study was conducted in order to assess the doses of UV required for different mortality rates in phage  $\Phi 2$ . 24 replicate populations of *Pseudomonas fluorescens* were initiated in 6 ml KB media in 30 ml sterile glass universals, and incubated at 28°C, shaken at 180 rpm for 48 hours. 60  $\mu$ l each culture was then transferred into a fresh microcosm, inoculated with 6  $\mu$ l ancestral phage stock and incubated for a further 48 h to allow phage populations to establish. At 48 h, 3 replicate populations were assigned to each one of 8 UV treatments: 0, 15, 30, 60, 100, 150, 300 or 600 mJoules  $\text{cm}^2$ . 3 ml mixed culture (containing both intracellular and extracellular phage) from each microcosm was transferred to a sterile 50 mm diameter Petri dish and placed into a UV chamber (GS Gene Linker, BIO-RAD Laboratories). The lids of the Petri dishes were then removed and the mixed cultures exposed to the specified dose of UV-C (254 nm) by running the appropriate program. After treatment, the lids were replaced, the cultures removed from the cross-linker, and retained in the Petri dishes at room temperature until all mixed cultures had been exposed to their relevant dose of UV. 1 ml samples of each mixed culture were then filter-sterilised and spot-plated for phage titration. The log-linear survival curve was then used to predict the UV doses that would incur 50% (LD50), 75% (LD75) and 90% (LD90) death of free phage. The model predicts LD50 at 281 mJoules  $\text{cm}^2$ , LD75 at 563 mJoules  $\text{cm}^2$  and LD90 at 935 mJoules  $\text{cm}^2$  (Fig. 3.1).

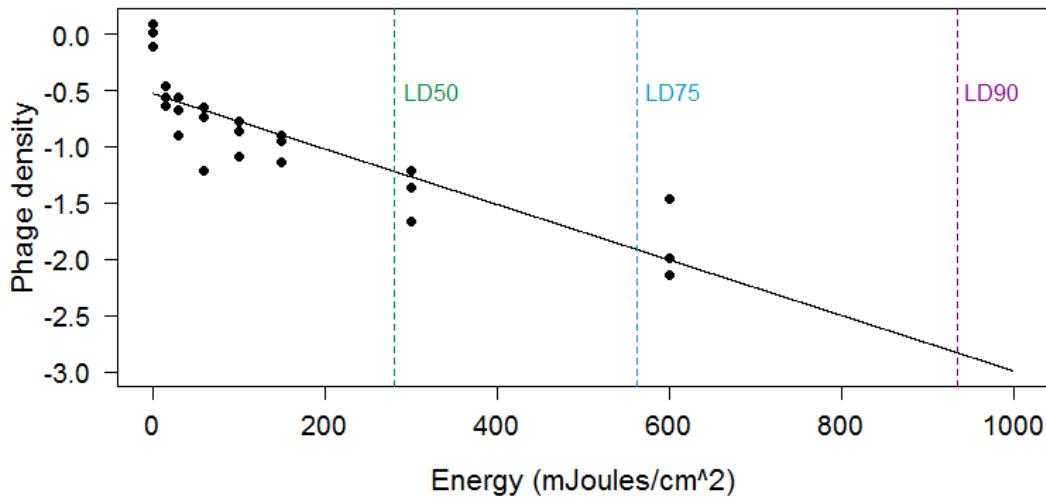


**Figure 3.1.** Pilot survival curve of log proportion of phage surviving different UV doses. Vertical lines indicate predicted doses for LD50 (green line), LD75 (blue line) and LD90 (purple line).

### Selection experiment

48 replicate populations of *Pseudomonas fluorescens* were initiated from 60  $\mu$ l saturated overnight cultures ( $\sim 10^7$  cells ml<sup>-1</sup>) in 6 ml KB in 30 ml sterile glass universals. Each population was inoculated with 6  $\mu$ l ancestral phage stock ( $10^{11}$  virions ml<sup>-1</sup>) and incubated at 28°C, shaken at 180 rpm. After 48 h growth, cultures were assigned to one of 2 evolution regimes: phage evolution only, where the host was removed after UV exposure and replaced with ancestral host at every transfer, or co-evolution with the host, where both host bacteria and phage were transferred after UV exposure and no host replacement took place. Populations under each evolution regime were additionally assigned to 4 UV treatments: LD0, LD50, LD75 or LD90 (0, 281, 563 and 935 mJoules cm<sup>2</sup>,

respectively). 6 replicate populations were assigned to each of the 8 treatment combinations. For irradiation, 3 ml of each mixed culture was transferred to a sterile 50 mm diameter Petri dish and placed into the UV chamber, without lids. These samples of whole culture, containing both phage particles and host cells, were then exposed to the appropriate dose of UV-C as described above. Populations assigned to the control LD0 treatment were transferred into a Petri dish as above, but not irradiated in the UV chamber. After all cultures had received their appropriate doses, for co-evolution treatments 60 µl mixed irradiated culture containing both phage virions and host cells was transferred to a fresh microcosm and incubated at 28°C, shaken at 180 rpm. For evolution treatments, 1 ml samples of mixed irradiated culture were filter-sterilised to remove host cells and 60 µl phage filtrate was transferred to a fresh microcosm, supplemented with 60 µl fresh ancestral saturated overnight non-irradiated culture of *P. fluorescens* and incubated at 28°C, shaken at 180 rpm. This regime was continued for 20 48 hour serial transfers (c. 130 bacterial generations). The order in which cultures received their dose was randomised to reduce the effects of any photo-reactivation that may have occurred in standing cultures.

### Population densities

At every 4<sup>th</sup> transfer, samples of each population were filter-sterilised and spot-plated for phage titration before UV dosing, and in co-evolution treatments bacterial populations were also plated from unfiltered samples for density determination. Aliquots of phage filtrate from all populations were stored at

-80°C, and aliquots of unfiltered culture from co-evolution treatments were frozen with 20% glycerol at -80°C.

### Phage life history

Filter-sterilised samples of phage populations from the LD0 and LD90 treatments were taken at the end of the selection experiment (transfer 20), amplified and assayed for life history traits following the methods described in chapter 2.

### Life history strategies

As life history strategies are made up of combinations of life history trait values rather than any individual trait in isolation, a principal components analysis was conducted on lysis time, burst size and adsorption rate to assess covariance and look for groupings by strategy.

### Sequence analysis

At the end of the experiment (Transfer 20), filter-sterilised  $\Phi$ 2 populations were Sanger sequenced (Applied Biosystems: ABI PRISM 3130xl Genetic Analyzer) for 5 genes believed to be important in interactions with the host and a control (Table 2.1, chapter 2). Genes were assembled and aligned using Geneious R7 (created by Biomatters. Available from <http://www.geneious.com/>).

Euclidean distances were calculated in R statistical package (R Core Team 2013) based on binary data of base differences from the ancestor. At each position where a particular base mutation occurred in at least one population, all

populations were given a score of 1 if they carried that particular base, 0 if they carried the ancestral base or 0.5 if there was a polymorphism of ancestral and mutant bases. Where two different base mutations occurred between populations at any particular position, that position was scored twice. A neighbour-joining tree of genetic distances between the populations was constructed and rooted by the ancestor.

## Statistical analysis

All statistical analyses were conducted in R statistical package (R Core Team 2013). Life history traits and mutation events were analysed using standard ANOVAs of trait by treatment, correlations between traits were analysed using Pearson's product moment correlations and variance in life history traits was analysed using an F-test of variance by treatment.

## Results

### Phage & bacterial densities

Phage density in evolving and co-evolving populations from the four UV treatments were measured at every fourth 48h transfer by spot-plating filter-sterilised samples. Bacterial density was also measured in co-evolving populations at every fourth transfer by plating unfiltered samples. There was no significant effect of UV on phage end-point (transfer 20) density (Fig. 3.2. ANOVA;  $F = 1.678$ , d.f. = 3, 40,  $p = 0.187$ ) or variance in phage end-point density (Bartlett test of homogeneity of variances:  $K^2 = 5.98$ , d.f. = 3,  $p = 0.113$ ), nor

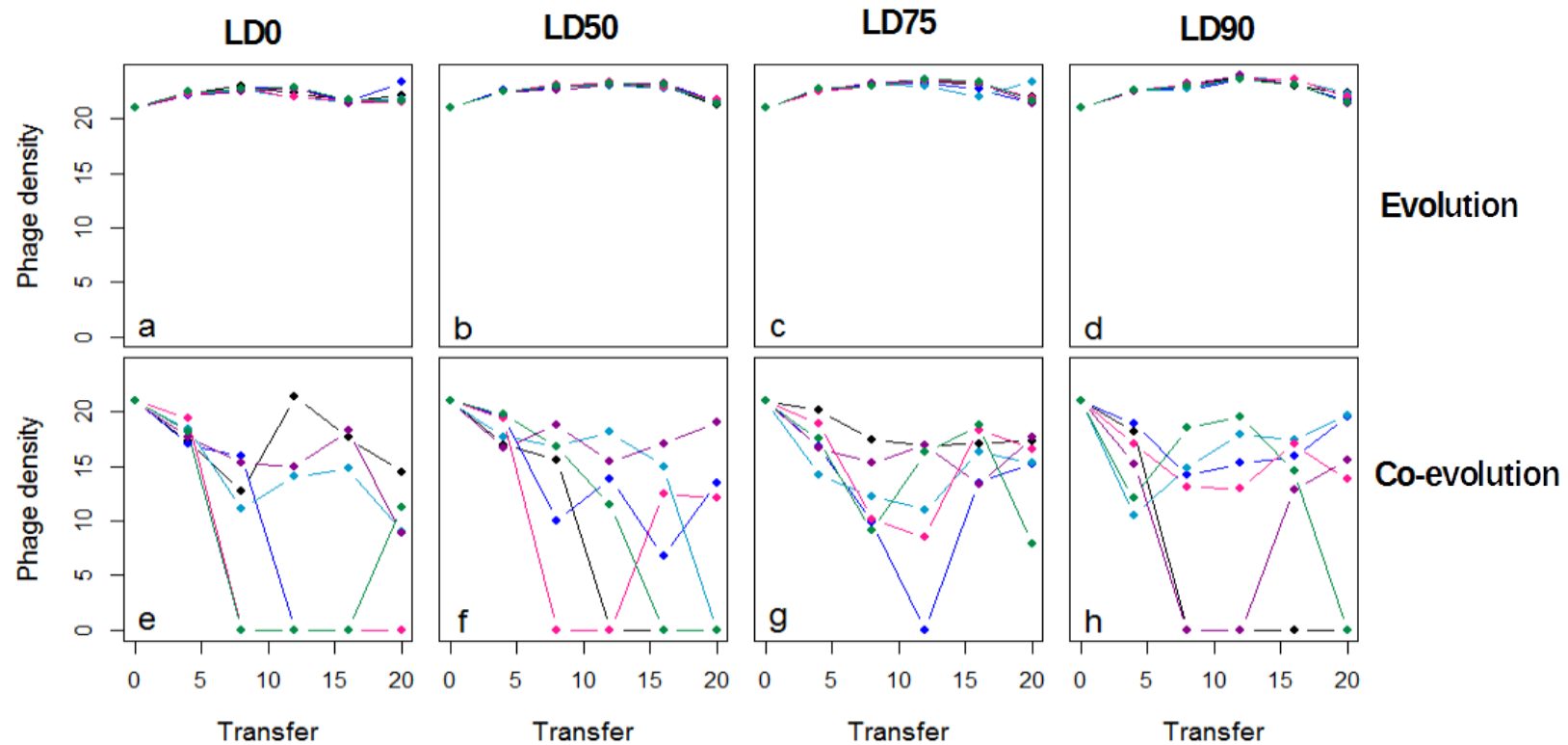


**Figure 3.2.** Log<sub>10</sub> Phage density measured every fourth transfer throughout the selection experiment in 6 replicate populations of each treatment. Panels a-d show phage density from evolving populations at 0 (a), 50 (b), 75 (c) and 90% (d) mortality UV treatments. Panels e-h show phage density from co-evolving populations at 0 (e), 50 (f), 75 (g) and 90% (h) mortality UV treatments. Colours represent individual replicate populations. There was no significant effect of UV on phage end-point (transfer 20) density (ANOVA;  $F = 1.678$ , d.f. = 3, 40,  $p = 0.187$ ). Phage densities were lower (ANOVA;  $F = 62.21$ , d.f. = 1, 40,  $p < 0.001$ ) and displayed more variance in co-evolution than evolution treatments (Bartlett test of homogeneity of variances:  $K^2 = 85.59$ , d.f. = 1,  $p < 0.001$ ).

bacterial end-point density (Fig. 3.3. ANOVA;  $F = 2.185$ , d.f. = 3, 19,  $p = 0.123$ ) or variance in bacterial end-point density (Bartlett test of homogeneity of variances:  $K^2 = 2.136$ , d.f. = 3,  $p = 0.545$ ). Phage densities were lower (Fig. 3.2. ANOVA;  $F = 62.21$ , d.f. = 1, 40,  $p < 0.001$ ) and displayed more variance in co-evolution than evolution treatments (Bartlett test of homogeneity of variances:  $K^2 = 85.59$ , d.f. = 1,  $p < 0.001$ ).

LD0 and LD90 treatments were chosen for further analysis as the extremes of the selection conditions, which would be most likely to elucidate the effects of UV stress on life history evolution. LD50 and LD75 treatments were excluded in order to reduce the time and expense needed for analysis.

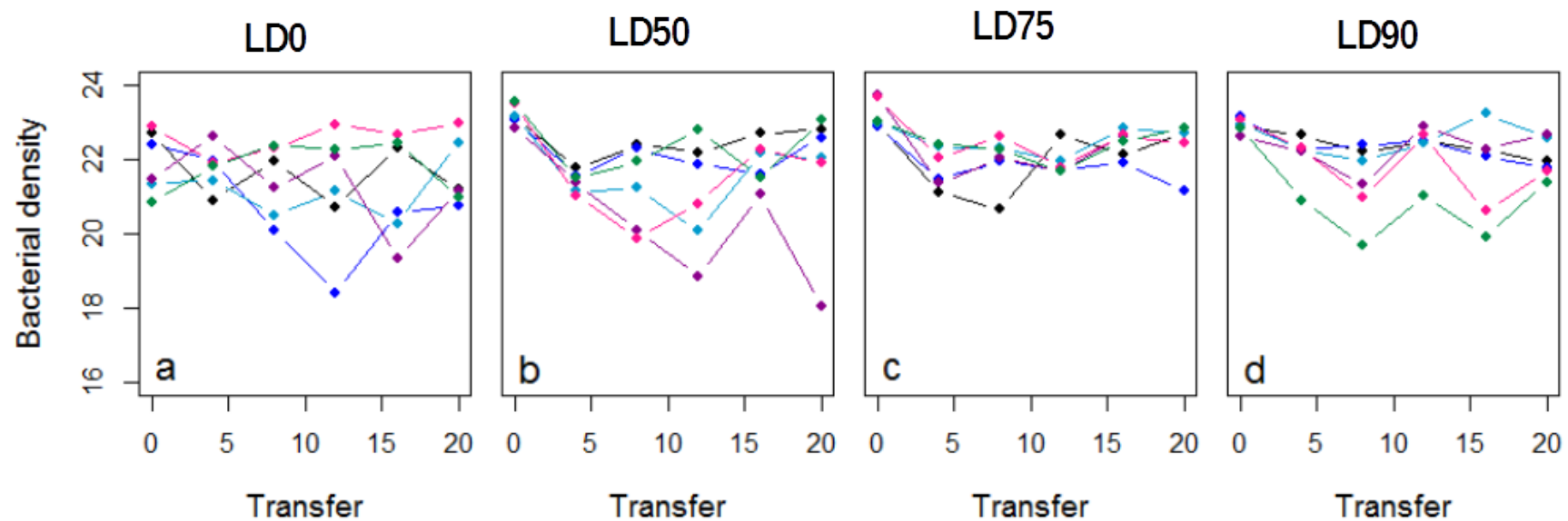


**Figure 3.3.**  $\text{Log}_{10}$  Bacterial density measured every fourth transfer throughout the selection experiment in 6 replicate populations of each treatment. Panels show bacterial density from co-evolving populations at 0 (a), 50 (b), 75 (c) and 90% (d) mortality UV treatments. Colours represent individual replicate populations. There was no significant effect of UV on bacterial end-point (transfer 20) density (ANOVA;  $F = 2.185$ , d.f. = 3, 19,  $p = 0.123$ )

## Phage life history

Samples of filter-sterilised phage populations from the end of the selection experiment (transfer 20) were assayed for life history traits adsorption rate, lysis time and burst size. Five of the co-evolution populations failed to amplify and are excluded from the rest of the analysis. From this point the levels of replication are: co-evolution & UV LD0  $n = 3$ , co-evolution & UV LD90  $n = 4$ , evolution & UV LD0  $n = 6$ , evolution & UV LD90  $n = 6$ .

There was no significant effect of UV dose on adsorption rate (Fig. 3.4.a. ANOVA;  $F = 0.696$ , d.f. = 1, 15,  $p = 0.417$ ). Adsorption rate was significantly slower in co-evolved than evolved populations (ANOVA;  $F = 63.16$ , d.f. = 1, 15,  $p < 0.0001$ ), and this effect was independent of UV dose (ANOVA; EVOLUTION  $\times$  UV:  $F = 0.709$ , d.f. = 1, 15,  $p = 0.413$ ). There was no significant difference in variance of adsorption rate between UV treatments (Levene's test for homogeneity of variance:  $F = 0.3$ , d.f. = 3, 15,  $p = 0.83$ ).

There was no significant effect of UV dose on lysis time (Fig. 3.4.c. ANOVA;  $F = 0.497$ , d.f. = 1, 15,  $p = 0.492$ ). There was a non-significant trend towards slower lysis in co-evolved than evolved populations (ANOVA;  $F = 3.39$ , d.f. = 1, 15,  $p = 0.085$ ), and this effect was independent of UV dose (ANOVA; EVOLUTION  $\times$  UV:  $F = 0.145$ , d.f. = 1, 15,  $p = 0.709$ ). There was a non-significant trend towards greater variance in lysis timing in populations from the coevolution-LD90 group than any other treatment (Levene's test for homogeneity of variance:  $F = 2.29$ , d.f. = 3, 15,  $p = 0.12$ ).

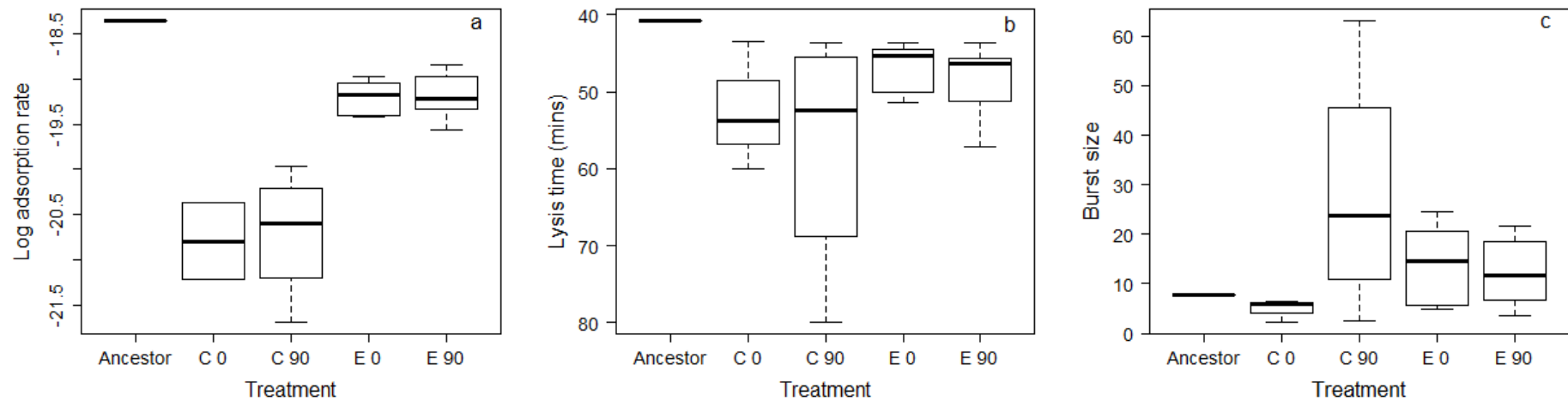


**Figure 3.4.** Life history box and whisker plots of evolved (transfer 20) phage populations from 0% (Evolved (E)  $n=6$ , co-evolved (C)  $n=3$ ) and 90% (Evolved  $n=6$ , co-evolved  $n=4$ ) mortality UV treatments and the ancestor ( $n=1$ ). Boxes display the median and interquartile range, and whiskers display the maximum and minimum values of the traits. Panel a shows adsorption rate, which was not affected by UV treatment (ANOVA;  $F = 0.696$ , d.f. = 1, 15,  $p = 0.417$ ), but was significantly slower in co-evolved than evolved populations (ANOVA;  $F = 63.16$ , d.f. = 1, 15,  $p < 0.0001$ ). Panel b shows lysis time, which was not affected by UV treatment (ANOVA;  $F = 0.497$ , d.f. = 1, 15,  $p = 0.492$ ), but showed a non-significant trend towards later lysis in co-evolved than evolved populations (ANOVA;  $F = 3.39$ , d.f. = 1, 15,  $p = 0.085$ ). Panel c shows burst size, which was not affected by UV treatment (ANOVA;  $F = 1.062$ , d.f. = 1, 15,  $p = 0.319$ ), nor significantly different between co-evolved and evolved treatments (ANOVA;  $F = 0.13$ , d.f. = 1, 15,  $p = 0.724$ ).

There was also no significant effect of UV dose on burst size (Fig. 3.4.b. ANOVA;  $F = 1.062$ , d.f. = 1, 15,  $p = 0.319$ ), nor any significant effect of evolution treatment (ANOVA;  $F = 0.13$ , d.f. = 1, 15,  $p = 0.724$ ). There was a non-significant trend towards an interaction between UV dose and evolution treatment on burst size (ANOVA; EVOLUTION x UV:  $F = 3.097$ , d.f. = 1, 15,  $p = 0.099$ ), which suggests that UV exposure may increase burst size in co-evolution treatments only. There was a non-significant trend towards greater variance in burst size in populations from the coevolution-LD90 group than any other treatment (Levene's test for homogeneity of variance:  $F = 2.77$ , d.f. = 3, 15,  $p = 0.078$ ).

Correlations between pairs of traits were sought in order to elucidate trade-offs. In general among all populations, a faster adsorption rate was associated with an earlier lysis time (Fig. 3.5; Pearson's product-moment correlation:  $t = -2.22$ , d.f. = 17,  $p = 0.04$ ), although this trend did not hold within any one treatment (Pearson's product-moment correlations: evolution-LD0:  $t = -2.1$ , d.f. = 4,  $p = 0.1$ ; evolution-LD90:  $t = -0.12$ , d.f. = 4,  $p = 0.9$ ; coevolution-LD0:  $t = -2.73$ , d.f. = 1,  $p = 0.22$ , coevolution-LD90:  $t = -0.37$ , d.f. = 2,  $p = 0.74$ ). Among all populations there was no correlation between burst size and adsorption (Pearson's product-moment correlation:  $t = -0.53$ , d.f. = 17,  $p = 0.68$ ), or burst size and lysis time (Pearson's product-moment correlation:  $t = -1.37$ , d.f. = 17,  $p = 0.18$ ), but at LD90, evolution populations showed a significant positive relationship between increased burst size and faster lysis (Fig. 3.6. Pearson's product-moment correlation:  $t = -3.6$ , d.f. = 4,  $p = 0.02$ ).

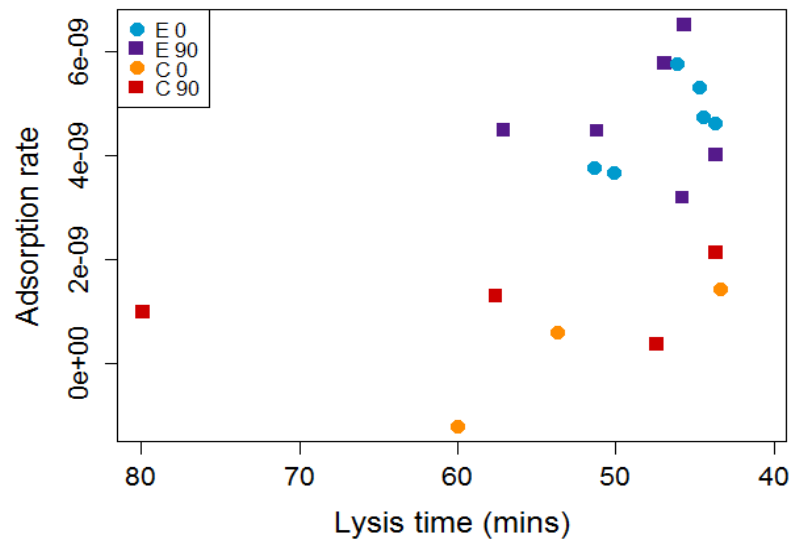


**Figure 3.5.** Correlation between adsorption rate and lysis time in evolved populations (transfer 20) from 0% (Evolved n=6, blue circles, co-evolved n=3, orange circles) and 90% (Evolved n=6, purple squares, co-evolved n=4, red squares) mortality UV treatments. Across all populations from all treatments combined, there was a positive correlation between fast adsorption and early lysis (Pearson's product-moment correlation:  $t = -2.22$ , d.f. = 17,  $p = 0.04$ ), but this trend did not hold within any one treatment (Pearson's product-moment correlations: evolution-LD0:  $t = -2.1$ , d.f. = 4,  $p = 0.1$ ; evolution-LD90:  $t = -0.12$ , d.f. = 4,  $p = 0.9$ ; co-evolution-LD0:  $t = -2.73$ , d.f. = 1,  $p = 0.22$ , co-evolution-LD90:  $t = -0.37$ , d.f. = 2,  $p = 0.74$ ).

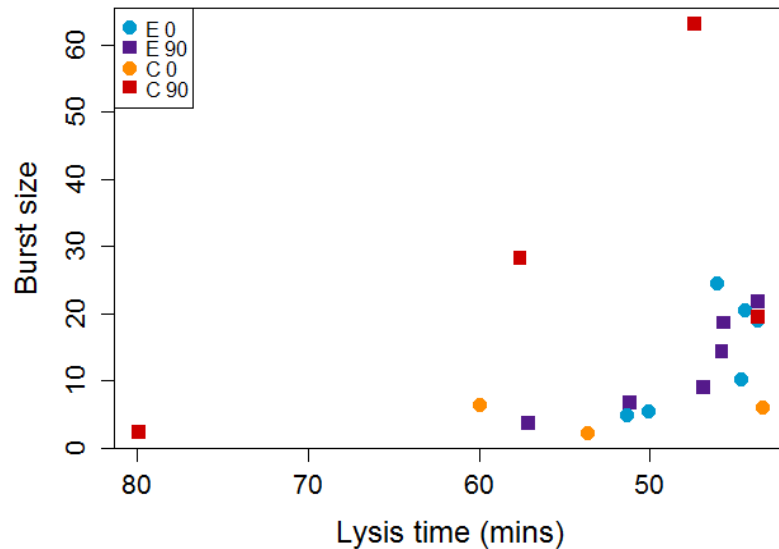


**Figure 3.6.** Correlation between burst size and lysis time in evolved populations (transfer 20) from 0% (Evolved n=6, blue circles, co-evolved n=3, orange circles) and 90% (Evolved n=6, purple squares, co-evolved n=4, red squares) mortality UV treatments. Across all populations from all treatments combined, there was no correlation between burst size and lysis time (Pearson's product-moment correlation:  $t = -1.37$ , d.f. = 17,  $p = 0.18$ ), but at LD90, evolution populations showed a significant positive relationship between increased burst size and faster lysis (Pearson's product-moment correlation:  $t = -3.6$ , d.f. = 4,  $p = 0.02$ ).

In order to investigate holistic life history strategies among these key traits, covariance was analysed using principle components analysis. The principal components analysis explained all of the variation in the data in principal components 1 (88%) and 2 (12%). PC1 was associated with burst size and lysis time, while PC2 was associated with adsorption rate, and loosely with lysis time (Fig. 3.6.a). Populations from evolution treatments were grouped closely together in trait space regardless of UV treatment, suggesting that there was little divergence in strategy between populations from the two UV treatments (Fig. 3.6.b). Conversely, in co-evolution populations there was a stark difference in life history strategies between LD0 populations, which are clustered more closely together and share similar trait space to evolution populations, and LD90 closely together and share similar trait space to evolution populations, and LD90

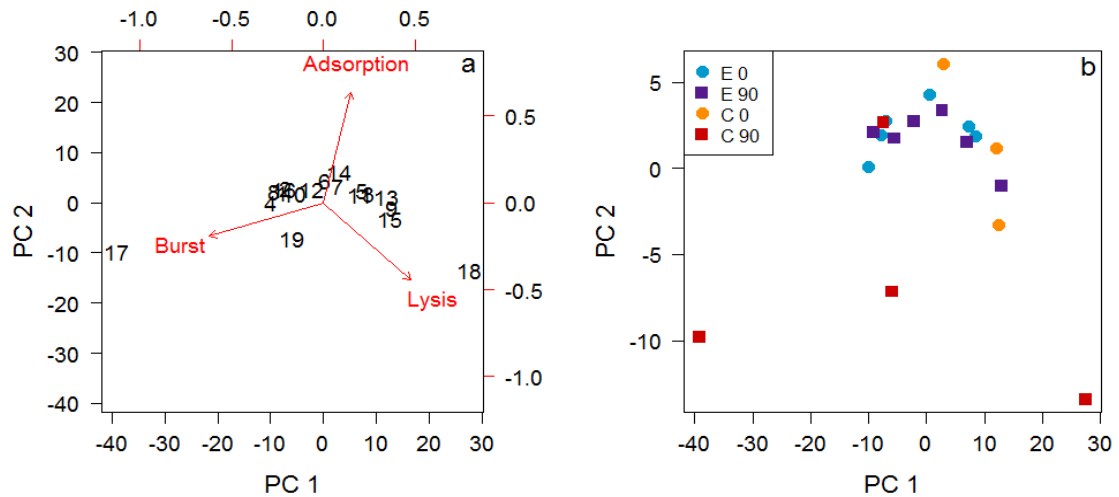


**Figure 3.7.** Principal components analysis. Panel a is the loadings biplot showing the principal component scores of the individual populations (lower x axis = PC1, left y axis = PC2), and the relative loadings of the life history variables (red arrows, upper x and right y axes). Numbers correspond to individual populations. Panel b is the traits biplot, which shows the location of each population from the 0% (Evolved n=6, blue circles, co-evolved n=3, orange circles) and 90% (Evolved n=6, purple squares, co-evolved n=4, red squares) mortality UV treatments in trait space according to principal components scores on PC1 and PC2.

populations, whose strategies varied widely and all but one population fell far from the main cluster of evolution populations.

## Phage evolution

Evolved phage populations were Sanger sequenced at the end of the selection experiment (transfer 20) in 5 genes believed to be important in controlling interactions with the host, and a control (see table 2.1, chapter 2). A number of mutations were identified in the genes studied, which are presented in table 3.1. The majority of mutational events were found in gene *SBWP25\_0036*, which encodes for the tail fibre protein, followed by genes *SBWP25\_0032* and *SBWP25\_0027* which encode for a tail tubular protein and predicted virion structural protein, respectively. Only a few mutations were found in genes *SBWP25\_0034* and *SBWP25\_0035* which encode for a predicted lysozyme and an internal virion structural protein, respectively, and one mutation was found in one population from treatment coevolution-LD90 in the control gene *SBWP25\_0040*, which encodes for a predicted phage lysozyme.

There was no significant effect of UV treatment on the number of mutations (Fig. 3.8. GLM:  $z = 0$ , d.f. = 15,  $p = 1$ ), but there were significantly more mutations in co-evolution treatments compared to evolution treatments (Fig. 3.8. GLM:  $z = -5.15$ , d.f. = 15,  $p < 0.0001$ ). In fact, only two mutation events were observed in evolution treatments: one A-G (R) polymorphism at position 1340 on gene *SBWP25\_0032* which occurred in just one evolution-LD90 population, and a T-A mutation at position 1433 on gene *SBWP25\_0036* which occurred in all

**Table 3.1.** The locations and identities of mutations on the genes sequenced from the end-point (transfer 20) populations. Positions (in base pairs from the start of each gene) are indicated at the top of the table, and the mutations found at that position (base differences from the ancestor) are identified at the bottom of the table. Rows correspond to individual populations. + indicates the presence of the identified mutation in the population, and = indicates the presence of the identified polymorphism.

Gene	SBWP25_0027					SBWP25_0032								SBWP25_0034			SBWP25_0035	
Position	74	161	262	275	331	113	388	476	569	868	1195	1340	1351	2170	1807	1808	2514	2498
C 0:																		
1	-	-	-	-	+	-	+	-	-	-	-	-	-	-	-	+	-	-
4	-	-	+	-	-	-	-	+	-	-	+	-	-	-	-	-	-	-
6	-	-	-	+	-	-	-	+	-	-	-	-	-	-	-	-	-	-
C 90:																		
2	-	-	-	-	+	-	-	-	+	-	-	-	-	=	-	-	-	+
3	-	-	-	-	+	+	-	+	-	-	-	-	-	-	-	-	-	+
4	-	-	-	-	-	-	-	+	-	+	-	-	-	-	-	-	-	-
5	=	+	-	-	-	-	-	+	-	-	-	-	+	-	+	-	+	-
E 0:																		
1	-	-	-	-	-	-	-	-	-	-	-	-	-	-	-	-	-	-
2	-	-	-	-	-	-	-	-	-	-	-	-	-	-	-	-	-	-
3	-	-	-	-	-	-	-	-	-	-	-	-	-	-	-	-	-	-
4	-	-	-	-	-	-	-	-	-	-	-	-	-	-	-	-	-	-
5	-	-	-	-	-	-	-	-	-	-	-	-	-	-	-	-	-	-
6	-	-	-	-	-	-	-	-	-	-	-	-	-	-	-	-	-	-
E 90:																		
1	-	-	-	-	-	-	-	-	-	-	-	-	-	-	-	-	-	-
2	-	-	-	-	-	-	-	-	-	-	-	-	-	-	-	-	-	-
3	-	-	-	-	-	-	-	-	-	-	-	-	-	-	-	-	-	-
4	-	-	-	-	-	-	-	-	-	-	-	-	-	-	-	-	-	-
5	-	-	-	-	-	-	-	-	-	-	-	-	-	-	-	-	-	-
6	-	-	-	-	-	-	-	-	-	-	-	=	-	-	-	-	-	-
Type (+)		T-G	G-A	C-T	Ins AAG	T-C		A-G	A-G	A-C	C-G		G-A		T-C	C-T	G-A	C-T
Poly (=)	R						R					R		K				

**Table 3.1 (continued).** The locations and identities of mutations on the genes sequenced from the end-point (transfer 20) populations. Positions (in base pairs from the start of each gene) are indicated at the top of the table, and the mutations found at that position (base differences from the ancestor) are identified at the bottom of the table. Rows correspond to individual populations. + indicates the presence of the identified mutation in the population, and = indicates the presence of the identified polymorphism.

Gene	SBWP25_0036																		SBWP25_0040
Position	290	307	308	370	995	1204	1217	1268	1271	1279	1284	1286	1287	1297	1298	1433	1562	1675	142
<b>C 0:</b>																			
1	-	-	+	-	+	+	-	+	+	-	-	-	-	-	+	-	-	-	-
4	-	+	-	-	-	+	+	-	-	+	-	+	+	+	-	-	-	+	-
6	+	-	-	+	-	+	-	-	-	+	-	+	+	+	-	-	+	-	-
<b>C 90:</b>																			
2	-	-	+	-	-	+	-	-	-	=	-	=	=	+	-	-	+	-	-
3	-	-	+	-	-	+	-	-	-	-	-	-	-	-	+	-	+	-	-
4	-	-	+	-	-	+	-	-	-	-	+	-	-	-	+	-	+	-	-
5	+	-	-	-	+	+	-	-	-	+	-	+	+	+	-	-	+	-	+
<b>E 0:</b>																			
1	-	-	-	-	-	-	-	-	-	-	-	-	-	-	-	+	-	-	-
2	-	-	-	-	-	-	-	-	-	-	-	-	-	-	-	+	-	-	-
3	-	-	-	-	-	-	-	-	-	-	-	-	-	-	-	+	-	-	-
4	-	-	-	-	-	-	-	-	-	-	-	-	-	-	-	+	-	-	-
5	-	-	-	-	-	-	-	-	-	-	-	-	-	-	-	+	-	-	-
6	-	-	-	-	-	-	-	-	-	-	-	-	-	-	-	+	-	-	-
<b>E 90:</b>																			
1	-	-	-	-	-	-	-	-	-	-	-	-	-	-	-	+	-	-	-
2	-	-	-	-	-	-	-	-	-	-	-	-	-	-	-	+	-	-	-
3	-	-	-	-	-	-	-	-	-	-	-	-	-	-	-	+	-	-	-
4	-	-	-	-	-	-	-	-	-	-	-	-	-	-	-	+	-	-	-
5	-	-	-	-	-	-	-	-	-	-	-	-	-	-	-	+	-	-	-
6	-	-	-	-	-	-	-	-	-	-	-	-	-	-	-	+	-	-	-
Type (+)	A-G	C-A	A-G	Del 12bp	T-A	G-A	G-C	C-G	C-T	T-A	T-C	A-G	C-A	A-G	C-A	T-A	C-A	A-G	
Poly (=)										W		R	M						R

evolution populations from both LD0 and LD90 treatments. Neither of these mutations were found in any population from the co-evolution treatments. Co-evolution-LD90 treatment populations also showed a greater variance in the number of mutational events between populations than in other treatments (Levene's test for homogeneity of variance:  $F = 11.74$ ,  $d.f. = 3, 15$ ,  $p = 0.0003$ ).

Figure 3.9 shows the frequencies of each identified mutational event in each gene within each treatment. In most genes, any one mutation was found in only one or two populations in any one treatment and there were many unique mutations which only occurred in one population in one treatment. In gene *SBWP25\_0036*, however, there were several mutations which occurred in the

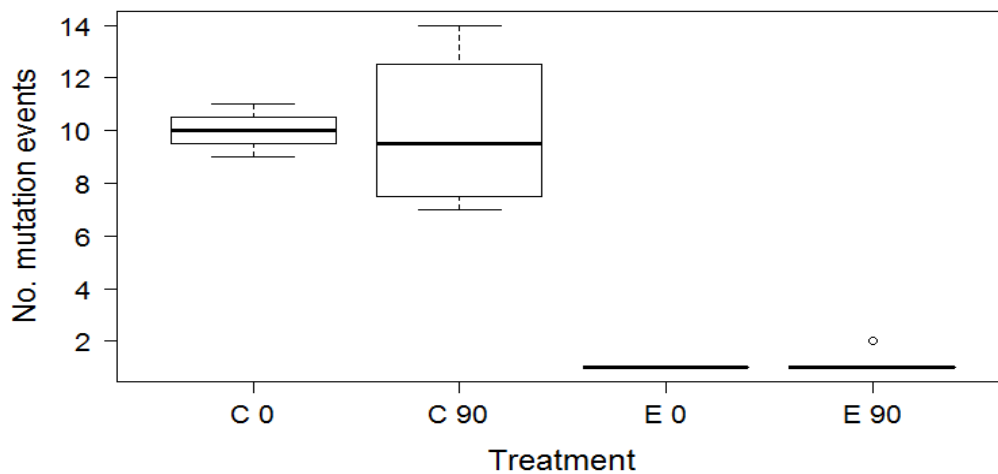


**Figure 3.8.** The number of mutation events across all genes sequenced from end-point (transfer 20) 0% (Evolved  $n=6$ , co-evolved  $n=3$ ) and 90% (Evolved  $n=6$ , co-evolved  $n=4$ ) mortality UV treatments. Boxes display the median and interquartile range, and whiskers display the maximum and minimum values. There was no significant effect of UV on the number of mutations between treatments (GLM:  $z = 0$ ,  $d.f. = 15$ ,  $p = 1$ ), but there were significantly more mutations in co-evolution treatments compared to evolution treatments (GLM:  $z = -5.15$ ,  $d.f. = 15$ ,  $p < 0.0001$ ).

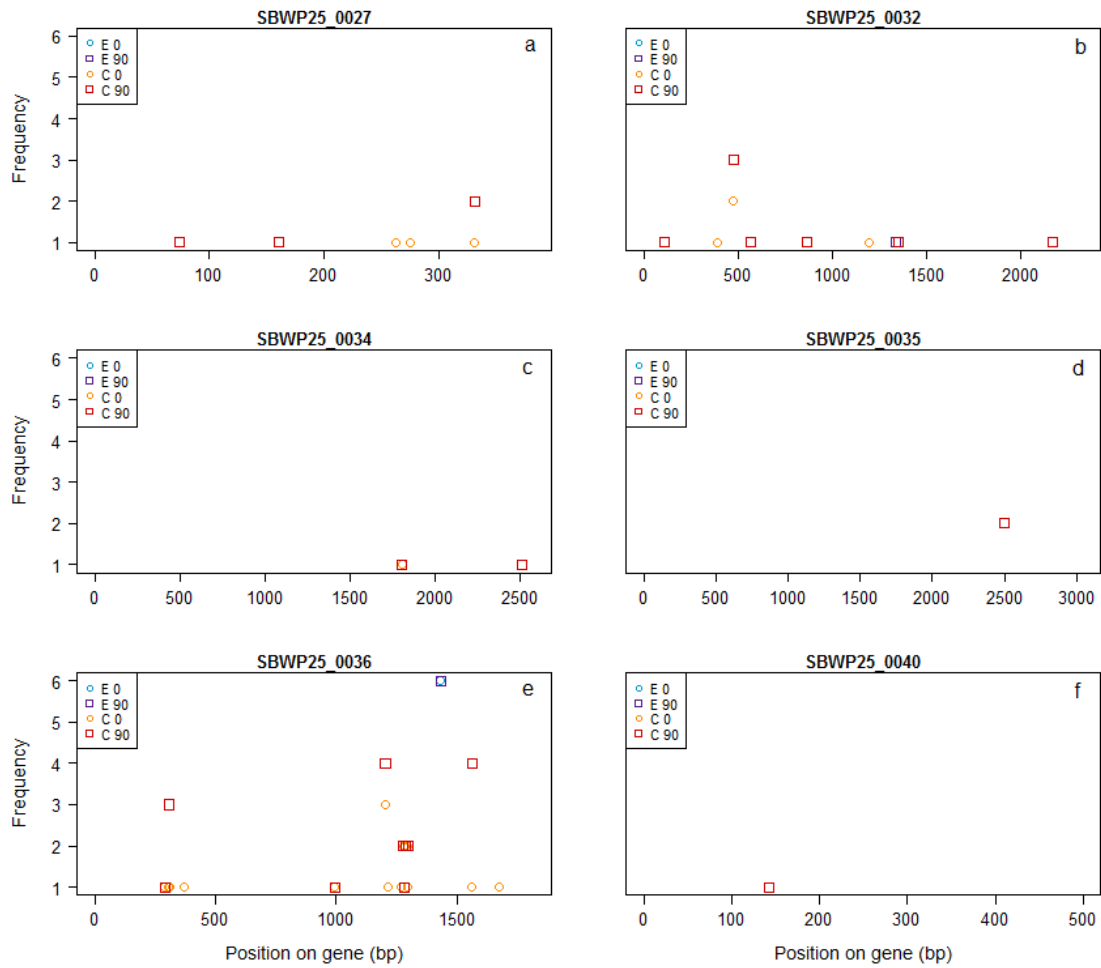


**Figure 3.9.** Frequency of each identified mutation in each gene in end-point (transfer 20) populations from 0% (Evolved n=6, blue circles, co-evolved n=3, orange circles) and 90% (Evolved n=6, purple squares, co-evolved n=4, red squares) mortality UV treatments. The x axis shows the bp position of mutations on the gene. a) gene *SBWP25\_0027*, b) gene *SBWP25\_0032*, c) gene *SBWP25\_0034*, d) gene *SBWP25\_0035*, e) gene *SBWP25\_0036*, f) gene *SBWP25\_0040*.

majority of populations within a treatment. With the exception of one mutation at 308 bp, all of the frequent mutations occurred between 1200 and 1600 bp.

Euclidean genetic distances of each population from the ancestor was higher in co-evolution treatments than evolution treatments in all of the genes studied (Fig. 3.10). A neighbour-joining tree of Euclidean distances is presented in figure 3.11. All evolution treatments cluster together on a single node with the exception of population evolution-LD90 6, which is located on a sister-node to the other evolution populations. Three of four coevolution-LD90 populations cluster closely together, with coevolution-LD90 5 clustering with two of the coevolution-LD0 populations, and coevolution-LD0 1 located on a separate but sister node to the other co-evolution populations. Evolution and co-evolution populations cluster separately from each other, but there is very little differentiation between LD0 and LD90 populations in the evolution treatment.

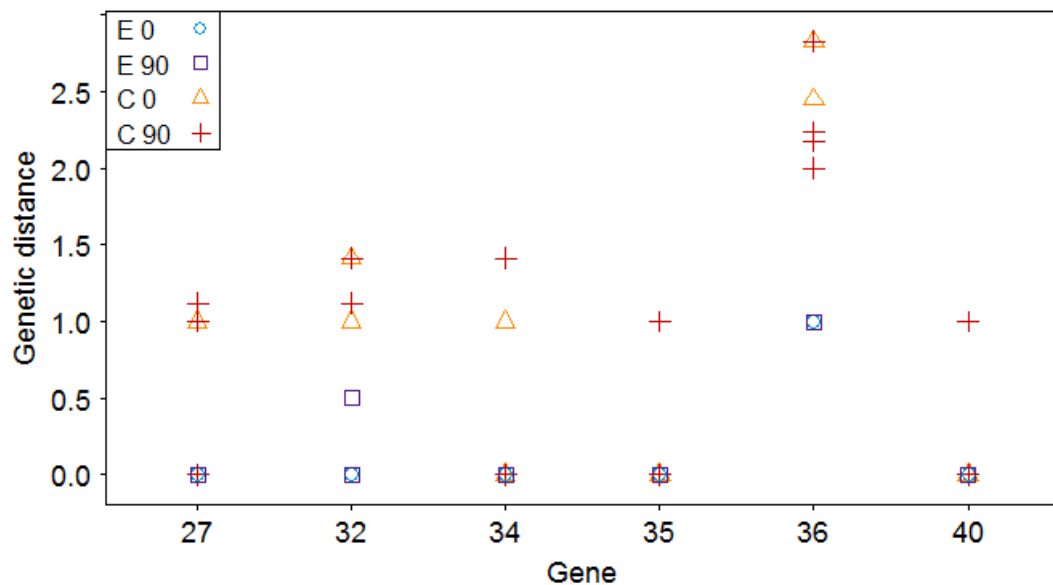


**Figure 3.10.** Pairwise euclidean distance from the ancestor in each gene in populations from 0% (Evolved n=6, blue circles, co-evolved n=3, orange triangles) and 90% (Evolved n=6, purple squares, co-evolved n=4, red crosses) mortality UV treatments. The x axis denotes the gene (*SBWP25\_0027* = 27, etc).

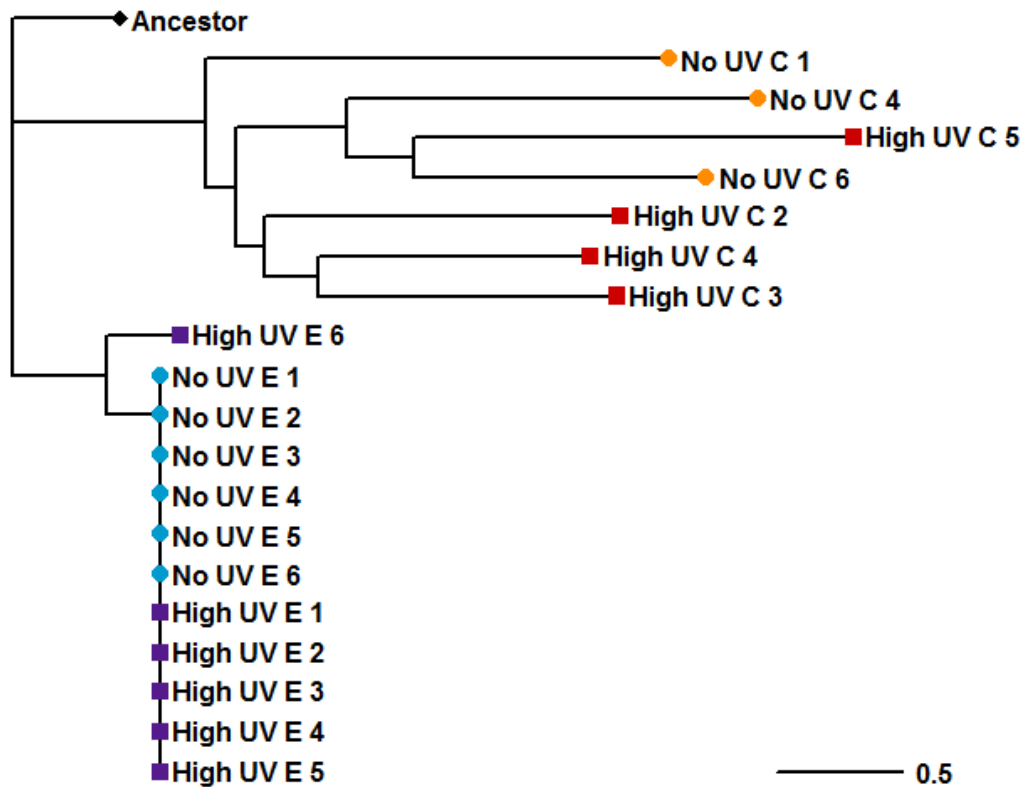


**Figure 3.11.** Neighbour-joining tree of pairwise Euclidean distances between 19 end-point (transfer 20) populations and the ancestor in all genes in table 2.1 (Chapter 2). Based on binary data of base substitutions from the ancestor, rooted by the ancestor (black diamond). 0% mortality populations are labelled No UV E (evolved, blue circles) and No UV C (co-evolved, orange circles). 90% mortality populations are labelled High UV E (evolved, purple squares) and High UV C (co-evolved, red squares).

In the co-evolution treatment, LD0 and LD90 populations cluster separately for the most part, with one LD90 population located within the LD0 cluster.

## Discussion

Evolved phage populations remained at stably high 48-h densities throughout the experiment, and co-evolved phage and bacterial populations suffered fluctuating densities typical of co-evolving populations in this system regardless

of UV treatments. Slower adsorption rate evolved in all treatments, with co-evolved treatments evolving slower adsorption rates than evolved treatments, contrary to predictions. There was no effect of UV treatment found in any life history trait, although there was a non-significant trend towards higher burst size and greater variation in both burst size and lysis time in co-evolved populations exposed to the highest dose of UV irradiation. A larger burst size may be an adaptation to increased extracellular mortality, as a larger number of progeny may increase the chances of a fraction surviving. There was a correlation between fast adsorption and early lysis across all treatments, but not within treatments, and high burst size was correlated with fast lysis only in evolution populations exposed to the highest dose of UV. There was little variation in life history strategy between evolved populations within or between UV treatments, but there was greater variation in co-evolved populations, and large variation evolved in co-evolved populations exposed to the highest dose of UV. Genetic analysis revealed very little molecular evolution in the evolution treatments within the genes studied, but much more mutation in the co-evolution treatments, and a greater variance in co-evolution populations exposed to the highest dose of UV. Genetic distances from the ancestor were higher in co-evolved treatments, but not greater in populations exposed to the highest dose of UV than those not exposed to UV. The mutation profiles (identity and frequency of given mutations) were sufficiently divergent between co-evolved populations exposed to the highest dose of UV and those not exposed to

UV that the majority of populations grouped according to UV treatment on a Euclidean distance tree, whilst evolved populations did not.

The observed evolution of reduced adsorption rate is at odds with standard life-history theory of parasite evolution under elevated ex-host mortality. However, evolution of reduced adsorption rate seems to be a general adaptation to laboratory conditions from an ancestor with an unusually high adsorption rate – slower adsorption rate also evolved contrary to theory in chapter 2. If this is the case, the further reduction in adsorption rate in co-evolved populations may simply be an artefact of the increased evolution rate under co-evolution (Paterson et al. 2010) allowing these populations to evolve closer to the optimum. An alternative explanation is that reduced adsorption rate could be a result of increased specialisation to non-ancestral host genotypes, or increased infectivity range reducing the ability of co-evolved phage to infect the ancestral host (Poullain et al. 2008). This conclusion is supported by the fact that several of the co-evolved populations failed to amplify on the ancestral host. Further work is necessary to determine between these alternative mechanisms.

It is surprising that UV dosing did not increase the mutation rate above the increase caused by co-evolution within the genes studied here. As the  $\Phi 2$  genome is relatively small, there may be very little evolutionary potential for phage-encoded UV repair (Bernstein 1981). As host-mediated repair is an efficient and ubiquitous process which only requires phage to adsorb to and penetrate the host, any phage-encoded resistance genes may be superfluous and lost in favour of a smaller genome which is more efficient to replicate. Instead,

an increased production of progeny leading to a higher burst size may increase the chances of some offspring surviving to infect irradiated hosts for photo-reactivation and excision. Also, phage may be under conflicting selection pressures for UV resistance and host infection. If any phage resistance mutations which confer resistance to UV also act to reduce infectivity or reproductive potential, then bacterial repair mechanisms will be harder to acquire, and therefore these mutations would reduce overall fitness, particularly under co-evolution. Alternatively, adaptive mutations may have occurred elsewhere on the genome that I was unable to detect here. As the genes I sequenced are involved with the infection process, they may be under purifying selection (Zwart et al. 2008), whereas genes elsewhere on the genome may be freer to accumulate mutations, and may be acting on life-history traits through epistasis or pleiotropy. Further study with whole-genome sequencing would uncover any such effects.

In evolution treatments, phage exposed to UV were re-introduced to ancestral hosts which had not been irradiated at each transfer. If phage are entirely reliant on host-mediated reactivation (which does not occur without host irradiation), this process may simply have decimated the population at each transfer, resulting in repeated bottle-necking with no opportunity for evolution of phenotypic or genotypic resistance. Alternatively, there may be molecular resistance evolution elsewhere on the genome which interacts epistatically with life-history evolution, resulting in no net change in phenotypic traits, nor in the life-history associated genes studied. It is beyond the scope of this study to

distinguish between these alternatives. Future study using irradiated ancestral host cells and/or whole-genome sequences are needed to elucidate this effect.

A lack of evolutionary potential is not appropriate to explain the patterns observed in co-evolution treatments, as these populations have not only undergone substantial evolution, but they also have the necessary conditions for reactivation. The main effect of UV dosing was an increase in variance of lysis timing and burst sizes, overall life history strategy and the number and identity of mutations between co-evolved populations. The current experiment is unable to distinguish whether these results are adaptive evolution or simply an effect of non-targeted mutagenesis caused by the damage and repair of DNA during UV exposure. It is also conceivable that any mutations that confer a direct benefit under UV exposure are located elsewhere on the genome and therefore not detected here. As bacterial cells were also exposed to UV in co-evolution treatments, bacterial mutation and repair may have had an effect on phage life history evolution. An increase in bacterial mutation rate could have resulted in a greater range of resistance profiles, driving the greater range of phage life history strategies we see here.

Co-evolution is known to exert strong selection pressure on phage  $\Phi 2$  through the Red Queen dynamics of repeated resistance and infectivity evolution (Paterson et al. 2010). Co-evolution with the host is also predicted to select for increased infectivity (fast adsorption rate) and large burst size, but faster lysis. Therefore, phage would have been under similar selection pressure for adsorption rate and burst size in the two co-evolution treatments, but opposing

selection pressures for lysis time between the two UV treatments. This may explain why life history strategy was more variable in UV-dosed populations along PC1, which was associated with lysis timing and burst size. It is perhaps not surprising then that there was no directional divergence in phenotype between co-evolution treatments, as phage faced a strong trade-off between adaptation to co-evolution and UV in lysis timing, which is interrelated with burst size and adsorption rate, resulting in increased variance in these traits also.

## Conclusions

This study was designed to assess the effects of UV exposure on the evolution of phage life history under both evolution and co-evolution. In evolution there was very little divergence in phenotype or genotype from the ancestor or between treatments, which suggests that resistance to UV in this phage is almost entirely dependent on host-mediated reactivation. In co-evolution there was increased variation in life-history traits and mutation in UV treatments but no clear directional evolution of phenotype or genotype above that observed in co-evolution populations not exposed to UV. The lack of directional evolution in phenotype is likely to be due to conflicting selection pressures from co-evolution and UV on lysis timing. It is beyond the scope of this study to determine whether the change in mutation profile between co-evolution populations exposed and not exposed to UV is due to adaptation or non-targeted random mutagenesis. Further studies would benefit from whole-genome sequencing to discover

potential adaptive mutations elsewhere on the genome and any epistatic effects which may have constrained the evolution of the genes studied here. Studies using evolution against an irradiated ancestral host would also help to elucidate any antagonism between co-evolution and UV resistance, as well as the potential for phage  $\Phi 2$  to evolve resistance without co-evolution.

## 4. The effects of phage on bacteria-plasmid dynamics

### Statement of collaboration

This experiment was conducted in collaboration with Dr. Ellie Harrison. We jointly conducted the selection experiment and the resistance assays, I plated phage samples for titration and Dr. Harrison assessed plasmid prevalence. Dr. Harrison conducted the time-shift analysis; all other analyses presented here are my own.

### Introduction

Conjugative plasmids are common in bacterial populations and act as agents of horizontal gene transfer, enhancing bacterial adaptation (Norman et al. 2009). Additionally, plasmids allow for a form of adaptive phenotypic plasticity in bacteria by acting as vectors of transiently beneficial genes among populations and between species that may be gained and lost as necessary (Eberhard 1990). These plasmid-encoded adaptations are often of profound ecological and clinical importance, such as resistance to heavy metal pollution (Silver & Misra 1988) and antibiotic resistance (Mazel & Davies 1999; Svara & Rankin 2011). In cystic fibrosis patients, *Pseudomonas aeruginosa* infection is associated with chronic phases of the disease, which can lead to fatal exacerbation of symptoms

(Deretic & Schurr 1994). Complicating the treatment of cystic fibrosis, *P. aeruginosa* is resistant to all reliable antibiotics, largely due to the carriage of multiple antibiotic-resistant plasmids and other mobile genetic elements (Livermore 2002).

Plasmids consist of a (usually) circular DNA genome of both core functional genes and potentially host-beneficial accessory genes. They can replicate independently within their bacterial hosts, and are subject to their own selection pressures (Harrison & Brockhurst 2012). The costs to host bacteria of carrying plasmids must be non-zero due to the biosynthetic costs of additional genetic material, and during cell replication plasmids can be lost during assortment into daughter cells, yet plasmids can be maintained at high frequencies. These realisations have prompted considerable interest in how plasmids are maintained in bacterial populations (e.g. Stewart & Levin 1977; Simonsen 1991). In environments where the benefits of plasmid carriage exceed the costs, plasmids are stably maintained at high frequency (Dionisio et al. 2005; Heuer et al. 2007). In the absence of such positive selection however, plasmids are expected to be lost from host populations due to purifying selection, unless counteracted by high rates of conjugative transfer or amelioration of the costs of carriage (Subbiah et al. 2011; Lundquist & Levin 1986; Harrison & Brockhurst 2012). Although the effects of many parameters such as conjugation rates, host density and degree of parasitism have been considered both empirically and in mathematical models (Simonsen 1991; Bergstrom et al. 2000), the effects of co-occurring parasites on plasmid persistence are yet to be examined. Multi-

parasitism is ubiquitous in nature (Mideo 2009; Read & Taylor 2001; Windsor 1998; Cox 2001) and can intensify or alter selection pressures on each individual party (Mideo 2009; Poulin 2001), so should not be ignored in attempts to quantify the existence conditions for plasmids. Bacteriophage, for example, are ubiquitous among bacteria and are a major cause of bacterial mortality (Proctor & Fuhrman 1990), so are likely to interact with plasmids either directly or indirectly.

*Pseudomonas fluorescens* carries the naturally associated conjugative mega-plasmid pQBR103 (Lilley & Bailey 1997b), which is 425kb. pQBR103 encodes a mercury resistance operon (Tett et al. 2007) which allows *P. fluorescens* to detoxify environmental mercury ions. When there is no environmental mercury, the biosynthetic costs of plasmid carriage is evidenced by a reduced growth rate in comparison to cells without the plasmid (Lilley & Bailey 1997; Ellis et al. 2007), and pQBR103 can be considered a parasite. At high levels of environmental mercury, however, pQBR103 confers a substantial growth benefit and can be considered a mutualist. As the concentration of environmental mercury varies within a landscape both spatially and temporally, the relationship between *P. fluorescens* and pQBR103 ranges from mutualistic through neutral to parasitic along a continuum proportional to mercury concentration.

pQBR103 and phage  $\Phi 2$  both occur commonly in natural populations of *P. fluorescens*, so phage are likely to impact upon plasmid fitness through their ecological and evolutionary effects on the host. Understanding the effects of co-

occurring naturally associated parasites on each other and their combinatorial effects on the host is important for disease management and prediction, and may be an important aspect to consider when designing medical interventions (Mideo 2009). If plasmid carriage reduces the ability of host bacteria to evolve resistance to phage due to biosynthetic costs, then phage infection will act to increase the cost of plasmid carriage and narrow the existence conditions for pQBR103. This effect could prove useful in the battle against plasmid-encoded antibiotic resistance and virulence factors in bacterial infections.

This study aims to elucidate the effects of phage predation on pQBR103 persistence and host-parasite dynamics, under various degrees of positive selection for pQBR103. We predict that phage infection will narrow the existence conditions for pQBR103 along the parasitism-mutualism continuum by exacerbating the costs of plasmid carriage and reducing host density. We therefore predict that the presence of  $\Phi 2$  will promote plasmid loss in the absence of selection for plasmid-encoded mercury resistance.

## Methods

### Selection experiment

48 microcosms were initiated with a single fresh colony of *Pseudomonas fluorescens* strain SBW25- $\Omega$ Gm containing the conjugative plasmid pQBR103, in 6 ml KB in 30 ml disposable glass universal tubes. These populations were incubated at a constant temperature of 28°C, at 180 rpm. After 48 h growth ( $\sim 10^7$  cells ml<sup>-1</sup>), 60  $\mu$ l of each population were transferred to fresh microcosms

and assigned to one of eight treatments: mercury free medium (0  $\mu\text{M}$   $\text{HgCl}_2$ ) or media containing 8, 16 or 32  $\mu\text{M}$   $\text{HgCl}_2$ , and with or without *P. fluorescens* bacteriophage SBW25 $\Phi$ 2 in a full factorial design with 6 replicate populations in each treatment (Transfer 1). At 32  $\mu\text{M}$   $\text{HgCl}_2$  pQBR103 is highly beneficial to the host, but at 0  $\mu\text{M}$   $\text{HgCl}_2$  pQBR103 carriage is costly to bacterial fitness, with intermediate concentrations of  $\text{HgCl}_2$  imposing intermediate costs/benefits to plasmid-carrying hosts (Harrison et al. 2014). Populations assigned to phage treatments were inoculated with 6  $\mu\text{l}$  of a  $10^{11}$  virions  $\text{ml}^{-1}$  ancestral stock suspension. All cultures were incubated at 28 °C, 180 rpm and 1% of culture transferred every 48h for 20 serial transfers (c. 130 bacterial generations).

### Population densities

At every 4<sup>th</sup> transfer, bacterial populations were plated for density, and  $\Phi$ 2 populations were filter-sterilised and spot-plated for titration. Aliquots of mixed culture were frozen with 20% glycerol at -80°C.

### Plasmid prevalence

At every 4<sup>th</sup> transfer, 10 individual colonies of *P. fluorescens* from each evolving population were PCR analysed for plasmid presence. Colonies were randomly selected from plated samples of each population and grown in 96-well plates for 48h at 28°C. These cultures were then screened for plasmid presence using primers targeting the mercury resistance operon *merA* (for: 5'-TGCAAGACACCCCCTATTGGAC-3' and rev: 5'-TTCGGCGACCAGCTTGATGAAC-3') and the putative origin of replication *oriV* (for: 5'-TGCCTAATCGTGTGTAATGTC-

3' and rev: 5'ACTCTGGCCTGCAAGTTTC-3'). Where <5 colonies screened positive for plasmid presence in a population, a further 90 colonies were analysed.

### Time-shift resistance assay

At every 4<sup>th</sup> transfer, 20 individual colonies of *P. fluorescens* were randomly selected from plated samples of each mercury-free population and grown in 96-well plates for 48h at 28°C. These cultures were then streak plated perpendicularly over pre-dried lines of filter-sterilised Φ2, on 1.2% KB agar. Colonies were streaked over lines of Φ2 from contemporary sympatric populations, 4 transfers in the past from the same evolving lineage and 4 transfers in the future. Plates were incubated inverted at 28°C. After overnight incubation, colonies were visually assessed for resistance to Φ2. Colonies were recorded as sensitive to Φ2 if their growth was markedly inhibited past the point at which they crossed the Φ2 line, and resistant if no inhibition was apparent.

### Statistical analysis

All statistical analyses were conducted in R statistical package (R Core Team 2013). Bacterial and phage end-point densities were analysed using ANOVAs and variance analysed with Bartlett's test of homogeneity of variance. Plasmid prevalence, bacterial resistance and mucoidy were analysed in generalised linear mixed effects models (with binomial errors) with phage treatment as a fixed effect, time and mercury treatment as covariates and population as a random effect.

## Results

### Plasmid prevalence

Plasmid prevalence was assessed by PCR every fourth transfer. Plasmids remained at or near fixation throughout the experiment in mercury-containing environments regardless of phage presence, whilst at 0  $\mu\text{M}$   $\text{HgCl}_2$  (where pQBR103 is parasitic) plasmid prevalence declined over time in both phage treatments (Fig. 4.1; Mercury x Time;  $z = 4.3$ ,  $n = 288$ ,  $p < 0.0001$ ). The decline in plasmid prevalence when parasitic was more pronounced in phage infected populations, with a decline to zero or very low frequency in 5 out of 6 populations, compared to stable maintenance of plasmid at intermediate frequencies in phage free populations ( $z = -3.1$ ,  $n = 72$ ,  $p = 0.002$ ). Plasmid prevalence was also more variable at transfer 20 in phage infected (range = 0-85%) than phage free (range = 69-88%) populations (F test of variances;  $F = 21$ ,  $\text{d.f.} = 5, 5$ ,  $p = 0.005$ ).

### Bacterial & phage densities

Bacterial density was measured every fourth transfer by plating samples of each population. In phage-containing populations, phage density was also measured by spot-plating filter-sterilised samples for phage titration. Bacterial end-point (transfer 20) density was high in all mercury treatments in the absence of phage, but was markedly reduced in phage infected populations regardless of mercury treatments (Fig. 4.2, ANOVA;  $F = 61.74$ ,  $\text{d.f.} = 1, 45$ ,  $p < 0.0001$ ).

Bacterial end-point density was more variable in phage-containing populations

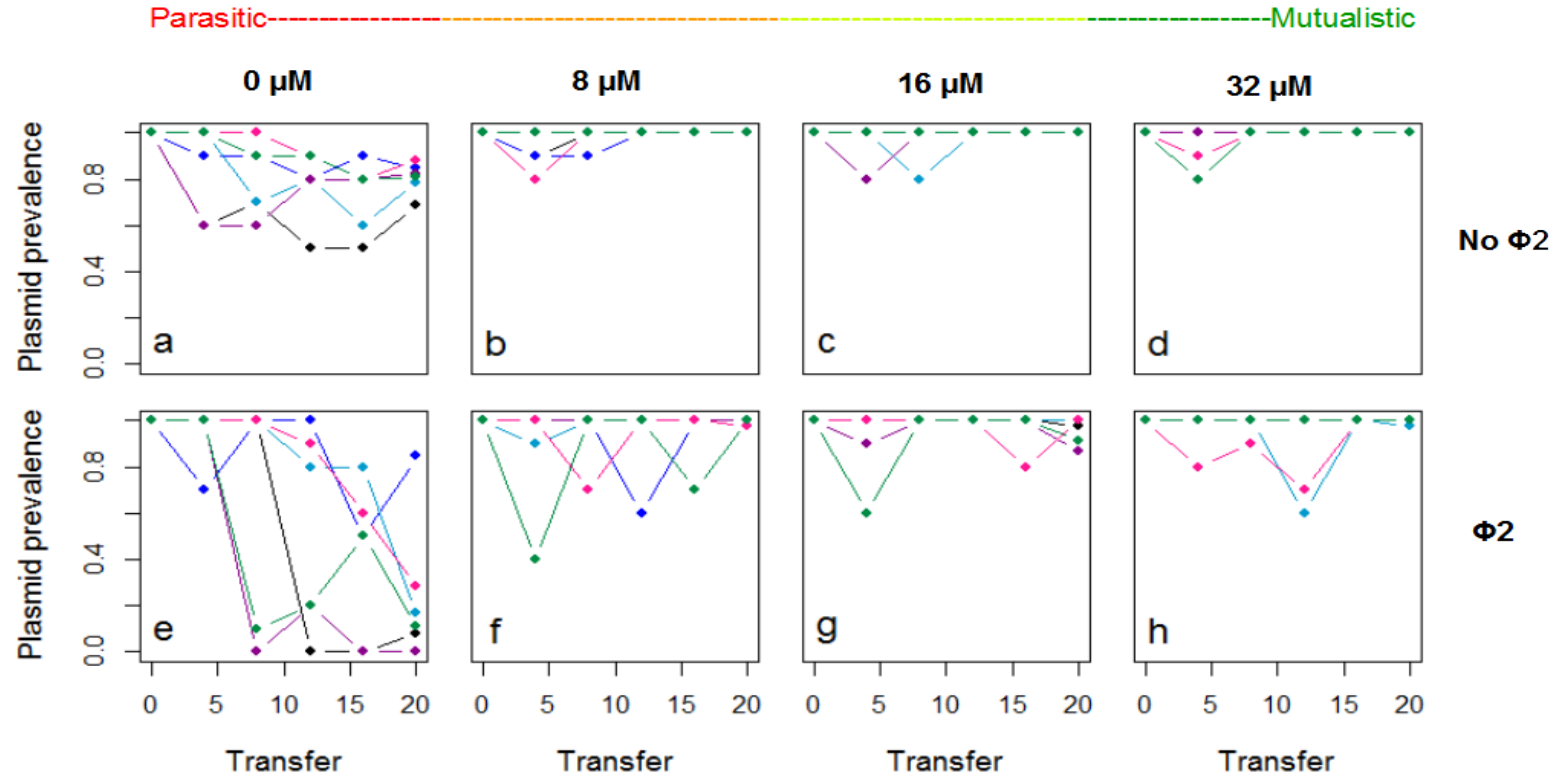


**Figure 4.1.** The proportion of plasmid-carrying cells over time in six replicate populations of each treatment. Panels a-d show plasmid prevalence in phage-free treatments from 0 (a), 8 (b), 16 (c) and 32 (d)  $\mu\text{M}$   $\text{HgCl}_2$ . Panels e-h show plasmid prevalence in phage-containing treatments from 0 (a), 8 (b), 16 (c) and 32 (d)  $\mu\text{M}$   $\text{HgCl}_2$ . Colours represent individual replicate populations. In mercury-containing populations, plasmid prevalence remained high regardless of phage treatment. At 0  $\mu\text{M}$   $\text{HgCl}_2$  plasmid prevalence declined over time in both phage treatments (Mercury x Time;  $z = 4.3$ ,  $n = 288$ ,  $p < 0.0001$ ). This decline was more pronounced in phage infected populations ( $z = -3.1$ ,  $n = 72$ ,  $p = 0.002$ ).

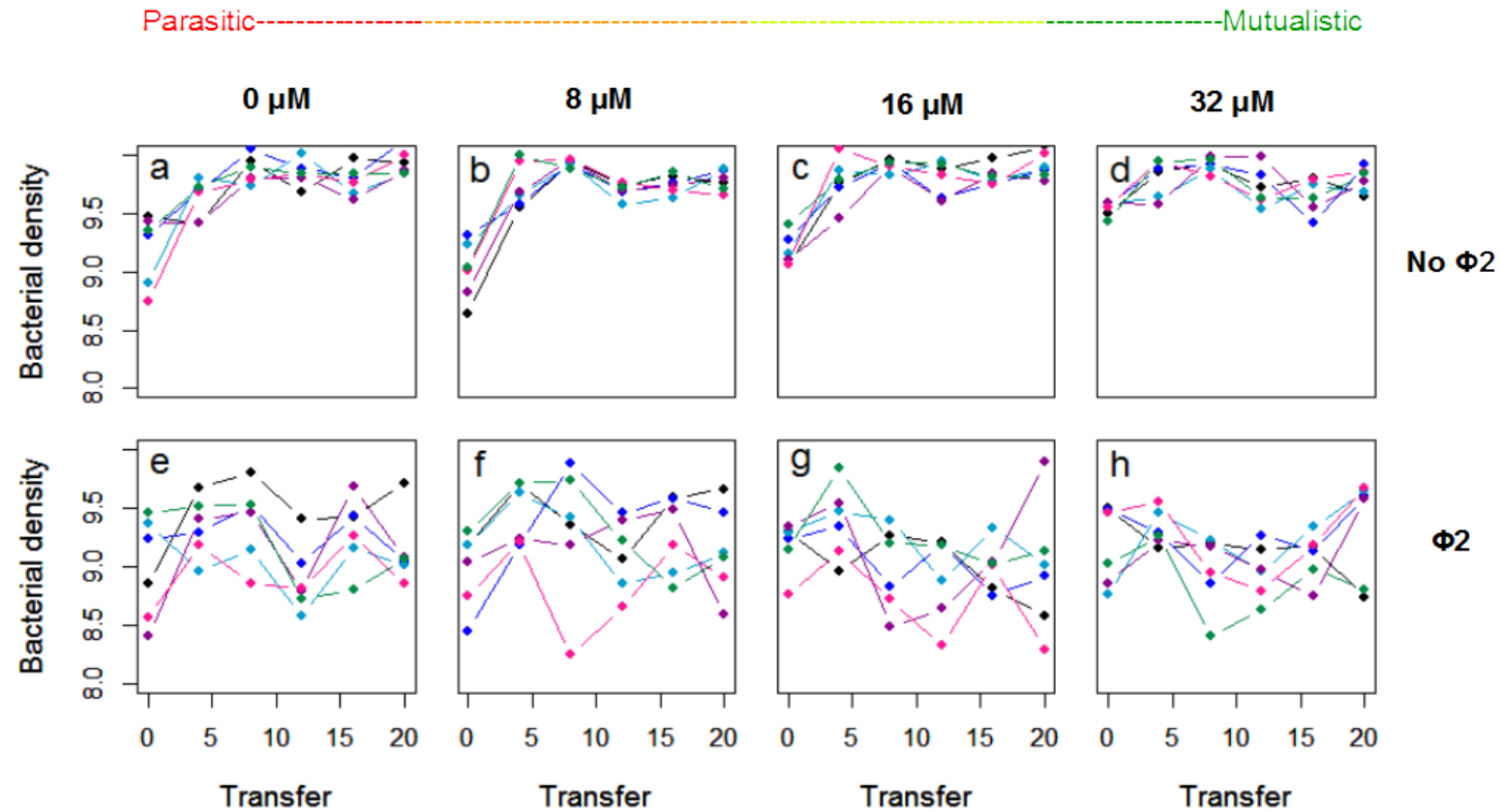


**Figure 4.2.** Bacterial density over time in 6 replicate populations of each treatment. Panels a-d show bacterial density in phage-free treatments from 0 (a), 8 (b), 16 (c) and 32 (d)  $\mu\text{M}$   $\text{HgCl}_2$ , and panels e-h show bacterial density in phage containing treatments from 0 (a), 8 (b), 16 (c) and 32 (d)  $\mu\text{M}$   $\text{HgCl}_2$ . Colours represent individual replicate populations. Bacterial end-point (transfer 20) density was high in all mercury treatments in the absence of phage, but markedly reduced in phage-containing populations regardless of mercury treatment (ANOVA;  $F = 61.74$ , d.f. = 1, 45,  $p < 0.0001$ )

(Bartlett test of homogeneity of variances:  $K^2 = 28.39$ , d.f. = 1,  $p < 0.0001$ ), but did not differ between mercury treatments (Bartlett test of homogeneity of variances:  $K^2 = 2.71$ , d.f. = 3,  $p = 0.438$ ). Phage end-point density and variance were also similar across phage infected treatments regardless of mercury concentration (Fig. 4.3, ANOVA;  $F = 0.225$ , d.f. = 1, 22,  $p = 0.64$ , Bartlett test of homogeneity of variances:  $K^2 = 0.704$ , d.f. = 3,  $p = 0.872$ ).

### **Bacterial resistance**

Resistance to past, future and contemporary phage was assayed using streak-platings of bacteria over pre-dried phage lines. There was a highly significant positive relationship between time-shift and bacterial resistance in mercury-free populations (Fig. 4.4,  $t = 4.81$ , d.f. = 60,  $p < 0.001$ ), indicating the incidence of selective sweeps of resistance mutations occurring in experimental populations.

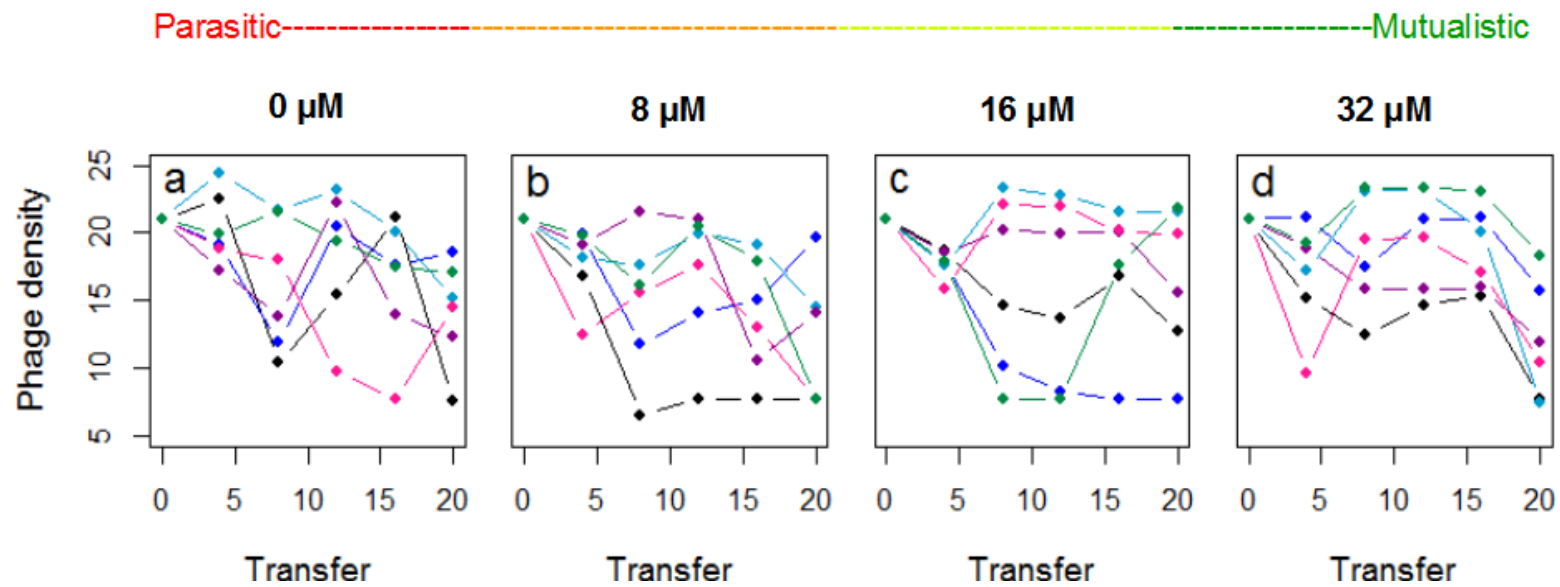


**Figure 4.3.** Phage density over time in 6 replicate populations of each treatment: 0 (a), 8 (b), 16 (c) and 32 (d)  $\mu\text{M}$   $\text{HgCl}_2$ . Colours represent individual replicate populations. Phage end-point (transfer 20) density was not affected by mercury concentration (ANOVA;  $F = 0.225$ , d.f. = 1, 22,  $p = 0.64$ ).

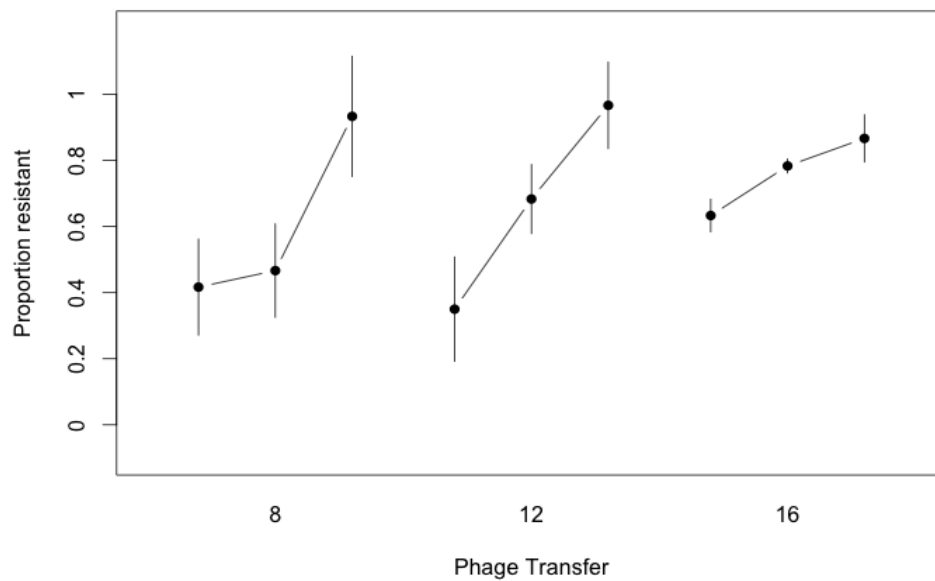


**Figure 4.4.** Rate of phage resistance evolution in bacterial populations at transfers 8, 12 and 16 in mercury-free populations. Points show the mean proportion of resistant clones from past (-4 transfers), present and future (+4 transfers) populations (left to right) when tested against contemporary sympatric phage populations. Means are averages of 6 replicate populations with error bars showing  $\pm 1$  standard error. There was a highly significant positive relationship between time-shift and bacterial resistance in mercury-free populations ( $t = 4.81$ ,  $d.f. = 60$ ,  $p < 0.001$ )

## Discussion

In the absence of positive selection for plasmid-encoded traits, theory predicts a loss of plasmids from the system unless counteracted by high rates of conjugation or amelioration of costs (Subbiah et al. 2011; Lundquist & Levin 1986; Harrison & Brockhurst 2012). We saw no purging of the plasmid in the absence of positive selection in phage-free populations, although plasmid prevalence was lower and more variable in mercury-free populations than in those under selection for plasmid-encoded mercury resistance. The loss or marked reduction of plasmids in the majority of phage-containing treatments

demonstrates that under no positive selection for plasmid-encoded traits, phage infection drives the loss of plasmids. This may be due to indirect competition for replication impeding the transmission ability of plasmids by phage. In phage infected cells, phage hijack the cellular replication machinery in order to replicate, which slows or halts bacterial, and therefore plasmid, replication as no daughter cells are produced. These cells are then lysed to release the new virions, which kills both the cell and effectively the plasmid by preventing both vertical transmission and conjugative transfer. Strong selection for phage resistance will confer a fitness benefit on bacterial cells that do not carry the plasmid, driving prevalence down. In the absence of phage predation, plasmids may be counteracting negative selection through high conjugation rates, which are not achievable in phage-containing populations due to the reduced density of host cells and the destruction of replication machinery caused by phage.

In phage-containing populations, there is considerable variability in the rate of plasmid loss between populations. Plasmids are maintained at high prevalence in each population until they are lost, often suddenly over just a few transfers. This transient bistability in an environment that selects against plasmid persistence suggests that plasmids may be hitch-hiking through linkage with positively-selected bacterial mutations. The selective sweeps of bacterial resistance to phage observed in this experiment are a likely candidate for hitch-hiking by plasmids, as modelled by Bergstrom et al. (2000). If resistance mutations arise in plasmid-containing cells or plasmids successfully transfer into new resistance mutants and those mutants are carried to fixation, the

plasmid may be able to hitch-hike to high frequency. Plasmid-free cells, however, are produced at a constant rate by segregation, and would have a growth rate advantage over plasmid-carrying cells. This would produce cycles of repeated fluctuations in the ratio of plasmid-carrying to plasmid-free cells, until a successful phage-resistance mutation arises in plasmid-free cells. When phage-resistance mutations arise in plasmid-free cells, the growth rate advantage over plasmid-carrying cells would quickly carry plasmid-free resistance to fixation, removing plasmid-carriers from the population.

Phage in this system are likely to impose strong indirect selection on plasmids to reduce the severity of their costs to bacteria through gene loss or reduced gene expression, and/or to increase their conjugation rate to counteract loss. As both phage and plasmids are ubiquitous in natural populations and likely to co-occur, phage are potentially important drivers of the evolution of these key plasmid traits. The dynamics observed here also highlight the potential importance of multi-parasitism on the impact of hitch-hiking. Not only does hitch-hiking affect bacteria-encoded chromosomal genes in linkage (Waite & Shou 2012; Morgan et al. 2012), but also traits encoded by plasmids, and potentially other mobile genetic elements.

In nature, selection for phage resistance may provide the necessary selective sweeps required for maintenance of plasmids by hitch-hiking during periods of absent positive selection, or between selective environments. Bergstrom et al. (2000) state that selective sweeps must be frequent in order to prevent incorporation of plasmid-encoded traits onto the bacterial chromosome. The

host-parasite antagonistic co-evolution of repeated resistance and counter-resistance in *P. fluorescens* and phage  $\Phi 2$  (Paterson et al. 2010), and other bacteria-phage systems may provide a suitable schedule of such selective sweeps for plasmid maintenance in natural environments.

These findings may also have implications for the use of phage therapy in treating bacterial infections. Theory suggests that semi-regular pulses of antibiotic resistance selection can maintain plasmids encoding resistance in bacterial populations despite periods of decline during the absence of selection (Svara & Rankin 2011). If co-infection with phage accelerates the loss of plasmids during periods of low or absent selection, this could shorten the interval needed between bouts of antibiotic use and reduce the evolutionary potential of antibiotic resistance in bacterial populations.

## Conclusions

This study was designed to assess the effects of multi-parasitism on the existence conditions for plasmids. Selection for resistance to phage both accelerated the loss of plasmids from mercury-free environments, and promoted hitch-hiking of plasmids on positively selected resistance mutations. These effects led to fluctuations in plasmid prevalence followed by rapid loss and extinction from populations. Therefore, multi-parasitism in this system limits the existence conditions for plasmid pQBR103.

## 5. Effects of plasmid carriage on phage life history and phage-host dynamics

### Statement of collaboration

This experiment was conducted in collaboration with Dr. Ellie Harrison. We worked together to design the experiment, and Dr. Harrison provided help and guidance on the analysis. I conducted the experiment and collected the data, and all final analyses shown here are my own.

### Introduction

Multiple virus genotypes or species co-infecting a single host cell is a common occurrence in nature and can have profound consequences for virus fitness (Turner 2005). Models of virulence evolution under multi-parasitism predict that genotypes exhibiting a “prudent” phenotype (characterised in phage by a long latent period and late lysis) will suffer a fitness disadvantage in competition with more virulent genotypes which are able to sequester more host resources and lyse sooner, thereby gaining secondary infections at a faster rate (Frank 1996; Nowak & May 1994). This selection for fast lysis will result in higher virulence of phage under multi-parasitism than in single infections. In experiments with *E. coli* and temperate lambdoid phage, Refardt (2011) demonstrated that when induced to lyse, lysis timing was always

controlled by the faster-lysing phage type in double infections. This fast lysis was associated with a competitive advantage over types with much later lysis, with competitive ability following a hierarchical pattern between 11 phage varying in lysis timing. Hamilton (1972) noted that relatedness could be a major factor influencing the evolution of life history in mixed infections. He hypothesized that when members of the same clone or related clones would suffer as a result of host resource depletion, more prudent life histories will evolve to enhance inclusive fitness. However, when competing strains or species are unrelated, the focal parasite benefits from increased virulence, as only unrelated competitors will suffer the costs of host depletion. This “tragedy of the commons” strategy of over-exploitation of the host in unrelated mixed infections has since featured in many theoretical models of virulence evolution (Chao et al. 2000; Frank 1996; Levin & Bull 1994), and have been demonstrated empirically in phage T4 (Eshelman et al. 2010). In the RNA phage  $\Phi 6$ , the effects of multi-parasitism follow a classical prisoner's dilemma strategy of game theory due to shared intracellular products produced by these phage. Cheats evolve when two co-infecting strains are unrelated, which sequester the intracellular products made by cooperators, reducing the overall productivity of phage and consequently reducing rather than increasing virulence in mixed infections (Turner & Chao 1999). Host response to multi-parasitism will also inevitably impact upon parasite fitness. Broad resistance phenotypes may evolve in bacterial populations exposed to multiple genotypes of phage (A. R. Hall et al. 2011; A. Hall et al. 2011), causing reduced fitness for phage and promoting the

evolution of costly infectivity traits (Poullain et al. 2008) which may impact upon life history. Alternatively, specific resistance mutations to locally adapted phage may reduce bacterial capability to resist invading phage genotypes, resulting in increased fitness of the rare genotype in mixed phage infections .

The effects of mobile genetic elements such as plasmids on phage life history are likely to be similar to the effects of non-related antagonistic competitors through their physiological and ecological effects on the host. Plasmids are a common feature of microbial communities and carry a variety of ecologically and clinically important traits such as heavy metal tolerance (Silver & Misra 1988; Lilley & Bailey 1997a) and antibiotic resistance (Archer & Johnston 1983; Mazel & Davies 1999). In environments where plasmids enhance bacterial fitness, they are maintained at high frequency in host populations (Dionisio et al. 2005; Heuer et al. 2007), and so are likely to impact upon phage fitness both in natural and clinical settings. The biosynthetic costs of plasmid carriage will restrict the host's ability to endure the costs of phage infection, thereby reducing the host resources available for phage progeny production; effectively an indirect competition between plasmid and phage. This indirect competition for host resources may select for increased virulence through faster lysis in a “tragedy of the commons” type response. The costs of plasmid carriage may also reduce the capacity of the host to evolve resistance to phage. Phage resistance mutations are often detrimental to bacterial fitness in the absence of phage due to antagonistic pleiotropy (Lenski 1988), which demonstrates the substantial costs of resistance evolution. Therefore, bacteria carrying plasmids may have limited

capacity to endure further decreases in fitness imposed by phage resistance evolution, which will result in decreased resistance to phage and reduce the rate of resistance/infectivity co-evolution. The dual costs of phage predation and plasmid carriage will negatively impact on bacterial growth, reducing the population density (as in phage-infected plasmid-carrying populations in chapter 4). Reduced host density may select for a more prudent phage life history strategy with a reduced adsorption rate and later lysis (Abedon et al. 2003a; Abedon 1989; Crossan et al. 2007; Wang et al. 1996).

The current literature on phage and multi-parasitism is focused on the effects of multiple genotypes or species of phage infecting host populations (Turner & Chao 1999; Turner 2005; Refardt 2011; Eshelman et al. 2010), and how the degree of relatedness influences virulence. The effects of mobile genetic elements on phage life history and phage-host dynamics are yet to be explored.

In chapter 4, we demonstrated that there was an antagonistic relationship between phage  $\Phi 2$  and plasmid pQBR103 in *P. fluorescens*, and that the persistence of the plasmid when phage were present depended upon the degree of positive selection for plasmid-encoded mercury resistance. In this chapter, I investigate the effects of plasmid carriage on phage life history evolution and phage-host dynamics. I predict that, due to the physiological costs of plasmid carriage, there will be reduced bacterial resistance to phage, and phage will consequently persist at higher density in plasmid-carrying populations. As plasmid carriage is predicted to limit the host resources available to phage for reproduction, a more virulent life history strategy may be favoured.

Alternatively, the predicted reduction of bacterial density in plasmid-carrying populations may select for a more prudent life history strategy.

## Methods

### Selection experiment

12 microcosms were initiated in 6 ml KB with 8  $\mu\text{M}$   $\text{HgCl}_2$  in 30 ml sterile disposable glass universals. 8  $\mu\text{M}$   $\text{HgCl}_2$  was used, as this concentration is an approximately neutral environment for plasmid carriage, where it imparts neither a strong positive or negative effect on the host, but is sufficient for maintenance of plasmid prevalence. 6 microcosms were inoculated with a single fresh colony of *Pseudomonas fluorescens* strain SBW25- $\Omega\text{Gm}$  (plasmid-free) and 6 were inoculated with the same strain containing the conjugative plasmid pQBR103 (plasmid-containing). These populations were incubated at 28°C, shaken at 180 rpm. After 48 h growth ( $\sim 10^7$  cells  $\text{ml}^{-1}$ ), 60  $\mu\text{l}$  of each population were transferred to fresh microcosms and inoculated with 6  $\mu\text{l}$  of a  $10^{11}$  virions  $\text{ml}^{-1}$  *P. fluorescens* bacteriophage SBW25 $\Phi$ 2 ancestral stock suspension (Transfer 1). All cultures were incubated at 28 °C, 180 rpm and 1% of mixed culture transferred to a fresh 6 ml microcosm every 48h for 20 serial transfers (c. 130 bacterial generations).

### Population densities and bacterial morphology

At every 4<sup>th</sup> transfer, bacterial populations were plated for density and colony morphology determination, and  $\Phi$ 2 populations were filter-sterilised and spot-

plated for titration. Aliquots of mixed culture were frozen with 20% glycerol at -80°C. In order to assess any morphological adaptation, plated colonies were visually assessed for morphology and scored as either wild-type (usual smooth colony morphology), mucoid (raised, viscous colonies), fuzzy (fuzzy spreaders) or wrinkly (wrinkly spreaders).

### Plasmid prevalence

To confirm the presence of plasmid in plasmid-containing populations throughout the experiment, at every 4<sup>th</sup> transfer, 20 individual colonies of *P. fluorescens* from each evolving plasmid-containing population were PCR analysed for plasmid presence. Colonies were randomly selected from plated samples of each population and grown in 96-well plates for 48h at 28°C. These cultures were then screened for plasmid presence using primers targeting the mercury resistance operon *merA* (for: 5'-TGCAAGACACCCCCTATTGGAC-3' and rev: 5'-TTCGGCGACCAGCTTGATGAAC-3') and the putative origin of replication *oriV* (for: 5'-TGCCTAATCGTGTGTAATGTC-3' and rev: 5'-ACTCTGGCCTGCAAGTTTC-3'). The full PCR protocol is outlined in appendix II.

### Resistance assay

At every 4<sup>th</sup> transfer, 20 individual colonies of *P. fluorescens* were randomly selected from plated samples of each population and grown in 96-well plates for 48h at 28°C. These cultures were then streak plated over lines of filter-sterilised  $\Phi$ 2, which had been allowed to dry on 1.2% KB agar. Colonies were streaked over lines of  $\Phi$ 2 from contemporary sympatric populations, 4 transfers in the

past from the same evolving lineage and 4 transfers in the future. Plates were incubated inverted at 28°C. After overnight incubation, colonies were visually assessed for resistance to  $\Phi$ 2. Colonies were recorded as sensitive to  $\Phi$ 2 if their growth was markedly inhibited past the point at which they crossed the  $\Phi$ 2 line, and resistant if no inhibition was apparent.

### Phage life history

Filter-sterilised samples of phage populations were taken at the end of the selection experiment (transfer 20), amplified and assayed for life history traits on ancestral plasmid-free hosts following the methods described in chapter 2.

### Life history strategies

As life history strategies are made up of combinations of life history trait values rather than any individual trait in isolation, a principal components analysis was conducted on lysis time, burst size and adsorption rate to assess covariance and look for groupings by strategy.

### Sequence analysis

At the end of the experiment (Transfer 20), filter-sterilised  $\Phi$ 2 populations were Sanger sequenced (Applied Biosystems: ABI PRISM 3130xl Genetic Analyzer) for 5 genes believed to be important in interactions with the host and a control (Table 2.1, chapter 2). The full sequencing protocol is outlined in appendix II. Genes were assembled and aligned using Geneious R7 (created by Biomatters. Available from <http://www.geneious.com/>).

Euclidean distances were calculated in R statistical package (R Core Team 2013) based on binary data of base differences from the ancestor. At each position where a particular base mutation occurred in at least one population, all populations were given a score of 1 if they carried that particular base, 0 if they carried the ancestral base or 0.5 if there was a polymorphism of ancestral and mutant bases. Where two different base mutations occurred between populations at any particular position, that position was scored twice. A neighbour-joining tree of genetic distances between the populations was constructed and rooted by the ancestor.

In addition, a neighbour-joining tree of Euclidean distances was constructed which combined data from all evolved phage populations from all experiments in this thesis. The purpose of this combined tree was to investigate similarities and differences between populations from different experiments and seek evidence of different modes of evolution between treatments.

## Statistical analysis

All statistical analyses were conducted in R statistical package (R Core Team 2013). Outliers were identified using the Grubbs test for outliers (Komsta 2011) and excluded from analyses. Plasmid prevalence was compared at the beginning and the end of the experiment using a Welch's two sample t-test. Bacterial resistance and morphology were analysed in linear mixed effects models with binomial errors, plasmid treatment as a fixed effect, time as a covariate and population as a random effect. Life history traits were analysed using standard

ANOVAs of trait by treatment, correlations between traits were analysed using Pearson's product moment correlations and variance in life history traits was analysed using the Bartlett test of homogeneity of variance between treatments.

## Results

### Plasmid prevalence.

Plasmid prevalence was assessed by PCR every fourth transfer in plasmid-containing populations to confirm plasmid presence. Plasmid prevalence was maintained at or near fixation in plasmid-containing populations throughout the majority of the experiment in all but one population (Fig. 5.1.). In population 2, prevalence declined to 20%, so this population could no longer be considered

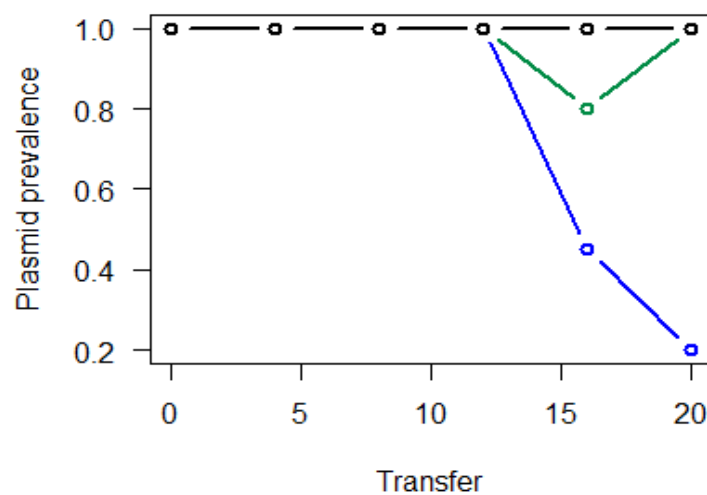


**Figure 5.1.** The proportion of plasmid-carrying cells over time in six replicate populations from the plasmid containing treatment. The black line represents 4 replicate populations which maintained plasmids in 100% of bacterial colonies tested. Other colours represent individual replicate populations. Prevalence in population 2 (blue line) declined to 20%, so this population was excluded from the rest of the analysis.

plasmid-containing and was removed from the rest of the analysis. The level of replication from this point was plasmid-free  $n=6$ , and plasmid-containing  $n=5$ .

### Phage & bacterial densities

To observe host-parasite dynamics, filter-sterilised samples of each evolving population were spot-plated for phage titration at every fourth transfer.

Unfiltered samples were also plated for bacterial density determination. In the absence of plasmid, bacterial density remained high throughout the experiment (Fig. 5.2.a), while phage density tended to peak at transfers 8-12 and then decline, final density varied between populations, and some populations neared extinction (Fig. 5.2.c). In the plasmid-containing populations however, bacterial density dropped to begin with, troughing between transfers 4-12, but recovered to high final density (Fig. 5.2.b). Bacterial end-point density (transfer 20) was lower in plasmid-carrying than in plasmid-free populations (Welch two sample t-test:  $t = 6.4192$ , d.f. = 5.2,  $p = 0.001$ ), and more variable (Bartlett test of homogeneity of variances;  $K^2 = 10.15$ , d.f. = 1,  $p = 0.001$ ). Phage, however, were maintained at high density in plasmid-containing populations, with final densities similar but much less variable compared to plasmid-free populations (Fig. 5.2.d, Welch two sample t-test:  $t = -1.303$ , d.f. = 4,  $p = 0.262$ . Bartlett test of homogeneity of variances;  $K^2 = 23.647$ , d.f. = 1,  $p < 0.001$ ).

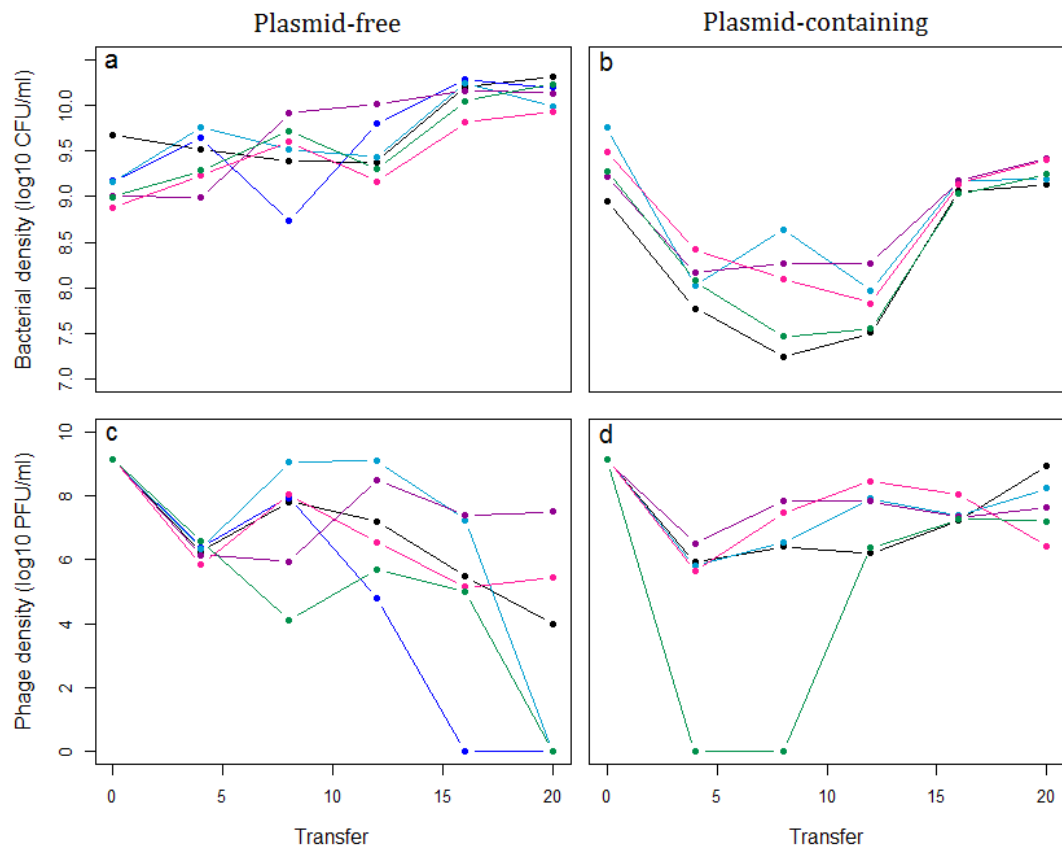


**Figure 5.2.** Bacterial and phage density in 6 replicate populations of each treatment. Panels a and b show bacterial density in plasmid-free and plasmid-carrying treatments, respectively. Panels c and d show phage density in plasmid-free and plasmid-carrying treatments, respectively. Colours represent individual replicate populations. Bacterial end-point density (transfer 20) was lower in plasmid-carrying than in plasmid-free populations (Welch two sample t-test:  $t = 6.4192$ , d.f. = 5.2,  $p = 0.001$ ). Phage final densities (transfer 20) were similar but much less variable in plasmid-containing than plasmid-free populations (Welch two sample t-test:  $t = -1.303$ , d.f. = 4,  $p = 0.262$ . Bartlett test of homogeneity of variances;  $K^2 = 23.647$ , d.f. = 1,  $p < 0.001$ ).

## Bacterial resistance and morphology

Bacterial morphology was visually assessed at every fourth transfer from plated samples of evolving populations. Resistance to past, future and contemporary phage was assayed using streak-platings of bacteria over pre-dried phage lines. Bacterial morphology differed strikingly between the two treatments (Fig. 5.3). In plasmid-free populations, there were transient episodes of mucoidy and fuzzy spreaders, whereas in plasmid-containing populations, mucoidy evolved very rapidly (within the first 4 transfers) and was maintained at much higher frequency throughout (Fig. 5.4.b,  $z = 5.99$ ,  $p < 0.0001$ ). In plasmid-free populations, bacteria evolved significantly higher levels of phage resistance throughout the experiment compared to plasmid-containing populations (Fig. 5.4.a,  $z = -2.430$ ,  $p = 0.015$ ).

## Phage life history

Samples of filter-sterilised phage populations from the end of the selection experiment (transfer 20) were assayed for life history traits adsorption rate, lysis time and burst size. There was a non-significant trend towards slower adsorption in plasmid containing compared to plasmid-free populations (Fig. 5.5.a; ANOVA;  $F = 4.665$ , d.f. = 1,8,  $p = 0.063$ ), and variance in adsorption rate was not significantly different between the two treatments (Bartlett test of homogeneity of variance;  $K^2 = 0.41$ , d.f. = 1,  $p = 0.522$ ).

There was no significant effect of plasmid presence on lysis time (Fig. 5.5.b; ANOVA;  $F = 0.19$ , d.f. = 1,8,  $p = 0.675$ ), and there was no significant difference in

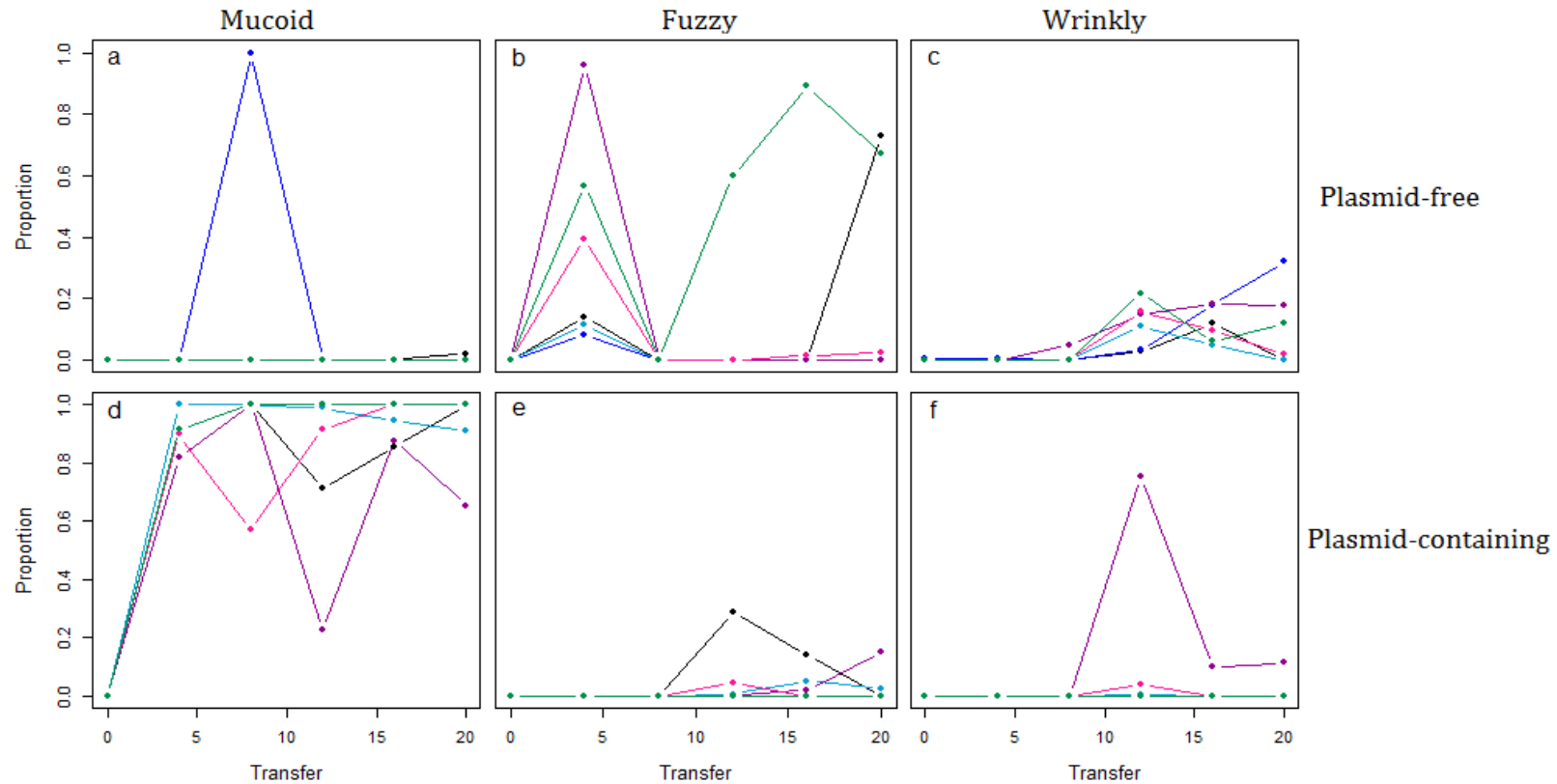


**Figure 5.3.** Bacterial colony morphologies which differ from the ancestral smooth colony type in 6 replicate populations of each treatment. Panels a, b and c show the proportion of all bacterial colonies that were mucoid colonies , fuzzy-spreader colonies and wrinkly-spreader colonies respectively in plasmid-free populations. Panels d, e and f show the proportions of these different phenotypes in plasmid-carrying treatments. Colours represent individual replicate populations. In plasmid-free populations, there were transient episodes of mucoidy and fuzzy spreaders. In plasmid-containing populations, mucoidy evolved rapidly and was maintained at much higher frequency throughout ( $z = 5.99$ ,  $p < 0.0001$ ).

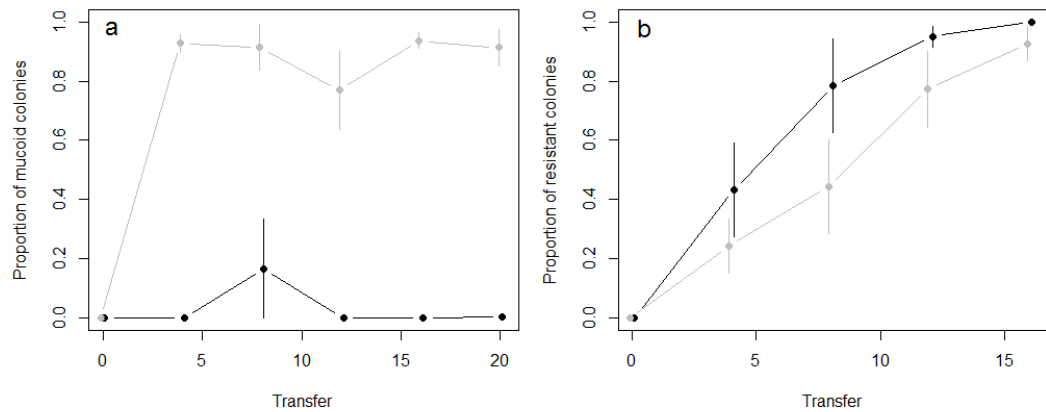


**Figure 5.4.** Proportion of a) phage resistant colonies and b) mucoid phenotype colonies through time for plasmid-free (black) and plasmid-containing (grey) populations. Error bars show 1 standard error for a mean of six independent populations. In plasmid-free populations, bacteria evolved significantly higher levels of phage resistance ( $z = -2.430$ ,  $p = 0.015$ ) and maintained a much higher frequency of mucoidy ( $z = 5.99$ ,  $p < 0.0001$ ) throughout the experiment compared to plasmid-containing populations.

variance between the two treatments (Bartlett test of homogeneity of variance;  $K^2 = 0.048$ , d.f. = 1,  $p = 0.826$ ).

There was no significant effect of plasmid presence on burst size (Fig. 5.5.c; ANOVA;  $F = 0.349$ , d.f. = 1,8,  $p = 0.57$ ), and there was no significant difference in variance between the two treatments (Bartlett test of homogeneity of variance;  $K^2 = 0.294$ , d.f. = 1,  $p = 0.588$ ).

Correlations between pairs of traits were sought in order to elucidate trade-offs, however none of the life history traits were correlated with any other trait across treatments nor within treatments (Pearson's product moment correlations, data not shown).

In order to investigate holistic life history strategies among these key traits, covariance was analysed using principle components analysis. All of the

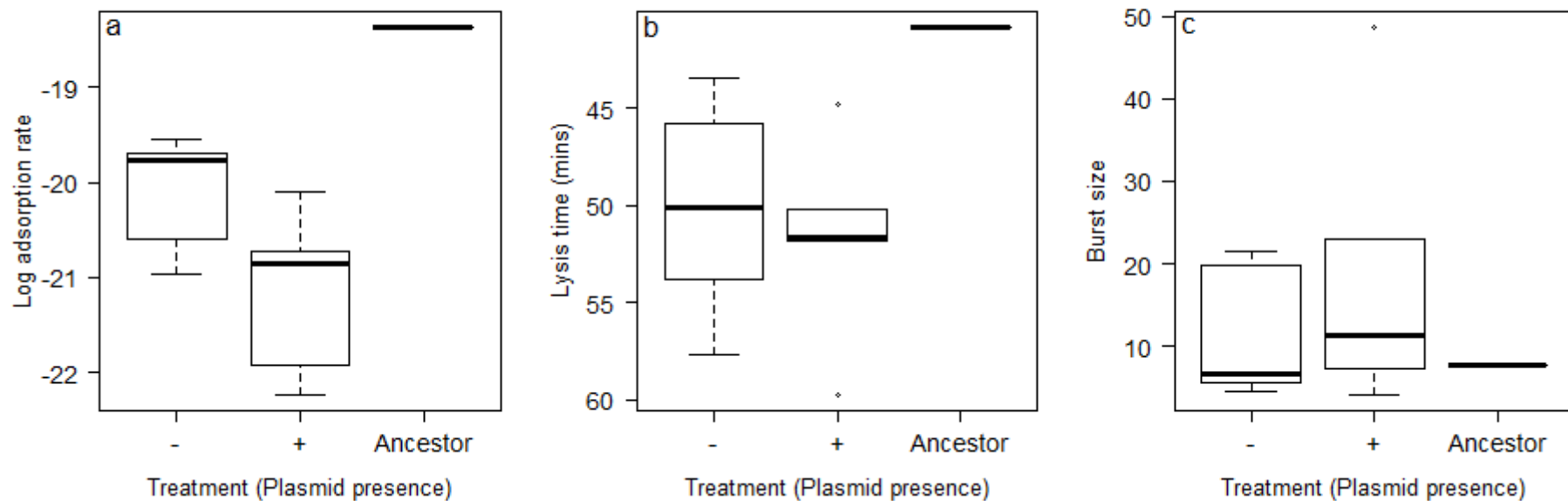


**Figure 5.5.** Life history box and whisker plots of evolved (transfer 20) phage populations from plasmid-free (n=6) and plasmid-containing (n=5) treatments, and the ancestor (n=1). Boxes display the median and interquartile range, and whiskers display the maximum and minimum values of the traits. Panel a displays adsorption rate, which shows a non-significant trend towards slower adsorption in plasmid containing compared to plasmid-free populations (ANOVA;  $F = 4.665$ , d.f. = 1,8,  $p = 0.063$ ). Panel b shows lysis time, which was not affected by plasmid presence (ANOVA;  $F = 0.19$ , d.f. = 1,8,  $p = 0.675$ ), and panel c shows burst size, which was also not affected by plasmid presence (Fig. 5.5.c; ANOVA;  $F = 0.349$ , d.f. = 1,8,  $p = 0.57$ ).

variance in the life history data was explained by PC1 (90%) and PC2 (10%). PC1 was strongly associated with burst size and with lysis, whilst PC2 was associated with adsorption rate and lysis (Fig. 5.6). There were no discernible groupings of the data according to PC1 and PC2, suggesting that there was large variance in phage life history strategy both with and without plasmids, and no divergence in strategy between the two treatments.

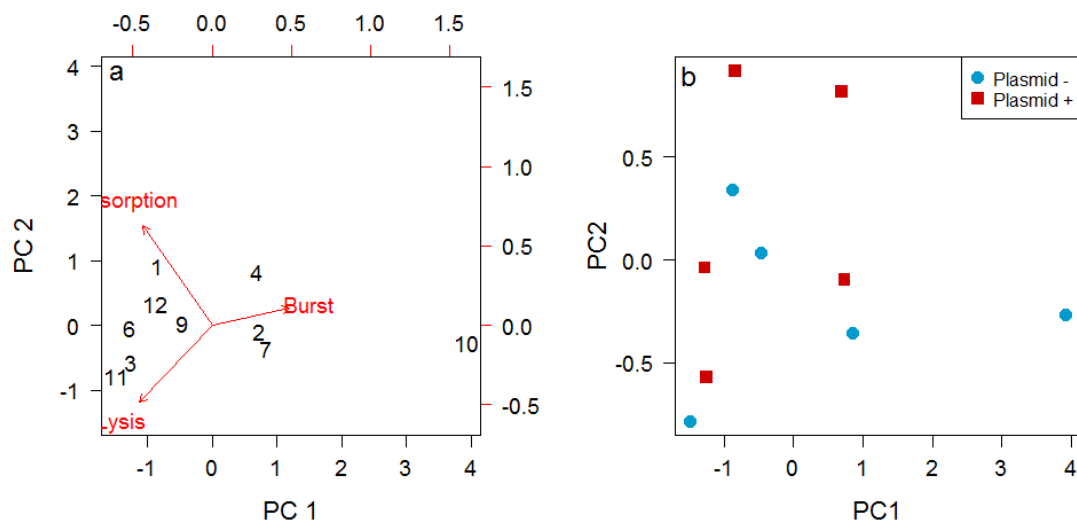


**Figure 5.6.** Principal components analysis. Panel a is the loadings biplot showing the principal component scores of the individual populations (lower x axis = PC1, left y axis = PC2), and the relative loadings of the life history variables (red arrows, upper x and right y axes). Numbers correspond to individual populations. Panel b is the traits biplot which shows the location of each population from the plasmid-free (n=5, blue circles) and plasmid-containing (n=5, red squares) treatments in trait space according to principal components scores on PC1 and PC2.

## Phage evolution

Evolved phage populations were Sanger sequenced at the end of the selection experiment (transfer 20) in 5 genes believed to be important in controlling interactions with the host, and a control (see table 2.1). Analysis of sequenced populations revealed possible contamination in population 3 from the plasmid-containing treatment. Removal of this population from analyses did not qualitatively alter the outcomes of phenotypic analyses, but did affect the genetic analyses. For this reason, I assumed that the contamination occurred during preparation for sequencing only, and this population was excluded from genetic analyses. From this point forward, the level of replication is: plasmid-free  $n=6$  and plasmid-containing  $n=4$ .

A number of mutations were identified in the genes studied, which are presented in table 5.1. The majority of mutational events were found in gene *SBWP25\_0036*, which encodes for the tail fibre protein, followed by gene *SBWP25\_0032* which encodes for a tail tubular protein. Only a few mutations were found in genes *SBWP25\_0027*, *SBWP25\_0034* and *SBWP25\_0035* which encode for a predicted virion structural protein, a predicted lysozyme and an internal virion structural protein, respectively, and no mutations were found in the control gene *SBWP25\_0040*, which encodes for a predicted phage lysozyme. There were significantly fewer mutations across all sequenced genes in plasmid-containing (range= 5-7, mean= 5.75) compared to plasmid-free (range= 9-11, mean= 9.8) populations (Fig. 5.7. GLM with Poisson error distribution;  $z = 15.98$ ,

**Table 5.1.** The locations and identities of mutations on the genes sequenced from the end-point (transfer 20) populations. Positions (in base pairs from the start of each gene) are indicated at the top of the table, and the mutations found at that position (base differences from the ancestor) are identified at the bottom of the table. Rows correspond to individual populations. + indicates the presence of the identified mutation in the population, \* indicates the presence of the alternative identified mutation and = indicates the presence of the identified polymorphism.

Gene	SBWP25_0027	SBWP25_0032					SBWP25_0034	SBWP25_0035
Position	331	476	820	857	895	1148	1807	250
<b>Plasmid-free:</b>								
1	+	-	-	-	-	-	-	-
2	+	-	-	-	-	-	-	-
3	+	+	-	-	-	-	-	-
4	+	-	-	-	-	-	-	-
5	+	-	-	-	-	-	-	-
6	+	+	-	-	+	-	+	+
<b>Plasmid-containing:</b>								
1	+	-	+	-	-	-	-	-
4	-	-	-	+	-	-	-	-
5	-	-	-	+	-	-	-	-
6	-	-	-	+	-	-	-	-
Type (+)	Ins AAG	A-G	A-G	A-C	A-G	C-T	T-C	G-A

**Table 5.1 (continued).** The locations and identities of mutations on the genes sequenced from the end-point (transfer 20) populations. Positions (in base pairs from the start of each gene) are indicated at the top of the table, and the mutations found at that position (base differences from the ancestor) are identified at the bottom of the table. Rows correspond to individual populations. + indicates the presence of the identified mutation in the population, \* indicates the presence of the alternative identified mutation and = indicates the presence of the identified polymorphism.

[illegible]

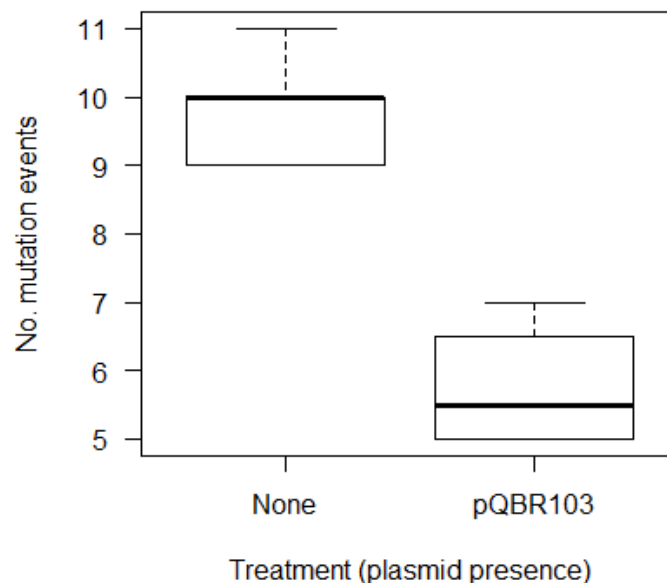


**Figure 5.7.** The number of mutation events across all genes sequenced in plasmid-free (n=6) and plasmid-containing (n=4) treatments. Boxes display the median and interquartile range, and whiskers display the maximum and minimum values. There were significantly fewer mutations across all sequenced genes in plasmid-containing compared to plasmid-free populations (GLM with Poisson error distribution;  $z = 15.98$ , d.f. = 7,  $p = << 0.0001$ ).

d.f. = 7,  $p = << 0.0001$ ). The variance in the number of mutation events was not significantly different between treatments (Levene's test for homogeneity of variance:  $F = 0.18$ , d.f. = 1, 7,  $p = 0.685$ ).

Figure 5.8 shows the frequencies of each identified mutational event in each gene within each treatment. In most genes, any one mutation was found in only one or two populations in any one treatment and there were several unique mutations which only occurred in one population in one treatment. In gene *SBWP25\_0036*, however, there were several mutations which occurred in the majority of populations within a treatment.

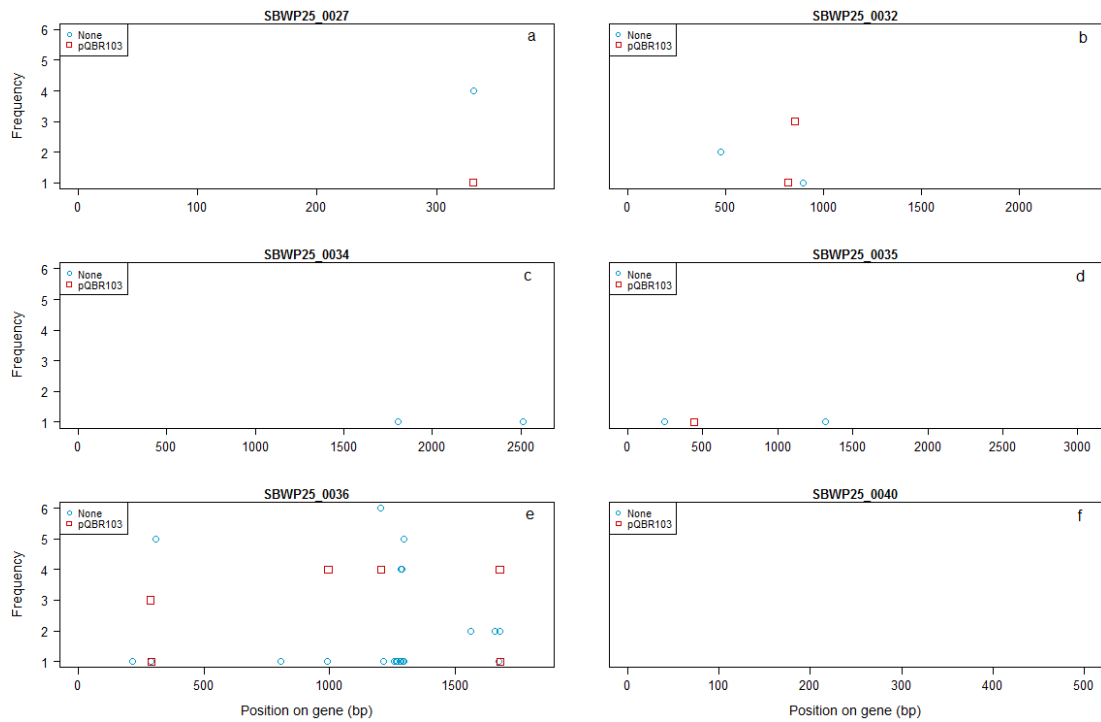


**Figure 5.8.** Frequency of each identified mutation in each gene in end-point (transfer 20) populations from plasmid-free (n=6, blue circles) and plasmid-containing (n=6, red squares) treatments. The x axis shows the bp position of mutations on the gene. a) gene *SBWP25\_0027*, b) gene *SBWP25\_0032*, c) gene *SBWP25\_0034*, d) gene *SBWP25\_0035*, e) gene *SBWP25\_0036*, f) gene *SBWP25\_0040*.

Euclidean genetic distances of each population from the ancestor were generally higher in plasmid-free treatments than plasmid-containing treatments (Fig. 5.9).

A neighbour-joining tree of Euclidean distances is displayed in figure 5.10.

Plasmid-free and plasmid-containing populations form two distinct groups, and branch lengths are shorter in plasmid-containing than plasmid-free populations.

The combined neighbour-joining tree of all evolved populations from all experiments is displayed in figure 5.11. In general, populations that evolved without co-evolution with the host (UV populations from the evolved treatments with high or no UV from chapter 3, and all populations from the spatial structure

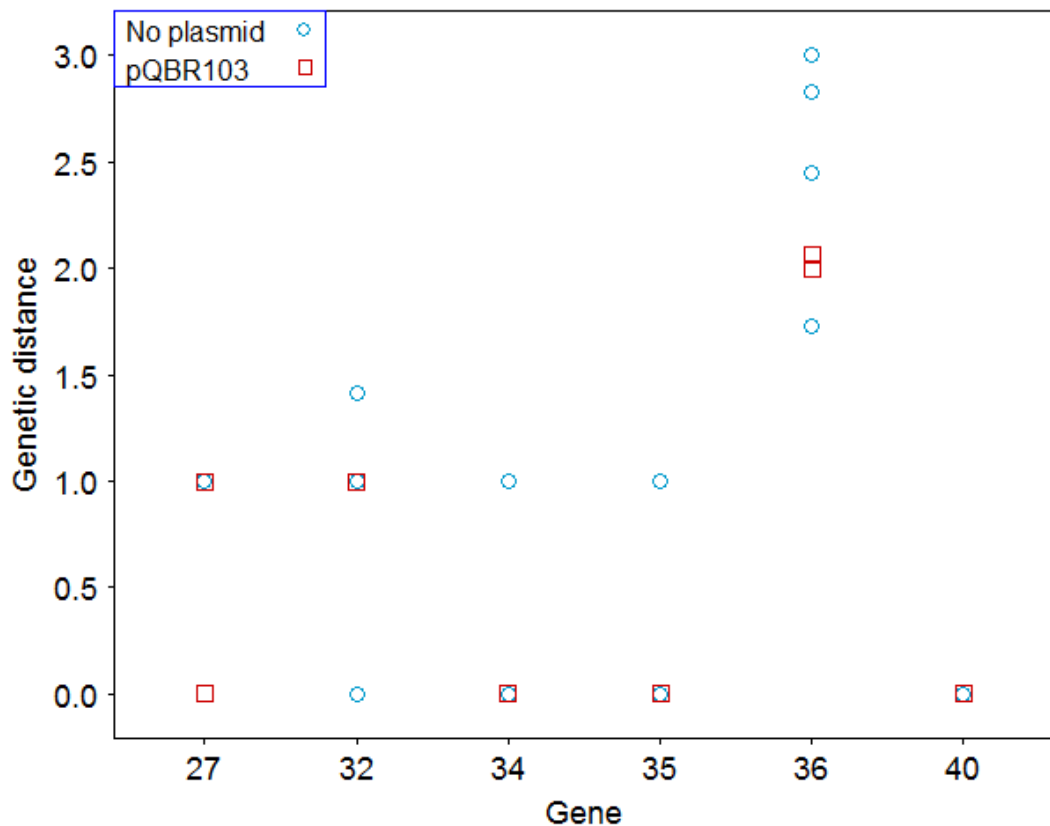


**Figure 5.9.** Pairwise euclidean distance from the ancestor in each gene in populations from plasmid-free (n=6, blue circles) and plasmid-containing (n=6, red squares) treatments. The x axis denotes the gene (*SBWP25\_0027* = 27, etc).

experiment from chapter 2) have the shortest branch lengths and group together separately from the populations that were co-evolved with the host (UV populations from the co-evolution treatments with high or no UV from chapter 3, and both plasmid-containing and plasmid-free populations from this chapter). Amongst the populations not co-evolved with the host, populations from the UV experiment (chapter 3) grouped separately from the spatial structure experiment (chapter 2). Amongst populations that were co-evolved with the host, plasmid-free populations from this chapter grouped with UV populations

(chapter 3), but plasmid-containing populations grouped separately from everything else within the co-evolution group.

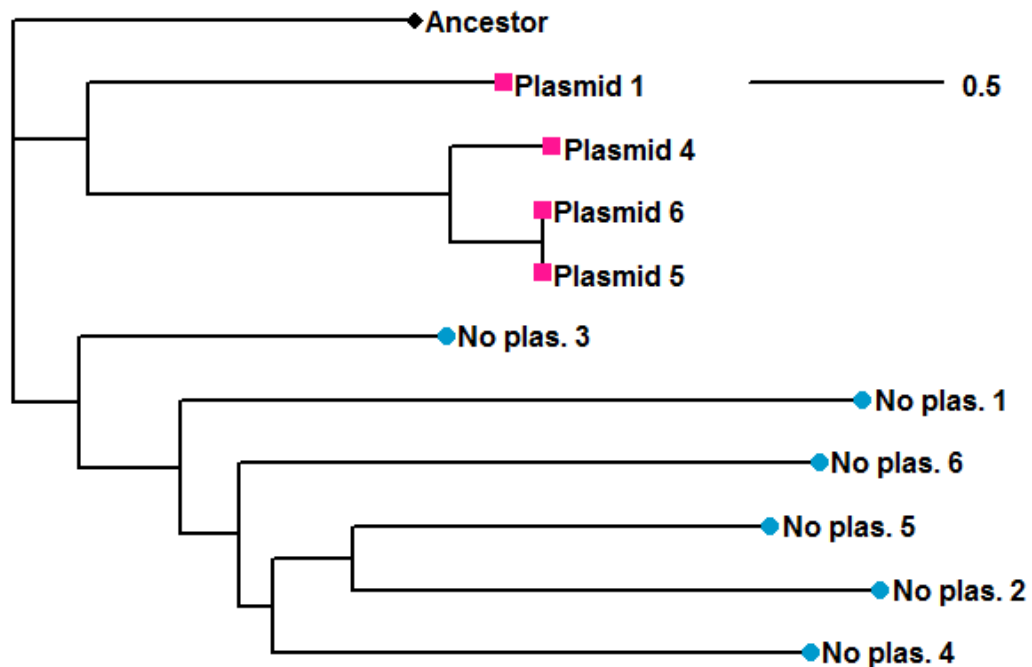


**Figure 5.10.** Neighbour-joining tree of pairwise Euclidean distances between 10 end-point (transfer 20) populations and the ancestor in all genes in table 2.1 (Chapter 2). Based on binary data of base substitutions from the ancestor, rooted by the ancestor (black diamond). Plasmid-free populations are labelled No plas. (blue circles). Plasmid-containing populations are labelled Plasmid (pink squares).

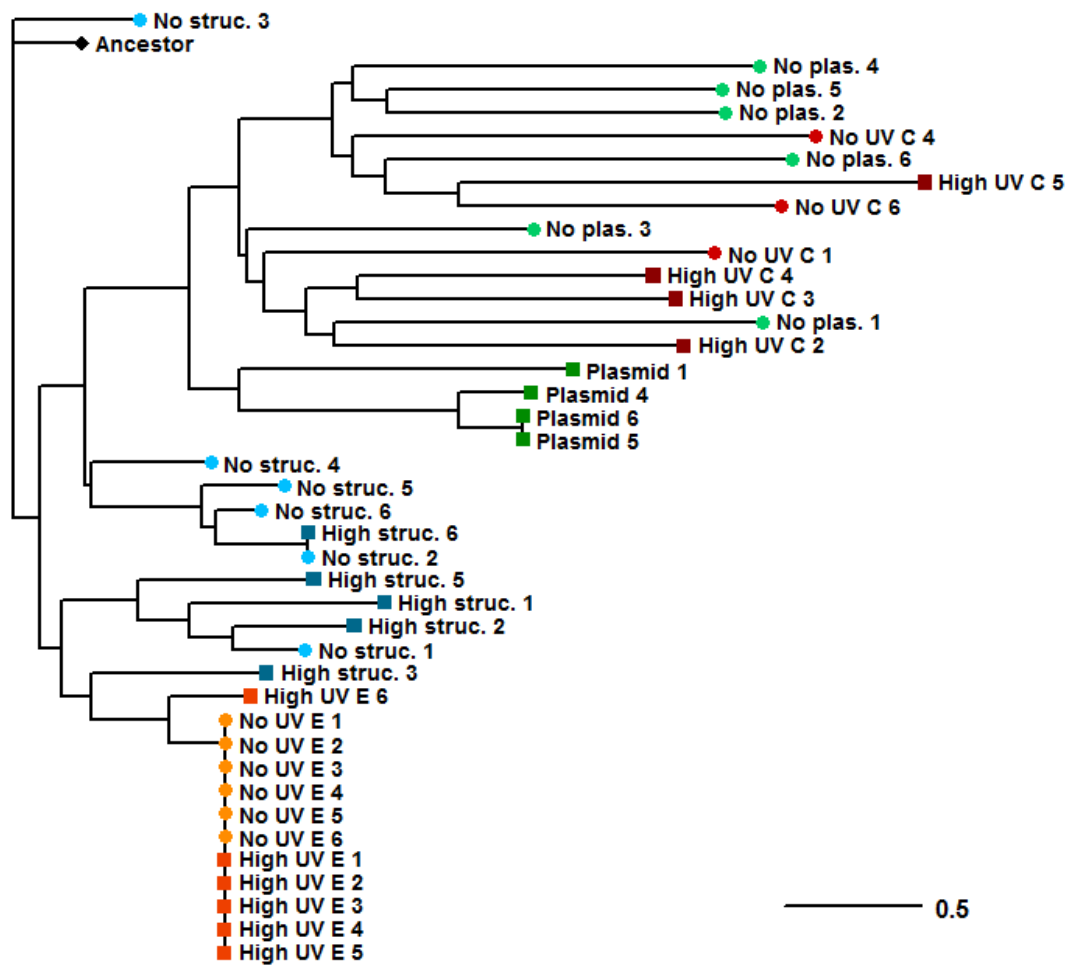


**Figure 5.11.** Combined neighbour-joining tree of pairwise Euclidean distances between 40 end-point (transfer 18 or 20) populations from chapters 2, 3 and 5, and the ancestor in all genes in table 2.1 (Chapter 2). Based on binary data of base substitutions from the ancestor, rooted by the ancestor (black diamond). 0% Pluronic populations from chapter 2 are labelled No struc, light blue circles. 16% Pluronic populations from chapter 2 are labelled High struc, dark blue squares. 0% mortality populations from chapter 3 are labelled No UV E (evolved, light orange circles) and No UV C (co-evolved, light red circles). 90% mortality populations from chapter 3 are labelled High UV E (evolved, dark orange squares) and High UV C (co-evolved, dark red squares). Plasmid-free populations from chapter 5 are labelled No plas. (light green circles). Plasmid-containing populations from chapter 5 are labelled Plasmid (dark green squares).

## Discussion

Plasmid carriage in host populations under phage predation in this system produced a reduction in host resistance to phage as predicted due to the physiological costs associated with plasmid carriage. An interesting finding which was not predicted is the promotion of mucoid conversion in plasmid carriers. Mucoidy in *Pseudomonads* is believed to be a general response to various stressors, and is known to afford some resistance to phage, as it produces a protective capsule around the cell which is believed to make adsorption more difficult (Fischer et al. 2004; Scanlan & Buckling 2012). Mucoid conversion is caused by the overproduction of alginate, which results in a viscous, opaque culture and raised, viscous colonies. The initial drop in bacterial density under the dual burden of plasmid carriage and phage predation indicates an additive fitness cost, more than that experienced with either parasite alone. The high levels of mucoid conversion observed in plasmid-carrying populations in this experiment may therefore represent a faster and less costly defence against phage predation than resistance mutation in bacteria already burdened with the biosynthetic costs of plasmid carriage. Resistance mutations to phage are known to frequently cause antagonistic pleiotropic effects which negatively affect bacterial fitness in phage-free environments (Lenski 1988). Although the mucoid phenotype is also costly to bacteria in the absence of phage (Scanlan & Buckling 2012), it is likely that mucoidy incurred lower fitness costs than antagonistic pleiotropic mutations.

Mucoidy offers only partial resistance to an evolving phage enemy, so overall resistance to phage was reduced in plasmid-carrying populations, whilst in plasmid-free populations the usual antagonistic co-evolution observed in this system kept resistance high. Towards the end of the experiment in plasmid-carrying populations we saw a recovery of both resistance and bacterial densities, although neither reached the levels seen in plasmid-free populations. This suggests that either resistance mutations may begin to arise later in plasmid-carrying populations at low frequencies, allowing recovery of the population, or that there is an amelioration of the costs of either plasmid carriage or mucoidy. Further work is needed to distinguish between these possible effects. Mucoidy in Pseudomonads is best studied in *Pseudomonas aeruginosa*, where it is a common feature of clinical isolates from cystic fibrosis patients (Deretic & Schurr 1994). In cystic fibrosis, mucoid conversion is a key virulence factor and is associated with acute symptoms and a poor prognosis for patients (Li et al. 2005; Henry et al. 1992). Plasmids encoding for antibiotic resistance are known to occur in *P. aeruginosa* in cystic fibrosis patients (Livermore 2002), and a number of phage and prophage have been successfully isolated from the lungs and sputum of cystic fibrosis patients (Tejedor et al. 1982), suggesting that plasmid-phage co-infection may be common in this system. If mucoidy in cystic fibrosis infections is caused by interactions between plasmids and phage, it raises serious concerns for the use of phage therapy to treat these and other bacterial infections where mucoidy is associated with disease severity.

Phage life history remained similar between the two plasmid treatments, except a non-significant trend towards slower adsorption in plasmid-containing populations. This is consistent with the evolution of a more prudent life history strategy in the plasmid-containing treatment. Life history theory predicts that in structured environments such as in our mucoid populations, phage will evolve slower adsorption rates in order to allow virions to diffuse further before attachment, thereby avoiding “kin shading” competition with identical genotypes (Abedon & Culler 2007a; Wild et al. 2009; Boots & Sasaki 1999). Mucoidy in the plasmid-carrying populations may therefore have driven the evolution of a slower adsorption rate. This is consistent with the fact that although plasmid-carrying populations had fewer mutations overall, most of the mutations were found on gene SBWP25\_0036, which encodes the tail fibre protein. The tail fibre protein is known to be an important determinant of specificity of binding in  $\Phi 2$  (Paterson et al. 2010), so is likely to be the main source of variation in adsorption rate. Alternatively, reduced adsorption rate could be a result of increased specialisation to non-ancestral host genotypes reducing the ability of co-evolved phage to infect the ancestral host (Poullain et al. 2008).

Phage density was maintained at high levels throughout the experiment in plasmid-containing populations, despite the lack of mutation indicating a reduced rate of infectivity evolution. This is consistent with the notion that the host is evolving mucoidy in place of resistance mutations, freeing phage from antagonistic co-evolution. An alternative explanation for this effect is that spatial

structure provided by mucoidy may have promoted a more stable co-existence of phage and the host by providing temporary refugia from phage attack. In the related species *Pseudomonas aeruginosa* and its phage PP7, spatial heterogeneity constrained phage evolution by providing ephemeral refugia for susceptible bacteria that served to replenish sensitive hosts at each transfer (Brockhurst et al. 2006). It is beyond the scope of this work to determine between these possible effects. Regardless of the mechanism, the lack of antagonistic co-evolution observed in this experiment has resulted in a reduced evolutionary rate in phage from plasmid-containing populations, as evidenced by the shorter genetic distance from the ancestor in phage from plasmid-carrying populations.

When combined with all other co-evolving populations in this thesis, plasmid-containing populations group together on a separate node in the neighbour-joining tree. This lends further support to the idea of a lack of antagonistic co-evolution in this treatment and an alternative trajectory of evolution. Phage released from an antagonistic arms race, but faced with mucoid host cells may instead be evolving specialisation to mucoidy, which would allow them to maintain the high densities observed in this experiment. Alternatively, direct or indirect interactions with plasmids may be driving a novel evolutionary trajectory such as increased efficiency of resource use. Further investigation into the function of these different evolutionary trajectories is necessary to elucidate the drivers and consequences of this alternative route.

## Conclusions

Plasmid carriage impedes the evolution of phage resistance mutations in *Pseudomonas fluorescens*, but promotes mucoid conversion. Mucoid conversion selects for phage with reduced adsorption rates, but there is no overall shift in life history strategy. The restriction of host resistance to phage frees phage from antagonistic co-evolution, reducing the evolutionary rate and allowing them to evolve specialism to persist at higher frequency in the host population. These findings raise concerns for the use of phage therapy in systems where antibiotic resistance is carried on plasmids and mucoidy is associated with disease severity, such as in cystic fibrosis.

## 6. General Discussion

Parasite life history theory predicts that lifetime reproductive success evolves through differential allocation to life history traits constrained by trade-offs (Stearns 1992; Stearns 1989). These life history traits govern the characteristics of parasites such as their virulence, transmission and infection phenotypes, so understanding their evolution is important for infectious disease prediction and management (Poulin 1996). Evolution in trade-offs is driven by abiotic and biotic factors in the environment, with different environments selecting for different optimal life history values (Poulin 1996; Combes 2001; Goldhill & Turner 2014). Whether or not parasites are able to reach their optima may be constrained by phylogeny, physiology and/or ecology, so optimality models may not provide the whole picture (Bull & Wang 2010; Heineman & Bull 2007). The increasingly popular field of experimental evolution is a powerful tool allowing researchers to gain a fuller understanding of the factors and constraints involved in parasite life history evolution (Brockhurst & Koskella 2013; Ebert 1998). In a series of evolution experiments, I explored the effects of common environmental factors on the life history evolution of bacteriophage  $\Phi 2$ , and the effects of co-occurrence of phage and plasmid on each other and the host. I discovered that the evolution of life history in this phage is sensitive to spatial structure, UV-C exposure and co-parasitism with plasmids, and that this evolution can be mediated by co-evolution with the host. I found no direct evidence of trade-offs between the key life history traits – in each experiment,

significant directional change due to treatment was observed in only one of the traits. However, evolved populations showed high variance in life history traits, which may have obscured evidence for trade-offs. There was some limited evidence for evolution of multiple life history strategies, but it is not clear whether these are adaptive strategies or simply an artefact of increased variance.

Most of the genetic mutation was found on gene *SBWP25\_0036* encoding for tail fibres, with some mutation on the other genes investigated under co-evolved treatments only. No direct link between mutation and phenotype could be elucidated, suggesting that evolution in life history is either governed by genes not examined in this thesis, or involves epistasis and pleiotropy with genes elsewhere on the genome (Scanlan et al. 2011).

In **Chapter 2** I explored the effects of spatial structure on phage evolving against a static ancestral host, and found that increased structure selects for later lysis, as predicted by models. However, the associated increase in burst size as predicted by theory was not observed. This suggests that the relationship between lysis time and burst size is not strictly linear as usually presumed (Abedon & Yin 2009; Goldhill & Turner 2014). Spatial structure was also found to break down the correlation between adsorption rate and lysis time, which suggests that lysis time can evolve independently of adsorption rate and burst size to some degree. There was some limited evidence of multiple life history strategies emerging in structured populations, suggesting that the evolution of life history is not always parallel, even between initially isogenic replicate

populations. I found similar variation in life history strategy in **Chapter 3** in UV-C irradiated populations, but it is not clear whether these were adaptive shifts towards multiple life history strategies or a consequence of non-targeted random mutagenesis. In **Chapter 3** I found no directional evolution of life history traits due to UV treatment in evolved populations, although this may be due to the absence of opportunity for photoreactivation. In co-evolved populations, UV irradiated populations evolved a larger burst size, and greater variance in both burst size and lysis time. A larger burst size may be an adaptation to increased extracellular mortality, the larger number of progeny increasing the chances of a fraction surviving. The number of mutations in co-evolved populations were more variable in those evolved to UV-irradiation but not higher on average, and the identities of the mutations were different between UV-irradiated and not irradiated populations.

**Chapters 4 and 5** investigated the effects of co-occurrence of the common symbionts  $\Phi 2$  and plasmid pQBR103, which confers mercury resistance on the host. We found striking ecological effects of each symbiont on each other and on the host. In **chapter 4**, plasmid prevalence in the absence of mercury was stably intermediate in the absence of phage, but showed transient bistability followed by rapid extinction in populations under phage predation. This demonstrated that in this system, phage limit the existence conditions for plasmids. Plasmids are able to persist for short periods by hitch-hiking on phage resistance mutations, but eventually the dual costs of phage and plasmids on the host drive plasmids to extinction. **Chapter 5** assessed the impact of plasmids on phage life

history and phage-host dynamics when plasmids were positively selected. The presence of plasmids impeded the evolution of host resistance to phage, releasing phage from Red Queen dynamics. This resulted in a reduced rate of mutation in phage in plasmid-containing populations, as evidenced by shorter Euclidean distance from the ancestor. Interestingly, hosts developed a high prevalence of mucoidy in response to the dual burden of plasmids and phage, which we interpret to represent a less costly quantitative resistance mechanism than qualitative resistance mutations. It is unclear whether the reduced adsorption rate evolved in phage populations co-existing with plasmids represents an adaptation to the structured environment of a mucoid host, or to the reduced host density caused by the dual costs of hosting both parasites.

## Implications

The current work highlights the complex nature of life history evolution in parasites, even in relatively simple microorganisms such as phage. Although some general predictions, for example that spatial structure should select for prudence (Boots & Meador 2007) may hold (chapter 2), the specific mutational and phenotypic trajectory towards prudence may vary between species (Gallet, Tully, et al. 2009; Dennehy 2009) and even between populations. In  $\Phi 2$ , prudence in structured environments was achieved by the evolution of later lysis, but the expected correlations of lysis time with adsorption rate and burst size were not found, and lysis time was highly variable between populations. The failure of burst size in particular to covary with lysis time suggests that

trade-offs may not constrain the evolution of these traits as tightly as believed, and that multiple strategies may be in operation simultaneously. Therefore, general predictions of parasite life history evolution may be misleading, which raises questions about the suitability of predictive models in emerging disease prediction and management.

This thesis also emphasises the importance of considering the host's parasite community when predicting the behaviour of infections and the impact of medical intervention. The ever-increasing problem of antibiotic resistance, which is often plasmid-encoded (Livermore 2002), has prompted a recent revival of the study of phage as anti-bacterial agents. The data presented here offer both an encouragement and a caution to the field of phage therapy – whilst phage may accelerate the loss of antibiotic resistance carrying plasmids in the absence of positive selection for plasmid-encoded traits, the associated mucoid conversion could be a major issue when mucoidy affects the severity of symptoms and patient prognosis (Li et al. 2005; Henry et al. 1992). Additionally, phage therapy used simultaneously with antibiotics may not be effective at removing antibiotic resistant infections, as strong selection for plasmid encoded traits provided by antibiotic use may maintain plasmid prevalence regardless of phage presence. If phage therapy is to be successful, a carefully planned schedule of antibiotic and phage usage may be the best approach. As such, phage therapy may be best employed as an alternative to antibiotics, and only when mucoidy is not a major virulence factor.

Further studies would benefit from whole genome sequencing to identify potential adaptive mutations elsewhere on the genome and elucidate any epistatic or pleiotropic effects. Larger numbers of replicate populations and longer-term studies would help to determine whether the increased variation seen in the evolved populations does reflect the evolution of multiple adaptive strategies or simply an artefact of increased mutation rate. Competitive fitness assays between evolved populations would also contribute to our understanding of the fitness effects of the phenotypic and genetic evolution observed here.

## Conclusions

Experimental evolution with a host-parasite system reveals that the evolution of parasite life history is more complex than a single trajectory towards a predicted optimum, and constraints between life-history traits do not prevent some degree of independent evolution of individual life-history traits. Co-evolution with the host provides additional mutational input, resulting in a greater degree of evolution in co-evolved populations. It is important to consider the specific ecology of the focal parasite, its host and any co-occurring symbionts in order to make informed predictions of life history evolution, and general predictions may not be achievable. Co-parasitism with phage and plasmid may provide the necessary conditions for plasmid persistence under fluctuating selection for plasmid-encoded traits. The efficacy and suitability of phage as therapeutic agents against plasmid-encoded antibiotic resistance is complicated, and caution should be used to prevent potential exacerbation of disease symptoms.

## References

- Abedon, S.T., 1989. Selection for bacteriophage latent period length by bacterial density: A theoretical examination. *Microbial Ecology*, 18(2), pp.79–88.
- Abedon, S.T. & Culler, R.R., 2007a. Bacteriophage evolution given spatial constraint. *Journal of theoretical biology*, 248(1), pp.111–9.
- Abedon, S.T. & Culler, R.R., 2007b. Optimizing bacteriophage plaque fecundity. *Journal of theoretical biology*, 249(3), pp.582–92.
- Abedon, S.T., Hyman, P. & Thomas, C., 2003a. Experimental examination of bacteriophage latent-period evolution as a response to bacterial availability. *Applied and environmental microbiology*, 69(12), p.7499.
- Abedon, S.T., Hyman, P. & Thomas, C., 2003b. Experimental Examination of Bacteriophage Latent-Period Evolution as a Response to Bacterial Availability Experimental Examination of Bacteriophage Latent-Period Evolution as a Response to Bacterial Availability. , 69(12).
- Abedon, S.T. & Yin, J., 2009. Bacteriophage plaques: theory and analysis M. R. J. Clokie & A. M. Kropinski, eds. *Methods Mol Biol*, 501, pp.161–174.
- Alizon, S. et al., 2009. Virulence evolution and the trade-off hypothesis: history, current state of affairs and the future. *Journal of evolutionary biology*, 22(2), pp.245–59.
- Anderson, R. & May, R., 1982. Coevolution of hosts and parasites. *Parasitology*.
- Anderson, R.M. & May, R.M., 1978. Regulation and stability of host-parasite interactions: I. Regulatory processes. *Journal of Animal Ecology*, 47, pp.219–247.
- Archer, G. & Johnston, J., 1983. Self-transmissible plasmids in staphylococci that encode resistance to aminoglycosides. *Antimicrobial agents and chemotherapy*, 24(1), pp.70–77.
- Barber, I., Hoare, D. & Krause, J., 2000. Effects of parasites on fish behaviour: a review and evolutionary perspective. *Reviews in Fish Biology and Fisheries*, 10, pp.131–165.
- Bawden, F. & Kleczkowski, A., 1953. The behaviour of some plant viruses after exposure to ultraviolet radiation. *Journal of general microbiology*, 8, pp.145–156.
- Bergstrom, C.T., Lipsitch, M. & Levin, B.R., 2000. Natural selection, infectious transfer and the existence conditions for bacterial plasmids. *Genetics*, 155(4), pp.1505–19.
- Bernstein, C., 1981. Deoxyribonucleic acid repair in bacteriophage. *Microbiological reviews*, 45(1), pp.72–98.

- Bonhoeffer, S., Lenski, R.E. & Ebert, D., 1996. The curse of the pharaoh: the evolution of virulence in pathogens with long living propagules. *Proceedings. Biological sciences / The Royal Society*, 263(1371), pp.715–21.
- Boots, M. & Meador, M., 2007. Local interactions select for lower pathogen infectivity. *Science (New York, N.Y.)*, 315(5816), pp.1284–6.
- Boots, M. & Sasaki, A., 2002. Parasite-driven extinction in spatially explicit host-parasite systems. *The American naturalist*, 159(6), pp.706–13.
- Boots, M. & Sasaki, A., 1999. “Small worlds” and the evolution of virulence: infection occurs locally and at a distance. *Proceedings. Biological sciences / The Royal Society*, 266(1432), pp.1933–8.
- Boots, M. & Sasaki, A., 2000. The evolutionary dynamics of local infection and global reproduction in host-parasite interactions. *Ecology Letters*, 3(3), pp.181–185.
- Brockhurst, M., Buckling, A. & Rainey, P.B., 2006. Spatial heterogeneity and the stability of host-parasite coexistence. *Journal of evolutionary biology*, 19(2), pp.374–9.
- Brockhurst, M. & Morgan, A., 2007. Experimental coevolution with bacteria and phage: The *Pseudomonas fluorescens*— $\phi$ 2 model system. *Infection, Genetics and Evolution*, 7(4), pp.547–552.
- Brockhurst, M.A. & Koskella, B., 2013. Experimental coevolution of species interactions. *Trends in ecology & evolution*, 28(6), pp.367–75.
- Buckling, A. & Rainey, P.B., 2002. Antagonistic coevolution between a bacterium and a bacteriophage. *Proceedings. Biological sciences / The Royal Society*, 269(1494), pp.931–936.
- Bull, J.J., 2006. Optimality models of phage life history and parallels in disease evolution. *Journal of theoretical biology*, 241(4), pp.928–38.
- Bull, J.J., Pfennig, D.W. & Wang, I.-N., 2004. Genetic details, optimization and phage life histories. *Trends in Ecology & Evolution*, 19(2), pp.76–82.
- Bull, J.J. & Wang, I.-N., 2010. Optimality models in the age of experimental evolution and genomics. *Journal of evolutionary biology*, 23(9), pp.1820–38.
- Cavilla, C. & Johns, H., 1964. Inactivation and photoreactivation of the T-even phages as a function of the inactivating ultraviolet wavelength. *Virology*, 24, pp.349–358.
- Chao, L., Hanley, K. & Burch, C., 2000. Kin selection and parasite evolution: higher and lower virulence with hard and soft selection. *Quarterly review of Biology*, 75(3), pp.261–275.
- Charlesworth, B. & Langley, C.H., 1989. The population genetics of *Drosophila* transposable elements. *Annual review of genetics*, 23, pp.251–87.

- Clutton-Brock, T.H., Guinness, F.E. & Albon, S.D., 1982. *Red Deer: Behavior and Ecology of Two Sexes*, University of Chicago Press.
- Combes, C., 2001. *Parasitism: The Ecology and Evolution of Intimate Interactions*, University of Chicago Press.
- Cox, F.E., 2001. Concomitant infections, parasites and immune responses. *Parasitology*, 122 Suppl, pp.S23–38.
- Crossan, J., Paterson, S. & Fenton, A., 2007. Host availability and the evolution of parasite life-history strategies. *Evolution; international journal of organic evolution*, 61(3), pp.675–84.
- Day, T., 2001. Parasite transmission modes and the evolution of virulence. *Evolution*, 55(12), pp.2389–400.
- Dennehy, J.J., 2009. Bacteriophages as model organisms for virus emergence research. *Trends in microbiology*, 17(10), pp.450–7.
- Dennehy, J.J., Abedon, S.T. & Turner, P.E., 2007. Host density impacts relative fitness of bacteriophage Phi6 genotypes in structured habitats. *Evolution; international journal of organic evolution*, 61(11), pp.2516–27.
- Deretic, V. & Schurr, M., 1994. Conversion of *Pseudomonas aeruginosa* to mucoidy in cystic fibrosis: environmental stress and regulation of bacterial virulence by alternative sigma factors. *Journal of Bacteriology*, 176(10), pp.2773–2780.
- Dessau, M. et al., 2012. Selective pressure causes an RNA virus to trade reproductive fitness for increased structural and thermal stability of a viral enzyme. *PLoS genetics*, 8(11), p.e1003102.
- Dionisio, F. et al., 2005. The evolution of a conjugative plasmid and its ability to increase bacterial fitness. *Biology letters*, 1(2), pp.250–2.
- Domingo-Calap, P., Pereira-Gómez, M. & Sanjuán, R., 2010. Selection for thermostability can lead to the emergence of mutational robustness in an RNA virus. *Journal of evolutionary biology*, 23(11), pp.2453–60.
- Dulbecco, R., 1950. Experiments on photoreactivation of bacteriophages inactivated with ultraviolet radiation. *Journal of bacteriology*, 59(3), pp.329–347.
- Dulbecco, R., 1949. Reactivation of ultra-violet-inactivated bacteriophage by visible light. *Nature*, 163(4155), p.949.
- Dupont, S. & Thorndyke, M.C., 2009. Impact of CO<sub>2</sub>-driven ocean acidification on invertebrates early life-history – What we know, what we need to know and what we can do. *Biogeosciences Discussions*, 6(January), pp.3109–3131.
- Eberhard, W., 1990. Evolution in bacterial plasmids and levels of selection. *Quarterly Review of Biology*, 65(1), pp.3–22.

- Ebert, D., 1998. Experimental Evolution of Parasites. *Science*, 282(5393), pp.1432–1436.
- Ebert, D. & Bull, J.J., 2003. Challenging the trade-off model for the evolution of virulence: is virulence management feasible? *Trends in Microbiology*, 11(1), pp.15–20.
- Ellis, R.J. et al., 2007. Frequency-dependent advantages of plasmid carriage by *Pseudomonas* in homogeneous and spatially structured environments. *The ISME journal*, 1(1), pp.92–5.
- Ellison, S., Feiner, R. & Hill, R., 1960. A host effect on bacteriophage survival after ultraviolet irradiation. *Virology*, 266(63), pp.30–32.
- Eshelman, C.C.M. et al., 2010. Unrestricted migration favours virulent pathogens in experimental metapopulations: evolutionary genetics of a rapacious life history. *Philosophical transactions of the Royal Society of London. Series B, Biological sciences*, 365(1552), pp.2503–2513.
- Ewald, P., 1983. Host-parasite relations, vectors, and the evolution of disease severity. *Annual Review of Ecology and Systematics*, 14(1983), pp.465–485.
- Fischer, C.R. et al., 2004. The coexistence of *Escherichia coli* serotype O157:H7 and its specific bacteriophage in continuous culture. *FEMS microbiology letters*, 241(2), pp.171–7.
- Frank, S., 1996. Models of parasite virulence. *Quarterly review of Biology*, 71(1), pp.37–78.
- Gadgil, M. & Bossert, W., 1970. Life historical consequences of natural selection. *American Naturalist*, 104, pp.1–24.
- Gallet, R., Shao, Y. & Wang, I.-N., 2009. High adsorption rate is detrimental to bacteriophage fitness in a biofilm-like environment. *BMC evolutionary biology*, 9, p.241.
- Gallet, R., Tully, T. & Evans, M., 2009. Ecological conditions affect evolutionary trajectory in a predator–prey system. *Evolution*, 63(3), pp.641–651.
- Galvani, A.P., 2003. Epidemiology meets evolutionary ecology. *Trends in Ecology & Evolution*, 18(3), pp.132–139.
- Gardener, S. & Jones, J., 1984. A new solidifying agent for culture media which liquefies on cooling. *Journal of general microbiology*, pp.731–733.
- Goldhill, D.H. & Turner, P.E., 2014. The evolution of life history trade-offs in viruses. *Current opinion in virology*, 8C, pp.79–84.
- Gouagna, L.C. et al., 2004. *Plasmodium falciparum* malaria disease manifestations in humans and transmission to *Anopheles gambiae*: a field study in Western Kenya. *Parasitology*, 128(3), pp.235–243.

- Haine, E.R., Boucansaud, K. & Rigaud, T., 2005. Conflict between parasites with different transmission strategies infecting an amphipod host. *Proceedings of the Royal Society B: Biological Sciences*, 272(1580), pp.2505–10.
- Hall, A., Scanlan, P. & Buckling, A., 2011. Bacteria-phage coevolution and the emergence of generalist pathogens. *The American Naturalist*, 177(1), pp.44–53.
- Hall, A.R. et al., 2011. Host-parasite coevolutionary arms races give way to fluctuating selection. *Ecology letters*, 14(7), pp.635–42.
- Hamilton, W., 1972. Altruism and related phenomena, mainly in social insects. *Annual Review of Ecology and systematics*, 3(1972), pp.193–232.
- Harm, W., 1963. Mutants of phage T4 with increased sensitivity to ultraviolet. *Virology*, 19, pp.66–71.
- Harrison, E. et al., 2014. Bacteriophages limit the existence conditions for conjugative plasmids. *In review*.
- Harrison, E. & Brockhurst, M.A., 2012. Plasmid-mediated horizontal gene transfer is a coevolutionary process. *Trends in microbiology*, 20(6), pp.262–7.
- Hastings, A. & Harrison, S., 1994. Metapopulation dynamics and genetics. *Annual review of Ecology and Systematics*, 25(1994), pp.167–188.
- Heineman, R.H. & Bull, J.J., 2007. Testing optimality with experimental evolution: lysis time in a bacteriophage. *Evolution; international journal of organic evolution*, 61(7), pp.1695–709.
- Henry, R.L., Mellis, C.M. & Petrovic, L., 1992. Mucoïd *Pseudomonas aeruginosa* is a marker of poor survival in cystic fibrosis. *Pediatric Pulmonology*, 12(3), pp.158–161.
- Heuer, H., Fox, R.E. & Top, E.M., 2007. Frequent conjugative transfer accelerates adaptation of a broad-host-range plasmid to an unfavorable *Pseudomonas putida* host. *FEMS microbiology ecology*, 59(3), pp.738–48.
- Hudson, P., Dobson, A. & Newborn, D., 1998. Prevention of population cycles by parasite removal. *science*, 282(5397), pp.2256–2258.
- Jensen, K.H. et al., 2006. Empirical support for optimal virulence in a castrating parasite. *PLoS biology*, 4(7), p.e197.
- Jones, E.O., White, A. & Boots, M., 2010. The evolutionary implications of conflict between parasites with different transmission modes. *Evolution*, 64(8), pp.2408–16.
- Kamo, M. & Boots, M., 2006. The evolution of parasite dispersal, transmission, and virulence in spatial host populations. *Evolutionary Ecology Research*, pp.1333–1347.

- Kellogg, C. & Paul, J., 2002. Degree of ultraviolet radiation damage and repair capabilities are related to G+ C content in marine vibriophages. *Aquatic microbial ecology*, 27, pp.13–20.
- Kerr, B. et al., 2006. Local migration promotes competitive restraint in a host-pathogen “tragedy of the commons”. *Nature*, 442(7098), pp.75–8.
- Komsta, L., 2011. Outliers: Tests for outliers.
- Law, R., 1979. Optimal life histories under age-specific predation. *American Naturalist*, 114(3), pp.399–417.
- Leggett, H.C. et al., 2012. Experimental Evolution of Adaptive Phenotypic Plasticity in a Parasite. *Current Biology*, pp.1–4.
- Lenski, R., 1988. Experimental studies of pleiotropy and epistasis in *Escherichia coli*. I. Variation in competitive fitness among mutants resistant to virus T4. *Evolution*, 42(3), pp.425–432.
- Lenski, R. et al., 1991. Long-term experimental evolution in *Escherichia coli*. I. Adaptation and divergence during 2,000 generations. *American Naturalist*, 138(6), pp.1315–1341.
- Lenski, R. & Levin, B., 1985. Constraints on the Coevolution of Bacteria and Virulent Phage : A Model , Some Experiments , and Predictions for Natural Communities. *American Naturalist*, 125(4), pp.585–602.
- Levin, B.R. & Bull, J.J., 1994. Short-sighted evolution and the virulence of pathogenic microorganisms. *Trends in microbiology*, 2(3), pp.76–81.
- Levin, S. & Pimentel, D., 1981. Selection of intermediate rates of increase in parasite-host systems. *American Naturalist*, 117(3), pp.308–315.
- Lewontin, R.C., 1989. A natural selection. *Nature*, 339, p.107.
- Li, Z. et al., 2005. Infection and Lung Disease Progression in Children With Cystic Fibrosis. , 293(5), pp.581–588.
- Lilley, A. & Bailey, M., 1997a. Impact of plasmid pQBR103 acquisition and carriage on the phytosphere fitness of *Pseudomonas fluorescens* SBW25: burden and benefit. *Applied and environmental microbiology*, 63(4), pp.1584–1587.
- Lilley, A. & Bailey, M., 1997b. The acquisition of indigenous plasmids by a genetically marked pseudomonad population colonizing the sugar beet phytosphere is related to local environmental. *Applied and Environmental Microbiology*, 4(63), pp.1577–1583.
- Lion, S. & Baalen, M. Van, 2008. Self-structuring in spatial evolutionary ecology. *Ecology letters*, 11(3), pp.277–95.
- Lion, S. & Boots, M., 2010. Are parasites “prudent” in space? *Ecology letters*, 13(10), pp.1245–55.

- Livermore, D.M., 2002. Multiple mechanisms of antimicrobial resistance in *Pseudomonas aeruginosa*: our worst nightmare? *Clinical infectious diseases : an official publication of the Infectious Diseases Society of America*, 34(5), pp.634–40.
- Lu, Z., Breidt, F. & others, 2003. Isolation and characterization of a *Lactobacillus plantarum* bacteriophage, [Phi] JL-1, from a cucumber fermentation• 1. *International journal of food microbiology*, 84(2), pp.225–235.
- Lundquist, P. & Levin, B., 1986. Transitory derepression and the maintenance of conjugative plasmids. *Genetics*, (1977), pp.483–497.
- Luria, S., 1947. Reactivation of irradiated bacteriophage by transfer of self-reproducing units. *Proceedings of the National Academy of Sciences*, 33, pp.253–264.
- Luria, S., 1950. Type hybrid bacteriophages. *Genetics*, 35.
- Luria, S. & Dulbecco, R., 1949. Genetic recombinations leading to production of active bacteriophage from ultraviolet inactivated bacteriophage particles. *Genetics*, (March), pp.93–125.
- Maynard Smith, J., 1978. Optimization Theory in Evolution. *Annual Review of Ecology and Systematics*, 9(1), pp.31–56.
- Mazel, D. & Davies, J., 1999. Antibiotic resistance in microbes. *Cellular and molecular life sciences : CMLS*, 56(9-10), pp.742–54.
- Messenger, S.L., Molineux, I.J. & Bull, J.J., 1999. Virulence evolution in a virus obeys a trade-off. *Proceedings. Biological sciences / The Royal Society*, 266(1417), pp.397–404.
- Messinger, S.M. & Ostling, A., 2009. The consequences of spatial structure for the evolution of pathogen transmission rate and virulence. *The American naturalist*, 174(4), pp.441–54.
- Mideo, N., 2009. Parasite adaptations to within-host competition. *Trends in parasitology*, 25(6), pp.261–8.
- Miracle, M. & Serra, M., 1989. Salinity and temperature influence in rotifer life history characteristics. *Hydrobiologia*, pp.81–102.
- Morgan, A.D. et al., 2012. Selection on non-social traits limits the invasion of social cheats. *Ecology letters*, 15(8), pp.841–6.
- Murray, A. & Jackson, G., 1993. Viral dynamics II: a model of the interaction of ultraviolet light and mixing processes on virus survival in seawater. *Marine Ecology-Progress Series*, 102, pp.105–114.
- Nidelet, T., Koella, J.C. & Koltz, O., 2009. Effects of shortened host life span on the evolution of parasite life history and virulence in a microbial host-parasite system. *BMC evolutionary biology*, 9(1), p.65.

- Norman, A., Hansen, L.H. & Sørensen, S.J., 2009. Conjugative plasmids: vessels of the communal gene pool. *Philosophical transactions of the Royal Society of London. Series B, Biological sciences*, 364(1527), pp.2275–89.
- Nowak, M.A. & May, R.M., 1994. Superinfection and the evolution of parasite virulence. *Proceedings. Biological sciences / The Royal Society*, 255(1342), pp.81–9.
- De Paepe, M. & Taddei, F., 2006. Viruses' life history: towards a mechanistic basis of a trade-off between survival and reproduction among phages. *PLoS biology*, 4(7), p.e193.
- Pajunen, M., Kiljunen, S. & Skurnik, M., 2000. Bacteriophage phi Ye03-12, Specific for *Yersinia enterocolitica* Serotype O:3, Is Related to Coliphages T3 and T7. *Journal of Bacteriology*, 182(18), pp.5114–5120.
- Partridge, L. & Harvey, P., 1988. The ecological context of life history evolution. *Science*, 538(1985).
- Paterson, S. et al., 2010. Antagonistic coevolution accelerates molecular evolution. *Nature*, 464(7286), pp.275–8.
- Pedersen, A.B. & Fenton, A., 2007. Emphasizing the ecology in parasite community ecology. *Trends in ecology & evolution*, 22(3), pp.133–9.
- Phillips, W. & Cannon, L., 1978. Ecological observations on the commercial sand crab, *Portunus pelagicus* (L.), and its parasite, *Sacculina granifera* Boschma, 1973 (Cirripedia: Rhizocephala). *Journal of Fish Diseases*, 1, pp.137–149.
- Poulin, R., 2011. *Evolutionary Ecology of Parasites: (Second Edition)*, Princeton University Press.
- Poulin, R., 2001. Interactions between species and the structure of helminth communities. *Parasitology*, 122 Suppl, pp.S3–11.
- Poulin, R., 1996. The evolution of life history strategies in parasitic animals. *Advances in parasitology*, 37, pp.107–34.
- Poullain, V. et al., 2008. The evolution of specificity in evolving and coevolving antagonistic interactions between a bacteria and its phage. *Evolution; international journal of organic evolution*, 62(1), pp.1–11.
- Proctor, L. & Fuhrman, J., 1990. Viral mortality of marine bacteria and cyanobacteria. *Nature*, 343, pp.60–62.
- R Core Team, 2013. R: A language and environment for statistical computing.
- Rainey, P. & Travisano, M., 1998. Adaptive radiation in a heterogeneous environment. *Nature*, 32, pp.69–72.
- Rainey, P.B. & Bailey, M.J., 1996. Physical and genetic map of the *Pseudomonas fluorescens* SBW25 chromosome. *Molecular microbiology*, 19(3), pp.521–33.
- Read, A. & Taylor, L., 2001. The ecology of genetically diverse infections. *Science*, 292(5519), pp.1099–1102.

- Read, A.F., 1994. The evolution of virulence. *Trends in Microbiology*, 2(3), pp.73–76.
- Redpath, S.M. et al., 2006. Testing the role of parasites in driving the cyclic population dynamics of a gamebird. *Ecology letters*, 9(4), pp.410–8.
- Refardt, D., 2011. Within-host competition determines reproductive success of temperate bacteriophages. *The ISME journal*, 5(9), pp.1451–60.
- Rigaud, T. & Haine, E.R., 2005. Conflict between co-occurring parasites as a confounding factor in manipulation studies? *Behavioural processes*, 68(3), pp.259–62.
- Rodriguez, R. a et al., 2014. Photoreactivation of bacteriophages after UV disinfection: role of genome structure and impacts of UV source. *Water research*, 55, pp.143–9.
- Roff, D. a & Fairbairn, D.J., 2007. The evolution of trade-offs: where are we? *Journal of evolutionary biology*, 20(2), pp.433–47.
- Roychoudhury, P. et al., 2014. Fitness benefits of low infectivity in a spatially structured population of bacteriophages. *Proceedings of the Royal Society B: Biological Sciences*, 281.
- Scanlan, P.D. et al., 2011. Genetic basis of infectivity evolution in a bacteriophage. *Molecular ecology*, 20(5), pp.981–9.
- Scanlan, P.D. & Buckling, A., 2012. Co-evolution with lytic phage selects for the mucoid phenotype of *Pseudomonas fluorescens* SBW25. *The ISME journal*, 6(6), pp.1148–1158.
- Shao, Y. & Wang, I.-N., 2008. Bacteriophage adsorption rate and optimal lysis time. *Genetics*, 180(1), pp.471–82.
- Silver, S. & Misra, T.K., 1988. Plasmid-mediated heavy metal resistances. *Annual review of microbiology*, 42, pp.717–43.
- Simonsen, L., 1991. The existence conditions for bacterial plasmids: theory and reality. *Microbial ecology*, 22, pp.187–205.
- Slatkin, M., 1987. Gene flow and the geographic structure of natural populations. *Science*, 236, pp.787–792.
- Stearns, S., 1992. *The evolution of life histories*, OUP Oxford.
- Stearns, S., 1989. Trade-offs in life-history evolution. *Functional ecology*, 3(3), pp.259–268.
- Stewart, F. & Levin, B., 1977. The population biology of bacterial plasmids: a priori conditions for the existence of conjugationally transmitted factors. *Genetics*, 87, pp.209–228.
- Streisinger, G., 1956. The genetic control of ultraviolet sensitivity levels in bacteriophages T2 and T4. *Virology*, 2(1), pp.1–12.

- Subbiah, M. et al., 2011. Selection pressure required for long-term persistence of blaCMY-2-positive IncA/C plasmids. *Applied and environmental microbiology*, 77(13), pp.4486–93.
- Susi, H. & Laine, A.-L., 2013. Pathogen life-history trade-offs revealed in allopatry. *Evolution; international journal of organic evolution*, 67(11), pp.3362–70.
- Suttle, C. & Chen, F., 1992. Mechanisms and rates of decay of marine viruses in seawater. *Applied and Environmental Microbiology*, 58(11), pp.3721–3729.
- Svara, F. & Rankin, D.J., 2011. The evolution of plasmid-carried antibiotic resistance. *BMC evolutionary biology*, 11(1), p.130.
- Tejedor, C., Foulds, J. & Zasloff, M., 1982. Bacteriophages in sputum of patients with bronchopulmonary Pseudomonas infections. *Infection and immunity*, 36(1), pp.440–1.
- Tett, A. et al., 2007. Sequence-based analysis of pQBR103; a representative of a unique, transfer-proficient mega plasmid resident in the microbial community of sugar beet. *The ISME journal*, 1(4), pp.331–40.
- Turner, P., 2005. Parasitism between co-infecting bacteriophages. *Advances in Ecological Research*, 37(04).
- Turner, P. & Chao, L., 1999. Prisoner's dilemma in an RNA virus. *Nature*, 398(April), pp.441–443.
- Waite, A.J. & Shou, W., 2012. Adaptation to a new environment allows cooperators to purge cheaters stochastically. *Proceedings of the National Academy of Sciences of the United States of America*, 109(47), pp.19079–86.
- Walther, B. a & Ewald, P.W., 2004. Pathogen survival in the external environment and the evolution of virulence. *Biological reviews of the Cambridge Philosophical Society*, 79(4), pp.849–69.
- Wang, I., Smith, D. & Young, R., 2000. Holins: the protein clocks of bacteriophage infections. *Annual Reviews in Microbiology*, 54, pp.799–825.
- Wang, N., Dykhuizen, D. & Slobodkin, L., 1996. The evolution of phage lysis timing. *Evolutionary Ecology*, 10, pp.545–558.
- Watts, D.J. & Strogatz, S.H., 1998. Collective dynamics of “small-world” networks. *Nature*, 393(6684), pp.440–2.
- Weinbauer, M. & Wilhelm, S., 1997. Photoreactivation compensates for UV damage and restores infectivity to natural marine virus communities. *Applied and Environmental Microbiology*, 63(6).
- Weiss, R. a., 2002. Virulence and pathogenesis. *Trends in Microbiology*, 10(7), pp.314–317.
- Wild, G., Gardner, A. & West, S.A., 2009. Adaptation and the evolution of parasite virulence in a connected world. *Nature*, 459(7249), pp.983–6.

- Wilhelm, S. et al., 1998. Measurements of DNA damage and photoreactivation imply that most viruses in marine surface waters are infective. *Aquatic microbial ecology*, 14, pp.215–222.
- Wilhelm, S. & Weinbauer, M., 1998. The role of sunlight in the removal and repair of viruses in the sea. *Limnology and oceanography*.
- Windsor, D.A., 1998. Most of the species on Earth are parasites. *International journal for parasitology*, 28(12), pp.1939–41.
- Wommack, K. et al., 1996. Effects of sunlight on bacteriophage viability and structure. *Applied and Environmental Microbiology*, 62(4), pp.1336–1341.
- Wood, R.D., Skopek, T.R. & Hutchinson, F., 1984. Changes in DNA base sequence induced by targeted mutagenesis of lambda phage by ultraviolet light. *Journal of molecular biology*, 173(3), pp.273–91.
- Young, R., 2013. Phage lysis: do we have the hole story yet? *Current opinion in microbiology*, 16(6), pp.790–7.
- Young, R., 2014. Phage lysis: three steps, three choices, one outcome. *Journal of microbiology (Seoul, Korea)*, 52(3), pp.243–58.
- Young, R., Wang, I.-N. & Roof, W.D., 2000. Phages will out: strategies of host cell lysis. *Trends in Microbiology*, 8(3), pp.120–128.
- Young, R.Y., 1992. Bacteriophage Lysis: Mechanism and Regulation. *Microbiological reviews*, 56(3), pp.430–481.
- Zhang, Q.-G. & Buckling, A., 2011. Antagonistic coevolution limits population persistence of a virus in a thermally deteriorating environment. *Ecology letters*, 14(3), pp.282–8.
- Zwart, M.P. et al., 2008. Low multiplicity of infection in vivo results in purifying selection against baculovirus deletion mutants. *The Journal of general virology*, 89(Pt 5), pp.1220–4.

# Appendix I – Ancestral phage life history characterization

## Introduction

To standardise the genetic background of evolving populations, an isogenic high-titre ancestral stock is necessary. Here is described the method of obtaining the ancestral stock, and the development of methods for calculating the life history of populations. The life history trait values are calculated and presented here, for comparison to evolved populations.

## Methods

### Host growth curve

6 replicate microcosms were initiated consisting of 6 ml KB media in a sterile 30 ml glass universal. Each of these were inoculated with 6 µl saturated *P. fluorescens* SBW25 culture and incubated at 28°C, shaken at 180 revolutions per minute (rpm). Immediately following inoculation and every hour for 12 hours, each replicate population was sampled (200 µl) and the optical density (OD) measured at 630 nm using a Tecan Sunrise™ microplate reader. A further sample was taken at 24 hours. At 0, 4, 8, 12 and 24 hours, a 50 µl sample of each replicate was taken, serially diluted and plated on KB agar for colony forming unit (cfu) enumeration.

Growth rate was measured as  $\frac{\log(N_8) - \log(N_4)}{t_8 - t_4}$  where  $t_8$  and  $t_4$  are hours 8 and 4 respectively and  $N_8$  and  $N_4$  are the number of colony forming units (CFU) at hours 8 and 4 respectively.

## Preparation of high-titre ancestral $\Phi 2$ stock

### *Standard plaque assay*

A  $\Phi 2$  suspension was serially diluted, and 100  $\mu$ l of each dilution mixed with 100  $\mu$ l saturated *P. fluorescens* culture and 6 ml semi-soft KB agar in a sterile bijou bottle by gentle inversion three times. Each of these mixtures were poured onto a standard KB agar plate and allowed to dry before inversion and incubation at 28°C overnight.

### *Purification*

Following the standard plaque assay described above, one well-separated plaque was selected, excised from the plate and suspended in 1 ml KB media. This suspension was vortexed at high speed for 30 seconds, and filter sterilised using a 0.22  $\mu$ m Millipore syringe filter. The filtrate was plated in a standard plaque assay as described above, but with 10 replicate plates per dilution.

### *Amplification*

Following the purification step, the plates exhibiting semi-confluent lysis were selected, flooded with 6 ml KB media and incubated at room temperature for 1 hour to allow phage to desorb into the media. After incubation, the media was

removed and placed into a sterile 250 ml sterile duran bottle. Using a sterile glass spreader, the semi-solid agar layer of each plate was scraped into the duran. 100 µl of Chloroform was added and the bottle inverted 3 times, before incubation at 4°C overnight. The contents of the bottle were then filter-sterilised using a Steritop (Millipore) 250 ml filter cup attached to a vacuum pump. 1 ml aliquots of the final filtrate were stored frozen at -80°C in 1.2 ml cryovials with 20% glycerol. A standard plaque assay was performed to enumerate PFUs.

### Determination of optimal MOI

Phage grow optimally when inoculated at an MOI that is sufficiently large that invasion of the host population is successful and sufficiently small that susceptible host cells are not quickly depleted.

#### *Method*

Adapted from Lu et al. (2003). 12 replicate microcosms were initiated with a single fresh colony of *P. fluorescens* in 6 ml KB in 30 ml disposable glass universal tubes. These populations were incubated at a constant temperature of 28°C, at 180 rpm. After 48 h growth ( $\sim 10^7$  cells ml<sup>-1</sup>), 60 µl from each population were transferred to fresh microcosms. At mid-log growth, these microcosms were inoculated with  $\phi 2$  at an MOI of 10, 1, 0.1, 0.01, 0.001 or 0.0001 (in duplicate). A cell-free control microcosm was also inoculated with the density that would be an MOI of 1. These cultures were incubated for 3.5 hours at 28°C, shaken at 180 rpm. After incubation, cultures were centrifuged at 8000g for 5 minutes, the supernatant was filtered and plated for phage titration.

## Growth curve

Modified from the one-step growth curve method described by Pajunen, Kiljunen, & Skurnik (2000). 33 replicate microcosms were initiated with 100 µl saturated *P. fluorescens* culture in 6 ml King's B (KB) liquid media in sterile 30 ml glass universals and incubated shaken at 180 rpm at 28°C. At mid-log host growth, microcosms were inoculated with phage suspension at an MOI of 0.001. Immediately after inoculation and every 8 minutes for 80 minutes, 3 replicate microcosms were selected at random, sampled and removed. A 1 ml sample was taken and immediately filter sterilised to prevent further growth. At the end of the assay, all samples were spot-plated for titration.

A generalised additive model (GAM) was fitted to  $\log_{10}$  PFU ml<sup>-1</sup> against smoothed time and used to predict values to fit a smoothed curve to the data.

## Lysis time

Lysis time was calculated as the point of inflection during the exponential rise period.

## Burst size

Burst size was calculated as (from Dennehy et al. 2007, modified to take account

of adsorption):  $\frac{P_{max}}{P_{ads}}$  where  $P_{max}$  is the maximum free phage following

burst, and  $P_{ads}$  is the number of adsorbed phage, obtained by calculating

$P_0 - P_{min}$  where  $P_0$  is free phage at time 0, and  $P_{min}$  is free phage following adsorption, immediately before the rise period.

## Adsorption rate

24 replicate microcosms were initiated with 100 µl saturated *P. fluorescens* culture in 6 ml KB liquid media in sterile 30 ml glass universals and incubated shaken at 180 rpm at 28°C. At mid-log host growth, microcosms were inoculated with phage suspension at an MOI of 0.001. Immediately after inoculation and at 3, 6, 10, 15, 20, 25 and 30 minutes, 3 replicate microcosms were selected at random, sampled and removed. A 1 ml sample was taken and immediately filter sterilised. At the end of the assay, all samples were spot-plated for titration.

Adsorption rate is calculated as (adapted from Shao & Wang 2008):

$$r = \frac{\mu \ln(P_t/P_0)}{-(e^{\mu t} - 1)N_0} \quad \text{where } P_t \text{ is free phage density at 30 minutes, } P_0 \text{ and}$$

$N_0$  are phage and bacterial density at time 0 respectively,  $\mu$  is bacterial growth rate and  $r$  is the rate to be measured.

## Results

### Host growth curve

*P. fluorescens* cultures reached mid-log density at 6 hours post-inoculation, with an OD<sub>630 nm</sub> of 0.63 (Fig. A1.1), which equates to approximately 8x10<sup>8</sup> cells ml<sup>-1</sup>. The population growth rate was 0.01 cells min<sup>-1</sup>.

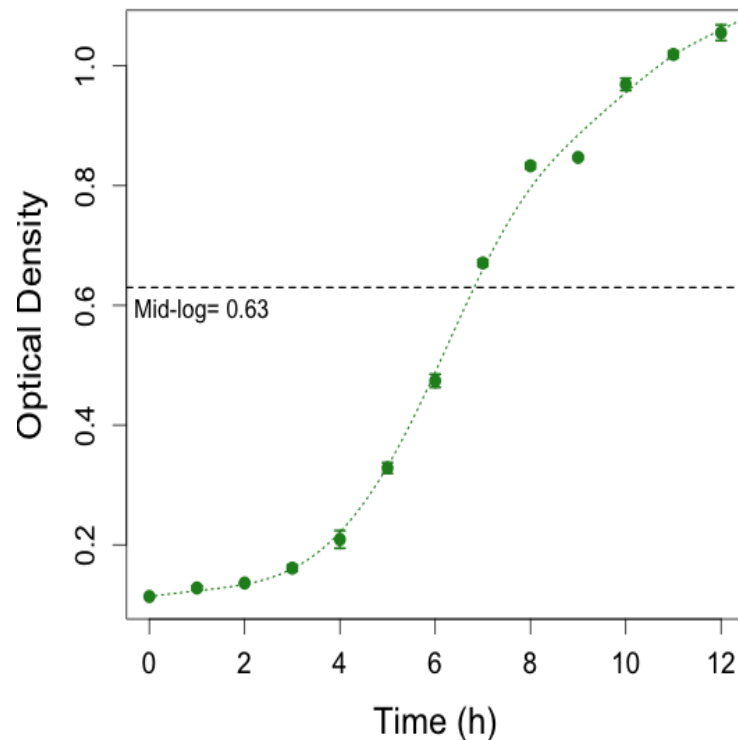


**Figure A1.1.** *P. fluorescens* growth curve. Error bars represent 1 standard error for a mean of 3 replicate populations. Dashed line shows mid-log density at OD<sub>630</sub> 0.63

### High-titre ancestral Φ2 stock

A high-titre ancestral Φ2 stock was obtained with  $1.2 \times 10^{11}$  PFU ml<sup>-1</sup> density.

### Optimal MOI

An MOI of 0.1 yields the highest phage density relative to inoculum density after 3.5 hours (Fig. A1.2), so is the optimal MOI for phage growth. A range of MOIs from 0.001-1 are also acceptable. In selection experiments, evolved phage

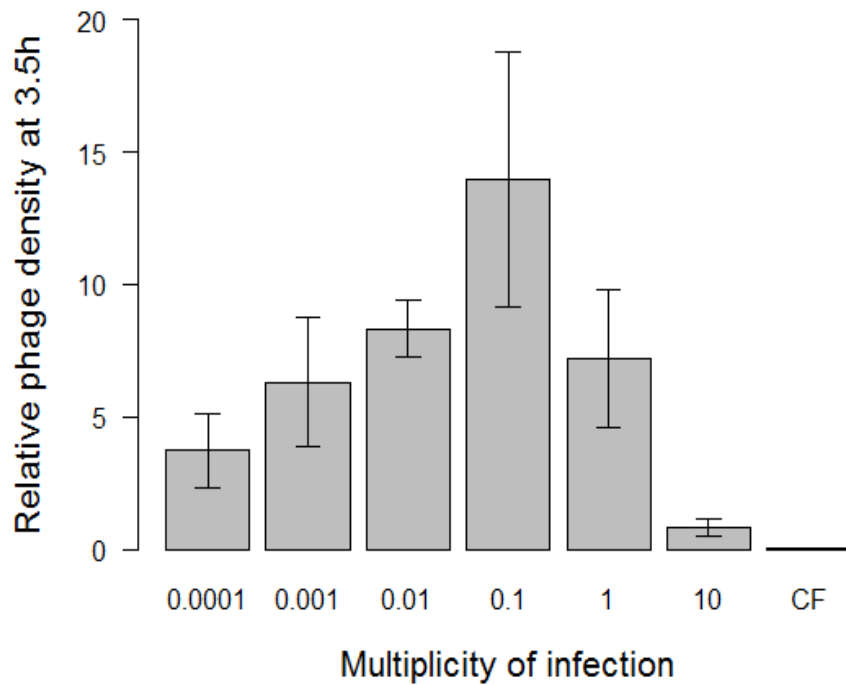


**Figure A1.2.** Relative phage density at 3.5 hours after inoculation at 6 different MOIs and a cell-free control (CF). Error bars represent 1 standard error for a mean of 2 replicate cultures

population densities were very low, so an optimal MOI was not achievable. MOI was standardised at 0.001 for all assays.

## Ancestral life history

The ancestral phage stock growth curve can be seen in figure A1.3. This isogenic stock has a lysis time of 40.8 minutes, a burst size of 7.8, a rise period slope of 13, and an adsorption rate of  $1.06 \times 10^{-8}$  virions cell<sup>-1</sup> ml<sup>-1</sup> min<sup>-1</sup>.

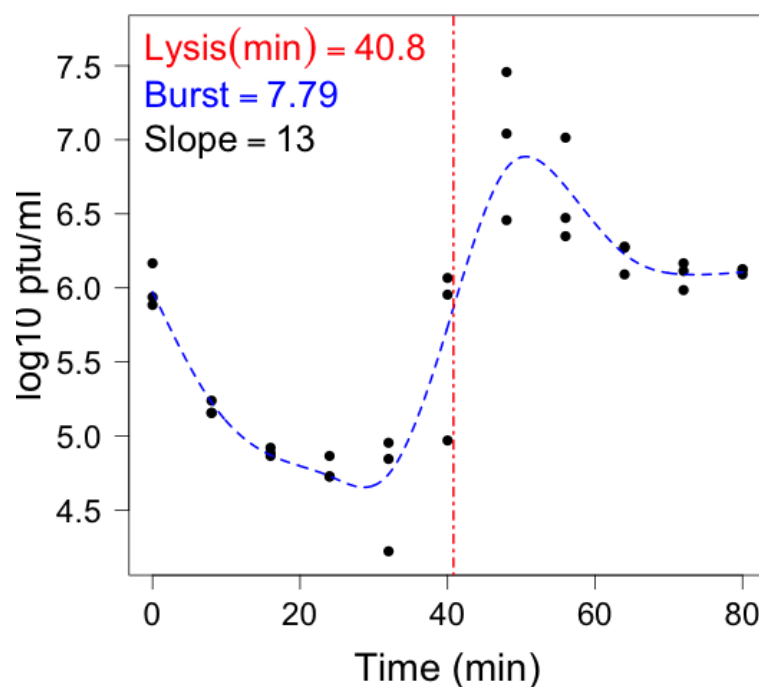


**Figure A1.3.** Ancestral stock growth curve with fitted GAM model (blue dashed line). Lysis time is indicated by the vertical red dashed line.

## References

- Dennehy, J.J., Abedon, S.T. & Turner, P.E., 2007. Host density impacts relative fitness of bacteriophage Phi6 genotypes in structured habitats. *Evolution; international journal of organic evolution*, 61(11), pp.2516–27.
- Lu, Z., Breidt, F. & others, 2003. Isolation and characterization of a *Lactobacillus plantarum* bacteriophage, [Phi] JL-1, from a cucumber fermentation • 1. *International journal of food microbiology*, 84(2), pp.225–235.
- Pajunen, M., Kiljunen, S. & Skurnik, M., 2000. Bacteriophage phi Ye03-12, Specific for *Yersinia enterocolitica* Serotype O:3, Is Related to Coliphage T3 and T7. *Journal of Bacteriology*, 182(18), pp.5114–5120.

Shao, Y. & Wang, I.-N., 2008. Bacteriophage adsorption rate and optimal lysis time. *Genetics*, 180(1), pp.471–82.

## Appendix II – Sequencing methods

### PCR

Target genes were amplified from each evolved population and the ancestor using 25 µl PCRs in a 96-well thermal cycling machine (Applied Biosystems Veriti™ 96-well Thermal Cycler). Each reaction consisted of 12.5 µl GoTaq® Green Master Mix (Promega), 1 µl each of 10 pmol forward and reverse primers (see Table A2.1 for primer sequences), 9.5 µl dd H<sub>2</sub>O and 1 µl phage population suspension (untreated). Thermal cycling conditions were: Heated lid at 100°C, initial denaturation at 95°C for 5 minutes, 35 cycles of 30 seconds at 95°C, 1 minute at 56°C and 1 minute at 72°C, with a final extension of 5 minutes at 72°C. Products were checked for size and presence by 1.4% agarose gel electrophoresis at 80 volts for 40 minutes.

### ExoSAP digest

PCR products were cleaned in 7 µl reactions containing 5 µl PCR product, 0.05 µl Exonuclease 1, 0.2 µl shrimp alkaline phosphatase (SAP), 0.7 µl 10x RX buffer and 1.05 µl dd H<sub>2</sub>O. Reactions were incubated for 45 minutes at 37°C and 15 minutes at 80°C, with a heated lid at 105°C in the 96-well thermal cycler.

## Cycle sequencing reaction

ExoSAP products were further amplified in preparation for sequencing in 10 µl reactions containing 1 µl ExoSAP product, 1 µl 5x buffer, 5.5 µl dd H<sub>2</sub>O, 0.5 µl Bigdye 3.1 and 2 µl 1.6 pmol forward or reverse primer. Reciprocal forward and reverse reactions were conducted for each primer set. Reactions were incubated for 25 cycles of: 10 seconds ramped to 96°C at 1°C sec<sup>-1</sup>, 5 seconds ramped to 50°C at 1°C sec<sup>-1</sup> and 4 minutes ramped to 60°C at 1°C sec<sup>-1</sup>, with a heated lid at 100°C in the 96-well thermal cycler.

## Precipitation and sequencing

In a skirted 96-well plate, 1.5 µl 3M C<sub>2</sub>H<sub>3</sub>NaO<sub>2</sub>, 31.25 µl 100% molecular grade ethanol and 7.25 µl dd H<sub>2</sub>O were combined with 10 µl cycle sequencing reaction product and incubated at room temperature for 15 minutes. These were then centrifuged at 3100 rpm for 45 minutes, and the supernatant discarded by centrifugation inverted at 600 rpm for 1 minute. DNA was washed by addition of 150 µl 70% molecular grade ethanol, centrifugation at 3100 rpm and discard of the supernatant as above. DNA was then resuspended in 10 µl Hi-Di formamide, and Sanger sequenced using 16-capillary electrophoresis on the ABI Prism 3130xl Genetic Analyser (Applied Biosystems).

## Analysis

Genes were assembled, aligned and analysed for mutations using Geneious R7 (created by Biomatters. Available from <http://www.geneious.com/>).

Fixed mutations were identified as single clear peaks that differed from the reference genome in both the forward and reverse sequences (NCBI accession number NC\_012660). Polymorphisms were identified as overlapping double high peaks that occurred in both the forward and reverse sequences.

**Table A2.1.** Primers used for phage gene sequencing

Gene	Part	Forward primer 5'-3'	Reverse primer 3'-5'
SBWP25_0027	1 of 1	GGACACCATGCGGCTAACAT	CCTCATCCCGATACTGCTGC
SBWP25_0032	1 of 4	TCAAGAAAGCTCGTACAAGAAC	TCCAACGCTTCTCAGCATC
SBWP25_0032	2 of 4	AAGGCACCTTCGCTTCCATC	CGTCATCTCATGCACACCAAC
SBWP25_0032	3 of 4	AATGGCAGCCTTCCAAGGAC	GCCACGGACATTGCTGAATAC
SBWP25_0032	4 of 4	TGGTCATTACGAGTACCTG	CCTGAACTGCTGATGGAAC
SBWP25_0034	1 of 4	ACCAGCGAGCAGTTCAATC	TGCCCTCAAACCTACCATCC
SBWP25_0034	2 of 4	TCTTCCAAGACGTGCTGACC	AGACATACGCCATCTGTGCC
SBWP25_0034	3 of 4	TCGGCGTACTCCCAAATC	ACTGGAACGACGACTCATAG
SBWP25_0034	4 of 4	TGTCTCCAACGTACAGTCC	TGCCATGTTCTTGATGAACC
SBWP25_0035	1 of 5	AACAGCATTGAACCCTGCC	AGTACATCCGTTGGAACGAG
SBWP25_0035	2 of 5	GTATCTGCTCAATGCCAGTC	CTTGTCCACACCCTTAATACC
SBWP25_0035	3 of 5	ACGTCATGCCTGATCCGAAC	CATCAGCAACGCTCTTGACC
SBWP25_0035	4 of 5	TCATGGAGAACTACGGCAC	GCATTCATAACGCCATCGAC
SBWP25_0035	5 of 5	AAGTTCATCCACTCCCACC	TTGCCAATATCTGCTGCAC
SBWP25_0036	1 of 3	TCCCGTACCAGAAGCAATCC	AGCGTACCTACAGCATCACC
SBWP25_0036	2 of 3	GCCGCACAGATCACTTATG	TGCAACAGTACACCAGATAAC
SBWP25_0036	3 of 3	GTATGTTCTCCAGCGGCAAC	TGCCAAACCGAACCGTTACC
SBWP25_0040	1 of 1	TTCGCCCAGTTGGTAAAGGT	AGGGCTAGGGCCACGATAAG